DISTRIBUTED OPTIMIZATION ALGORITHMS FOR INTER-REGIONAL COORDINATION OF ELECTRICITY MARKETS

by

Verónica Raquel Bósquez Fóti

A Dissertation

Submitted to the Faculty of Purdue University

In Partial Fulfillment of the Requirements for the degree of

Doctor of Philosophy

School of Industrial Engineering

West Lafayette, Indiana

May 2021

THE PURDUE UNIVERSITY GRADUATE SCHOOL
STATEMENT OF COMMITTEE APPROVAL

Dr. Andrew (Lu) Liu, Chair
School of Industrial Engineering

Dr. Gesualdo Scutari
School of Industrial Engineering

Dr. Paul Preckel
Department of Agricultural Economics

Dr. Douglas Gotham
Director, State Utility Forecasting Group

Approved by:
Dr. Abhijit Deshmukh

A Papá, porque, aunque ya no estés aquí, me motivas a ser la persona que viste en mí.

A Drága Édesanyámnak, mert életembe a legnagyobb áldás a lányod lenni volt.

ACKNOWLEDGMENTS

This work would not have been possible without the help of my advisor, Professor Andrew Liu, who patiently guided me over the years, strengthened the mathematical rigor of my work, and shared my interest in the operation of wholesale electricity markets. As a mid-career graduate student attempting to balance a job, parental duties, and academic work, I am grateful for Professor Liu's unwavering support and understanding, which were critical in getting me through the finish line. I am also thankful to Professor Oleg Wasynczuk, who encouraged me to pursue my academic ambitions and suggested working with Professor Liu.

I am indebted to Mr. Stephen Fernands who, in addition to being an outstanding boss, partially funded this research by supporting my academic work while I was employed at Customized Energy Solutions, Ltd.

Numerous hours of enlightening conversation with my friends and colleagues at MISO stakeholder meetings and electricity market conferences sparked my desire to explore big solutions to some of the shortcomings of the existing wholesale market design. I am especially thankful for my chats with Mr. Steve Leovy, whose relentless curiosity first got me thinking about how close seams management could get to the ideal scenario, and with Dr. Sergio Brignone, a sharp and brilliant critic of the implementation of wholesale markets, who made me see the huge cost of even small inefficiencies as an opportunity to consider bold remedies. Further, I will always be grateful to Dr. Dhiman Chatterjee, who gave me my first opportunity to work in the areas of wholesale electric markets and congestion management. He had confidence in my abilities much before I did and opened the door to a career that has brought to my life a great deal of satisfaction.

Finally, this work, and every accomplishment in my life, I partly owe to the support of my family. They are my rock, my inspiration, and my constant cheerleaders.

TABLE OF CONTENTS

LIST OF TABLES

LIST OF FIGURES

LIST OF ABBREVIATIONS

ADMM	Alternating direction method of multipliers
CTS	Coordinated transaction scheduling
ED	Economic dispatch
FERC	Federal Energy Regulatory Commission
FTR	Financial transmission right
ISO	Independent System Operator
ISO-NE	Independent System Operator of New England
LMP	Locational marginal price
M2M	Market-to-market
MISO	Midcontinent Independent System Operator
NERC	North American Electric Reliability Corporation
NYISO	New York Independent System Operator
RCF	Reciprocal coordinated flowgate
RTO	Regional Transmission Organization
SCED	Security-constrained economic dispatch
SCUC	Security-constrained unit commitment
UC	Unit commitment

ABSTRACT

In the US, seven regional transmission organizations (RTOs) operate wholesale electricity markets within three largely independent transmission systems, the largest of which includes five RTO regions and many vertically integrated utilities.

RTOs operate a day-ahead and a real-time market. In the day-ahead market, generation and demand-side resources are optimally scheduled based on bids and offers for the next day. Those schedules are adjusted according to actual operating conditions in the real-time market. Both markets involve a unit commitment calculation, a mixed integer program that determines which generators will be online, and an economic dispatch calculation, an optimization determines the output of each online generator for every interval and calculates locational marginal prices (LMPs).

The use of LMPs for the management of congestion in RTO transmission systems has brought efficiency and transparency to the operation of electric power systems and provides price signals that highlight the need for investment in transmission and generation. Through this work, we aim to extend these efficiency and transparency gains to the coordination across RTOs. Existing market-based inter-regional coordination schemes are limited to incremental changes in real-time markets.

We propose a multi-regional unit-commitment that enables coordination in the day-ahead timeframe by applying a distributed approach to approximate a system-wide optimal commitment and dispatch while allowing each region to largely maintain their own rules, model only internal transmission up to the boundary, and keep sensitive financial information confidential. A heuristic algorithm based on an extension of the alternating directions method of multipliers (ADMM) for the mixed integer program is applied to the unit commitment.

The proposed coordinated solution was simulated and compared to the ideal single-market scenario and to a representation of the current uncoordinated solution, achieving at least 58% of the maximum potential savings, which, in terms of the annual cost of electric generation in the US, could add up to nearly $7 billion per year. In addition to the coordinated day-ahead solution, we develop a distributed solution for financial transmission rights (FTR) auctions with minimal information sharing across RTOs that constitutes the first known work to provide a viable option for market participants to seamlessly hedge price variability exposure on cross-border transactions.

1. INTRODUCTION

In April 1996, the Federal Energy Regulatory Commission (FERC) issued Order 888 [45], promoting wholesale competition in electric supply through open access to high voltage electric transmission systems. As a result, Independent Transmission Operators (ISOs) were established to administer open access tariffs in a non-discriminatory fashion. In Order 2000 [46], issued in December 1999, FERC established Regional Transmission Organizations (RTOs) and encouraged utilities to join them [15]. Order 2000 defined a minimum set of functions for an RTO that, in addition to the administration and design of an open access transmission tariff, include the management of congestion in the transmission system via market-based mechanisms that provide economic incentives to market participants to generate or consume electricity in a way that avoids overloading transmission facilities.

Currently, seven ISOs operate in the US, within three largely independent transmission systems (the Eastern, Western and Texas interconnections) (Figure 1.1), serving approximately two thirds of the country's population. All US ISOs are also established as RTOs, with operational authority over all transmission facilities under their control.

Where more than one transmission operator exists in an interconnected system, RTOs are also responsible for inter-regional coordination. However, the efficiencies introduced to the utilization of the transmission system by the implementation of market-based mechanisms to manage congestion, have not been extended to the flow across RTO regions. Considerable amount of electricity is exchanged between interconnected regions, yet the optimization processes utilized to schedule generation and load within RTOs is not extended to the coordination across RTOs. Any existing interregional coordination schemes fall short from approximating the system-wide minimum cost dispatch and are mostly limited to the real-time markets, as described in [33] and [5]. Consequently, decisions regarding which generation resources will be running during each hour of the day are largely made without optimizing cross-border transactions.

In 2010, a study performed by ISO New England's external market monitor, valued the cost of the inefficiency of transfers across the New York ISO interface at $200 million a year [43]. Considering that the study was performed for a maximum interchange of 500 MW, and that, for example, the hourly average interchange on the MISO-PJM interface was 2.7 GW in 2019 [44], even a small increase in interchange efficiency could bring considerable savings.

Figure 1.1. ISO/RTO regions[1]

Beyond increasing the economic efficiency of the operation of the transmission network with the current generation mix, improving the coordination across electricity markets constitutes an important step in the improved utilization of renewable resources. A recent report commissioned by US clean energy groups [20] argues for the need of improved inter-regional planning as the generation resource mix moves towards large amounts of wind and solar generation. In [9], the cost of transition to a 100% renewable electric supply is evaluated under various inter-regional coordination scenarios. The paper concludes that a scenario where states implement their emissions reduction plans independently would result in a cost of $135/MWh, versus $73/MWh in a coordinated scenario where a country-wide approach is adopted for the transition to clean

[1] Image from ISO/RTO Council (https://isorto.org/).

electric power, and where considerable new transmission is built to reinforce current inter-regional ties and to interconnect the currently independent regions.

But the construction of large inter-regional transmission infrastructure will not be efficiently utilized unless the investment is accompanied with market structures that allow the transfer of electric power across market regions to respond to economic signals. The current coordination schemes allow for very limited response to economic signals across RTO boundaries.

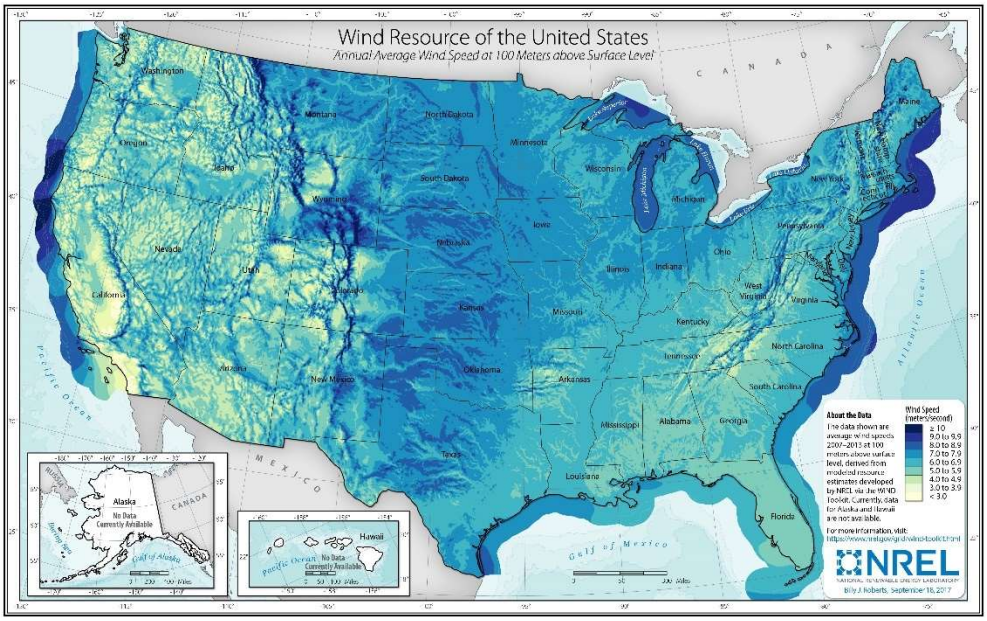

Figure 1.2. Average wind speed map of the US[2]

Figure 1.2 and Figure 1.3 show the geographic distribution of wind and solar generation potential in the US, respectively. As seen in Figure 1.2, onshore wind resources are located far from most demand, and in the case of the Upper Midwest, wind generation must be transported long distances to reach demand in the Eastern part of the country. Solar generation potential is found mostly on the southern part of the country, as shown in Figure 1.3. In order to achieve optimal utilization, power from renewable resources must travel, not only across several RTO regions, but between areas with centrally cleared markets and areas where such markets do not yet exist.

[2] https://www.nrel.gov/gis/wind.html

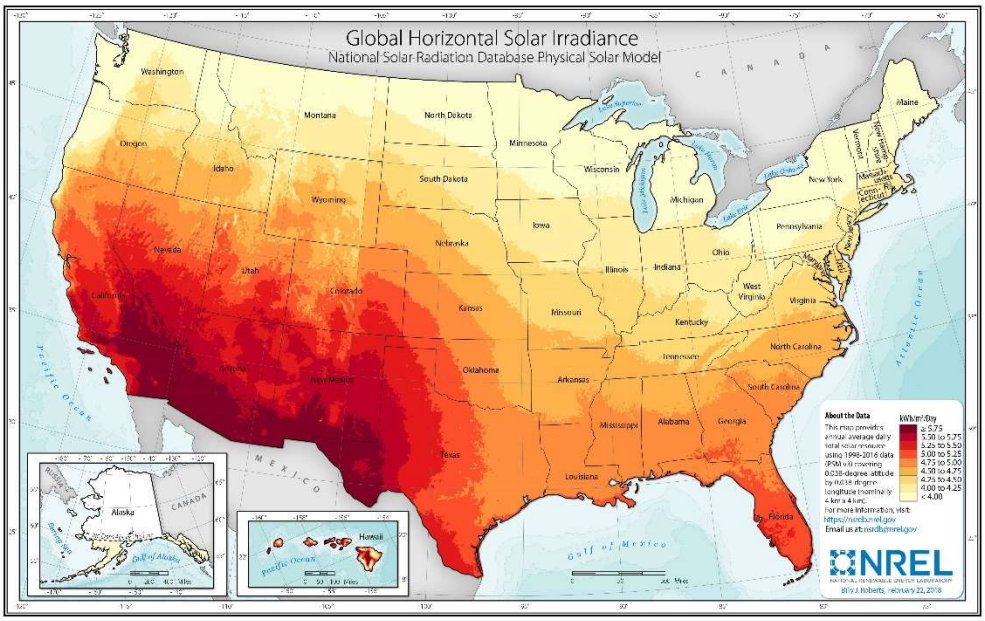

Figure 1.3. Average solar irradiance map of the US[3]

The interregional coordination problem is not unique to the US. There are many other interconnected systems with more than one transmission operator. The various electricity market operators across the European Union, for example, are working towards better interregional coordination with the purpose of optimizing the utilization of transmission interconnections [19]. However, European markets are settled on zonal prices, where a single zone may span an entire national market or a large portion of it (Figure 1.4, obtained from [18]), whereas US RTO markets are settled on nodal or bus-level prices. In the European zonal market, transmission limits that are internal to the bidding zones are not considered in the pricing of electricity. Only transactions across bidding zones are limited by transmission constraints. In this work, we assume the entire transmission system is modeled by the market operator during the day-ahead market process in such a way that internal transmission constraints are enforced, and prices are calculated at a nodal level. While this is not the case in a zonal market, the formulation presented throughout this work can be adapted to a zonal model.

[3] https://www.nrel.gov/gis/solar.html

Figure 1.4. Bidding zone configuration in Europe as of September 2020 [18]

1.1 Current state of inter-regional coordination

US RTOs operate two-settlement markets that include a day-ahead and a real-time market. The day-ahead market receives bids and offers for the next day and determines, for each hourly interval, which generation units will be online and what will be their output level (or the power consumption of price-sensitive load). The day-ahead market produces forward prices for energy at every node in the system. The real-time market makes adjustments to the day-ahead schedules based on operating conditions, usually every five minutes, based on real-time bids and offers

submitted by participating generators and price-sensitive load. Additional detail regarding the clearing process of the day-ahead and real-time market is presented in sections 2.2, 2.3 and 2.4.

When more than one RTO operates on an interconnected transmission system, the flow through some transmission elements, especially those close to the boundary, will be driven by generation and load residing in several markets. To avoid overloading those facilities, some coordination must exist among RTOs. The most basic level of coordination, illustrated in Figure 1.5 (a), consists of splitting the transmission capacity of shared facilities prior to the market clearing calculations. This makes sure that no overloads occur, but may result in sub-utilization of transmission, where one area does not use the entirety of its share while the other could reduce costs by taking over the unused transmission capacity.

Most transmission operators do pre-allocate the capacity of shared transmission facilities by identifying facilities that are largely impacted by transactions in more than one area as reciprocal coordinated flowgates (RCFs) and managing congestion on those facilities using procedures defined by the North American Electric Reliability Corporation (NERC) [39].

In most RTOs, however, coordination occurs past the initial transmission share allocation. Figure 1.5 (b) illustrates market-to-market (M2M) procedures, where the capacity of shared constraints is re-allocated between real-time market intervals [33]. In M2M procedures, transmission capacity of overloaded RCFs is moved from one RTO to the other based on the value that each region assigns to the scarce transmission capacity. To achieve this goal, capacity is allocated based on the shadow price of the RCF constraint in the real-time economic dispatch (details of this optimization are presented in section 2.4) on both markets. A M2M settlement is needed after the fact to compensate the region that cedes part of its pre-allocated transmission capacity.

More recently, some RTOs have implemented Coordinated Transaction Scheduling (CTS), illustrated in Figure 1.5 (c), which does not directly re-allocate transmission capacity, but auctions import and export capacity available after the day-ahead market clears. Low participation in CTS has been tied to transaction fees and to the fact that it relies on RTO forecasts of real-time prices at the boundary, which are often inaccurate [44].

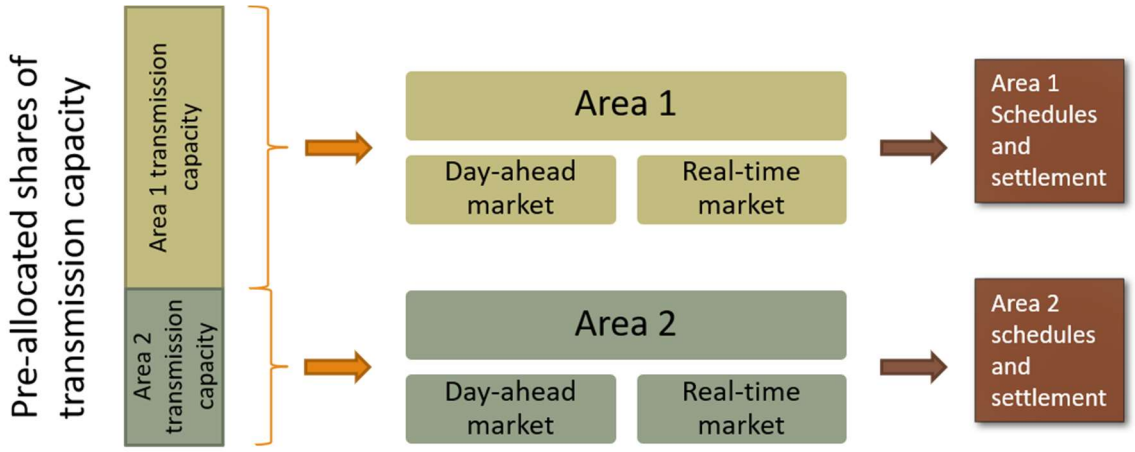

(a)

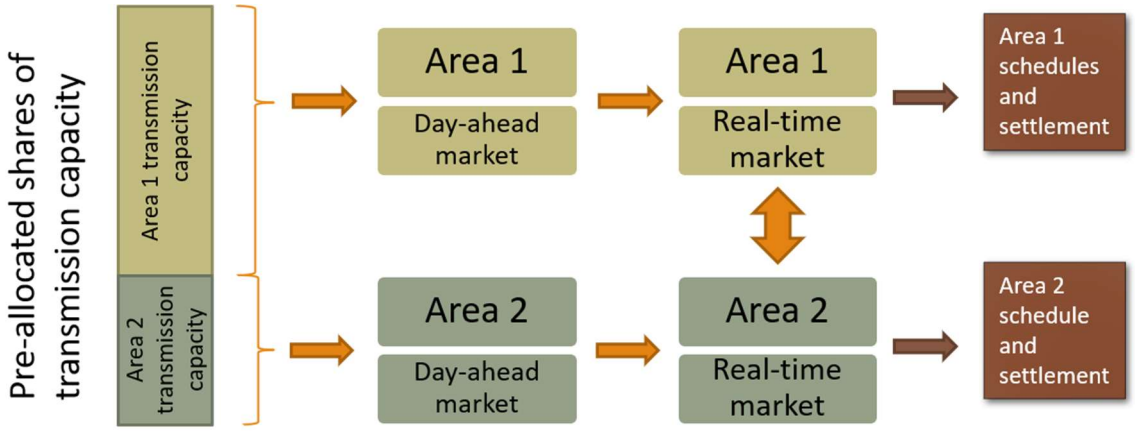

(b)

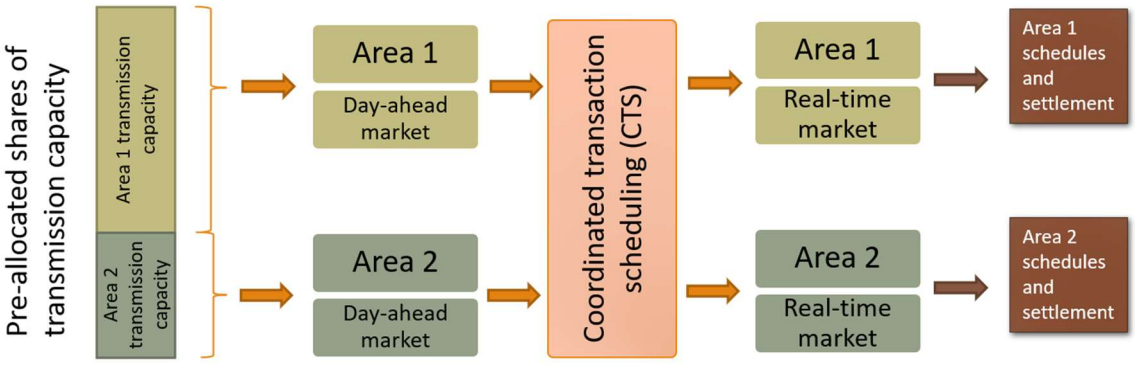

(c)

Figure 1.5. Existing inter-regional coordination schemes

Notwithstanding the existing inter-regional coordination schemes, inter-regional schedules often flow in uneconomic fashion, moving power from a high-priced area to a lower-priced area. Table 1.1 shows the information presented in the PJM State of the Market Report [2] that summarizes the number of hours during which the direction of real-time flows were inconsistent with real-time LMPs during the first nine months of 2020.

Table 1.1. Uneconomic inter-regional transactions Q1-Q3 2020 (PJM) [43]

Interface	Percentage of hours with real-time flow inconsistent with interface prices
MISO	32.70%
NYISO	50.50%
Neptune underwater transmission (NYISO)	33.20%
Linden variable frequency transformer (NYISO)	41.70%
Hudson DC line (NYISO)	52.50%

Cross-border transactions are often uneconomic because the current market design does not offer a practical way for market participants to submit price-sensitive cross-border transaction requests. CTS, which is a market from cross-border transactions that is separate from the day-ahead and real-time markets, runs within the real-time market timeframe and allows for price-sensitive transaction scheduling that is not based on actual prices, but on ISO estimates of real-time prices at the interface that are often incorrect.

1.2 Proposed inter-regional coordination approach

None of the existing coordination processes optimize the use of shared transmission capacity in the day-ahead market. Both M2M and CTS are real-time market processes. As such, decisions regarding which generators will be online are made without taking external transactions into account. This means that each region must meet its capacity requirements without consideration of external available resources. This may result in higher overall costs, and hinders the ability of generators to serve as capacity resources in external markets.

Naturally, optimal utilization of transmission and generation could be achieved by integrating the entire interconnected transmission system into a single market. However, moving to a single market is unlikely, since RTOs have functions that go well beyond market operations,

have a wide range of rules and market processes, and respond to different regulatory entities. Furthermore, to fully utilize the capacity of the transmission system, effective coordination schemes are not only needed across RTO regions, but also across RTO and non-RTO regions. Recognizing that, we propose a distributed unit commitment and dispatch approach that allows regions to retain their market rules, clearing and pricing algorithms, and settlement processes.

A multi-regional, day-ahead clearing process requires a distributed solution of the unit commitment (UC) problem, which is challenging. But given the large potential savings, it is worth considering solutions that may require increased computational capabilities and harmonization of the daily bidding and market clearing timelines across RTOs. In addition to improving the efficiency of transmission utilization, effective market-based congestion management across RTO borders would facilitate the investment on new energy sources delivered across regional markets by enabling cross-border capacity contracts and congestion management products. It would also provide price signals that highlight the best candidate locations for investment in new transmission.

In this work, we propose the use of a distributed optimization algorithm based on the alternating directions method of multipliers (ADMM) in [8]. ADMM has been applied to the unit commitment problems in [17], but the solution methods proposed there did not reach a feasible solution for our test cases. The algorithm we propose applies an approach developed from the one presented in [48] for the distributed solution of nonconvex optimization problems, taking advantage of the specific structure of the market clearing calculations.

The day-ahead clearing algorithm developed in this work simultaneously schedules price-sensitive cross-border transactions and determines the commitment and dispatch of generation and load. This allows for generation to be committed in one region to serve load or meet reserves requirements in another, when that is the least cost solution and meets system-wide transmission and operational constraints. Therefore, transactions across regional borders are automatically scheduled when economic.

Based on the test cases studied, the minimum savings achieved by applying the proposed algorithm instead of the current uncoordinated day-ahead clearing process were of 3.2% of the total cost, which in terms of the cost of electric power generation in the US represents approximately $7 billion per year.

Most of the previously proposed inter-regional coordination algorithms that address the operation of interconnected electric transmission systems with market-based congestion

management mechanisms stop short of offering a solution that tackles the unit commitment problem, precluding the full extension of the coordination into the day-ahead market clearing process where the large majority of the generation schedules are determined.

Under the existing inter-regional coordination schemes, there is usually a gap between the interface day-ahead prices as calculated by neighboring RTOs. This issue is replicated in the representation of the current price calculation shown within the simulation results in section 0. As discussed in detail in Chapter 5, this price gap results in market participants being unable to hedge their exposure to price variability on transactions across markets. The proposed coordinated solution eliminates the interface price gap.

In addition to a coordinated day-ahead market solution, we propose a coordinated auction for financial transmission rights (FTR) that allows for market participants to seamlessly procure the financial instruments required to hedge their exposure to price variability on cross-border transactions in the day-ahead market. While interest on these cross-border hedging instruments has existed in organized electricity markets for some time[4], to our knowledge no viable market design has been proposed to date.

The rest of the dissertation is organized as follows. Chapter 2 provides a description of the operation of RTO markets and the general formulation of the optimization models used in the market clearing processes. Chapter 3 presents the proposed design of a coordinated day-ahead market clearing process that relies on a distributed solution of the market clearing calculations using ADMM. A heuristic variation of ADMM for nonconvex problems is applied to the multi-area market clearing process. Simulation results that compare the application of the proposed multi-area solution algorithm to the single-area solution and to a representation of the existing uncoordinated multi-area solution. Chapter 4 addresses an important extension of the coordination across electricity markets by proposing a multi-area auction for financial transmission rights (FTRs). FTRs are financial instruments that play an important role in the implementation of market-based congestion management, as they allow transmission customers to reduce the risk associated with variable locational prices in RTO markets. Such risk is difficult to manage for transactions that span more than one RTO region without the availability of cross-border FTRs.

[4] Discussions in the MISO-PJM joint and common market initiative from August 2005 included discussions of coordinated auctions that never materialized (https://www.miso-pjm.com/working-groups/~/media/pjm-jointcommon/stakeholders-group/20050825/20050825-item-04a-cross-border-ftr.ashx).

Chapter 4 proposes a multi-regional FTR auction design that applies the distributed optimization methods from Chapter 3 to the auction clearing process. Chapter 5 addresses revenue adequacy and wealth transfer issues associated with the implementation of coordinated market clearing processes. In the same way that M2M procedures require payments to address transmission capacity sharing and revenue adequacy, we explore the settlement implications of optimizing the use of transmission capacity in FTR and day-ahead markets.

1.3 Literature review

Multi-area formulations of the economic dispatch problem have been proposed with the purpose of either improving computational performance through parallel calculations or allowing separate sub-regions to perform their own clearing calculations with limited information sharing while approaching the optimal solution at a regional level.

In [29], a method for a parallel solution to the optimal power flow (OPF) problem is presented. This paper predates RTOs and market-based congestion management. The authors highlight the method's applicability to interconnected systems where several utilities operate, where instead of a centralized dispatch calculation, each utility can calculate its own dispatch without explicit modeling of external networks or large amounts of information exchange; thereby, allowing different sub-regional rules and requiring minimal modification to each utility's economic dispatch algorithms. Other benefits of the distributed approach are cited in the paper, such as avoiding communications bottlenecks and reliability issues associated with a centralized dispatch center and anti-trust prohibitions against pooling of multi-utility data.

Since the publication of [29], many utilities have moved to a centralized dispatch performed by an ISO, with adequate communications infrastructure and geographically spread backup control centers. Throughout this work the interest in distributed OPF solutions focuses instead on coordination across ISO regions, which still requires limited external network modeling and information exchange and must also allow for a diverse set of market clearing rules.

The scenario modeled in [29] has each utility model its service area and buses shared with other utilities. Dummy generators are used at the border buses to mimic the effect of the external systems. The proposed regional decomposition relies on a linearized augmented Lagrangian approach to relax coupling constraints to improve convergence with respect to standard Lagrangian relaxation approaches.

A multi-area decomposition framework is also presented in [13], using a linearized economic dispatch algorithm that allows each area to perform its dispatch calculations independently. The authors cite cross-country coordination cases like the Central American integration project as potentially benefiting from the proposed approach. The algorithm is based on the Lagrangian relaxation decomposition. The parallel solution relies on the introduction of fictitious buses at the points of interconnection.

Lagrangian relaxation decomposition is also applied to the OPF problem in [50], [41] and [21] for the multi-area problem associated with separate regional transmission operators. In [30] various distributed versions of the distributed OPF problem were tested on a large system representing the Texas transmission network.

More recently, with the goal of allowing cross-ISO market coordination, a marginal equivalent decomposition that relies on exchange of marginal generation and binding constraint information is presented in [55], where convergence is proven for a sequential solution of the multi-area economic dispatch linear program. In [22], an algorithm based on multi-parametric programming is utilized to solve the economic dispatch problem with tie-line scheduling for the deterministic case, and proposes a technique that alternately uses the algorithm for the deterministic variant and a mixed-integer linear program to solve the robust problem that includes demand uncertainty.

A coordinated dispatch framework that optimizes the transaction amounts across ISOs was presented in [5]. This framework is derived from the decomposition of the single economic dispatch calculation into a hierarchical optimization with multiple area subproblems where the interchange amounts and the allocation of shared transmission capacity are linking variables. This approach addresses practical concerns by explicitly modeling transactions across regions and discussing the selection of the proxy bus (or bus aggregate) that represents the injection and withdrawal location for cross-border transactions. However, the proposed coordinated dispatch applies only to the real-time market, as there is no coordination in the unit commitment stage.

The results obtained in [5] served as basis for the Coordinated Transaction Scheduling (CTS) process implemented between several of the Eastern ISOs. CTS attempts to schedule cross-border transactions in a price-sensitive manner based on a priori price estimates[5] of real-time prices. The

[5] http://www.jointandcommon.com/-/media/committees-groups/stakeholder-meetings/pjm-miso-joint-common/20170822/20170822-item-03-coordinated-transaction-scheduling-update.ashx?la=en

dependence of CTS on the accuracy of ISO-generated estimates of real-time interface prices has proven to be a considerable implementation challenge [44] as it often results in cross-border transactions being scheduled in an uneconomic fashion based on actual real-time prices. No instance of cross-ISO coordination clears cross-border transactions and internal generation and load simultaneously.

While, as discussed, distributed solutions to the economic dispatch problem have been widely explored, multi-regional implementation of the unit commitment problem presents challenges associated with the binary nature of the commitment decision variables. Some approaches have been proposed, such as allowing generators to self-commit in a power pool setting [14], or applying heuristic methods to a simplified multi-regional commitment algorithm that does not enforce all transmission constraints [24], but enforces instead a limited set of tie-line and interchange limits [42].

In [17], the multi-regional DC unit commitment problem is solved using a heuristic extension of the alternating directions method of multipliers (ADMM) that attempts to overcome the oscillations and traps in local optima resulting from the nonconvexity of the unit commitment problem. When attempting to apply the algorithms proposed in [17] to the test cases developed for this dissertation, the direct application of ADMM to the unit commitment problem never resulted in solutions where multi-regional boundary conditions matched across the individual regional solutions. For the same test cases, the relaxation of binary variables proposed as an alternative initial step in resulted in [17], resulted in unit commitment solutions that did not lead to feasible economic dispatch solutions.

As an alternative to applying ADMM to the unit commitment problem in the manner described in [17], the semidefinite programming relaxation for the unit commitment problem proposed in [4] and [16] was used in order to apply ADMM to the relaxed unit commitment problem. The result was very similar to what was found by simply relaxing the binary constraints in the unit commitment, and generally yielded a coordinated solution that was infeasible with respect to the operational characteristics of generators.

ADMM was applied to the solution of a small unit commitment test case by using the formulation presented in [6] that, by adding a penalty term to the objective function, creates a locally convex problem that preserves the separable structure of the original problem. While this

approach did yield a solution for the small five-bus test case, the solution times even for the small case made the application of this algorithm impractical for larger problems.

A multi-regional unit commitment formulation based on a DC power flow is also presented in [3], in this case for unit scheduling under uncertain wind generation output. The multi-regional problem is also solved through an augmented Lagrangian relaxation approach, using the alternative problem principle (APP) instead of ADMM, claiming better convergence characteristics for non-convex problems. The algorithm presented requires sequential solution of each area unit commitment problem, but indicates that the use of techniques proposed in [13] would allow for parallel area solutions.

More recently, the Power Systems Engineering Research Center (PSERC) issued the final report of a research project including various topics aimed at approximating seamless inter-regional market operations [7]. The report recognizes the current inefficiencies in the coordination across interconnected electricity markets and the rising importance of such coordination as we face increased penetration of renewable generation. Work included within this research project proposes an algorithm for multi-area economic dispatch that uses a primal decomposition methods, allows for coordinated dispatch and does not require regional coordinators to share information beyond the state of boundary buses [25], but does not extend the coordinated solution to the unit commitment stage. Stochastic optimization is applied to the to the scheduling of tie-line flows and the multi-area solution of the economic dispatch problem in [28] and [27] to address the uncertainty around available renewable resources and demand. The same challenges associated with the increased impact of the intermittent nature of wind generation are tackled using robust optimization techniques applied to tie-line scheduling in [23]. Part of the research project addresses issues potentially leading to low participation in the CTS markets by proposing a generalized design that tackles the issue of limited transaction points [24] and analyzing the operation of CTS markets using game-theoretical models [40]. Instead of proposing incremental improvements to CTS, the coordinated market clearing algorithms proposed in this dissertation would eliminate the need for a separate market for cross-border transactions, as well as the need for an often-inaccurate selection of transaction points to represent cross-border power flow.

2. WHOLESALE ELECTRICITY MARKETS

This chapter introduces various concepts associated with the operation of power systems and US wholesale electric power markets. It first describes the electric power system and provides some historical context to the introduction of market-based congestion management in the US. The two-settlement market construct is described, and the detailed formulation of the market clearing optimization processes utilized throughout the dissertation is presented in 2.3 and 2.4. Section 2.4.1 provides a definition of locational marginal prices using a linear power flow formulation.

2.1 The electric power system

Generally speaking, the system that generates and transports electric power has three components, as summarized below and illustrated in Figure 2.1:

1. Generation: the set of devices that produce electric power from other sources such as fossil fuels, nuclear fuels, solar radiation, movement of water or wind, geothermal energy, etc.
2. Transmission: the set of wires, towers, transformers, breakers, DC lines and converters, protection equipment and other devices that transport electric power at high voltage (usually 100 kV and above) over long distances.
3. Distribution: the set of wires, poles, underground cables, transformers, and other devices that transport electric power at lower voltages from the delivery location of the transmission system to the end user.

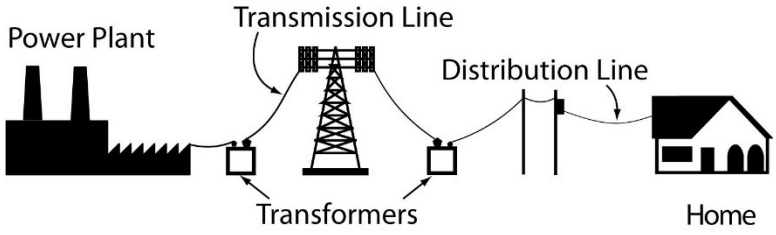

Figure 2.1. Components of the electric power system[6]

[6] Figure retrieved from the graphic library on the National Energy Education Development Project website (https://www.need.org/educators/).

Historically, the transmission system was built by vertically integrated utilities with the purpose of transporting energy from their owned generators, often located based on the availability of resources (hydro power, coal), to towns and cities they served. Competition in the electric power generation was first introduced by the Public Utilities Regulatory Policies Act (PURPA) of 1978, eventually leading to FERC Order 888, which promoted competition through non-discriminatory access to the high voltage transmission system and, with FERC Order 2000, the establishment of RTOs that manage congestion of the transmission system through market-based mechanisms. RTOs manage congestion of the transmission system by issuing operating instructions to power plants and price-sensitive load, aggregated at the point of delivery of the transmission system. The distribution system is outside the control of RTOs.

Within each ISO/RTO, the mandated market-based congestion management was implemented using locational marginal prices (LMPs) that are derived from a centrally cleared market. LMPs are a byproduct within the economic dispatch calculations. Details on the formulation of the economic dispatch problem and the calculation of LMPs are provided in section 2.4.1. The use of LMPs to price energy in electricity markets was first proposed by Schweppe et al. in [47]. The concept was further developed for its application in the operation of transmission networks, as presented in [11].

Prior to the implementation of LMP-based congestion management, overloads in the transmission system were addressed by curtailing transactions based on the impact they had on the overloaded facility and on the quality of the reserved transmission service. In general, however, the purchase of transmission service constituted a guarantee of physical access to the transmission system for load serving entities to deliver their owned or contracted generation to their load. With the implementation of RTO markets, transmission customers no longer had the same guaranteed transmission service, potentially exposing them to highly variable LMPs. In [26], Hogan introduced the concept of contract networks for transmission, which make holders of transmission rights financially indifferent to purchasing power at the LMP at the delivery location versus purchasing contracted generation at its location and paying loss charges from the generator location to the delivery point. These long-term[7] rights have been adopted in every US RTO under a variety of names. Throughout this work we refer to them as Financial Transmission Rights (FTRs).

[7] Usually granted or sold as monthly and yearly products.

2.2 The two-settlement market clearing

Market operators perform a series of optimization processes that generate dispatch instructions and price signals to deploy generation and demand-side management resources in the economically optimal manner, while avoiding violation of the physical limitations of transmission and generation facilities. US RTO markets run a two-settlement process that includes day-ahead and real-time markets. The day-ahead market is cleared based on expected conditions, issuing hourly schedules to allow sufficient time for operational planning, and generation start-up and shut-down procedures that may take several hours. The real-time or balancing market adjusts dispatch based on actual system conditions, with updated instructions usually issued with a frequency of five minutes or less.

The two-settlement market clearing process used in US wholesale electricity markets largely consists of unit commitment calculations followed by economic dispatch (ED) calculations. The unit commitment is a mixed-integer program that aims to minimize the total cost of serving load and meeting certain ancillary services requirements while maintaining feasibility of the dispatch with respect to the physical limitations of generation and transmission facilities. Equations (2.1) and (2.3) present a high-level formulation of the unit commitment problem, with additional detail of the formulation provided in section 2.3.

The economic dispatch calculations optimize the dispatch for a given generation commitment state. A high-level representation of the economic dispatch problem is shown in (2.2), with the detailed formulation used throughout this work shown in section 2.4. Locational Marginal Prices (LMPs) are a byproduct of the economic dispatch solution.

In a two-settlement process the RTO calculates and settles day-ahead and real-time markets. The day-ahead market produces forward prices for electricity and provides commitment instructions for generation units that may require advance notice to start up, either because of the physical limitations of the unit, or to plan for adequate fuel reserves and plant staffing. The real-time market adjusts dispatch instructions as needed due to deviations from planned conditions due to forecast errors, unplanned generation and transmission outages, and other unanticipated circumstances.

RTOs typically run unit commitment and economic dispatch processes that ensure the feasibility of the dispatch with respect to the limits of generation and transmission facilities under normal operating conditions and under a set of considered contingency scenarios.

The unit commitment problem is an optimal power flow that minimizes the total commitment and dispatch cost. A high-level generic formulation of a unit commitment is shown below:

$$\begin{aligned} &\min f(P,u) \\ &\text{s.t.} \\ &\quad g(P,Q,u,V,\theta) \le 0 \\ &\quad h(P,Q,u,V,\theta) = 0 \\ &\quad u \cdot P^{min} \le P \le u \cdot P^{max} \\ &\quad u \cdot Q^{min} \le Q \le u \cdot Q^{max} \\ &\quad u \in \{0,1\}, \end{aligned} \tag{2.1}$$

where the decision variables include P and Q, which are the vectors of real and reactive generator power output, u being the on/off state of each generating unit, and V, θ being the bus voltage magnitudes and phase angles, respectively. The general constraints g and h include nodal power balance equations, flow limits, ancillary service requirements, inter-temporal limits such as minimum run times, minimum down times, and ramp rates.

The economic dispatch is similar to the unit commitment calculation, but the generator statuses are fixed, setting the output of all offline units to zero. The output of online units have continuous feasible ranges between each unit's minimum and maximum limits.

$$\begin{aligned} &\min f(P) \\ &\text{s.t.} \\ &\quad g(P,Q,V,\theta) \le 0 \\ &\quad h(P,Q,V,\theta) = 0 \\ &\quad P^{min} \le P \le P^{max} \\ &\quad Q^{min} \le Q \le Q^{max}. \end{aligned} \tag{2.2}$$

The unit commitment model used in this work utilizes a DC approximation of the power flow equation and a quadratic generator cost model, resulting in a mixed integer program that can be written as:

$$
\begin{aligned}
&\min \frac{1}{2} P^T Q P + c^T P + c_u^T u \\
&\text{Subject to} \\
&A_{eq} \begin{bmatrix} P \\ u \\ \theta \end{bmatrix} - b_{eq} = 0 \\
&A \begin{bmatrix} P \\ u \\ \theta \end{bmatrix} - b \le 0 \\
&u \in \{0,1\} \\
&P^{min} \le P \le P^{max}.
\end{aligned}
\tag{2.3}
$$

Details on equation (2.3) and parameters $Q, c, c_u, A_{eq}, b_{eq}, A$ and b as defined in this work are provided in section 2.3.

2.3 Unit commitment formulation

The formulation of the unit commitment problem used in this work is adapted from [38] and [37]. Reserves requirements and contingency conditions are not explicitly included in this formulation, but their inclusion is a relatively straightforward extension of the formulation below.

$$\min \sum_{g,t} \mathcal{C}_g^{UC}(p_{g,t}, u_{g,t}, v_{g,t}, v_{g,t}^{HS}, w_{g,t}) \tag{2.4}$$

Subject to:

$$u_{g,t} - u_{g,t-1} = v_{g,t} - w_{g,t} \quad \forall t, g \tag{2.5}$$

$$v_{g,t}^H \le \sum_{\tau=t-1}^{\max(1, T_g^{cold} - T_{g,0}^D)} w_{g,t} \tag{2.6}$$

$$\forall t \in [\max(1, T_g^{cold} + T_g^0), TI], g$$

$$v_{g,t}^H \le v_{g,t} \quad \forall t, g \tag{2.7}$$

$$u_{g,t} = 1 \quad \forall t \in [1, T_g^U - T_g^0], g : u_g^0 = 1 \tag{2.8}$$

$$\sum_{\tau=t-T_{min}^U+1}^{t} v_{\tau,g} \le u_{g,t} \quad \forall t \in [T_g^U, TI], g \tag{2.9}$$

$$u_{g,t} = 0 \quad \forall t \in [1, T_g^D + T_g^0], g : u_g^0 = 0 \tag{2.10}$$

$$\sum_{\tau=t-T_{min}^D+1}^{t} w_{\tau,g} \le 1 - u_{g,t} \quad t \in [T_g^D, TI], g \tag{2.11}$$

$$\left.\begin{aligned} p_{g,t} &\le \left(P_g^{max} - P_g^{\min}\right)u_{g,t} - \left(P_g^{max} - P_g^{SU.\max}\right)v_{g,t} \\ p_{g,t} &\le \left(P_g^{max} - P_g^{\min}\right)u_{g,t} - \left(P_g^{max} - P_g^{SD.\max}\right)w_{g,t-1} \end{aligned}\right\} \quad \forall t, g : T_g^U = 1$$

$$\left.\begin{aligned} p_{g,t} \le \left(P_g^{max} - P_g^{\min}\right)u_{g,t} - \left(P_g^{max} - P_g^{SU.\max}\right)v_{g,t} \\ -\left(P_g^{max} - P_g^{SD.\max}\right)w_{g,t-1} \end{aligned}\right\} \quad \forall t, g : T_g^U \ge 2 \tag{2.12}$$

$$-RD_g \le p_{g,t} - p_{g,t-1} \le RU_g \quad \forall t, g \tag{2.13}$$

$$\sum_{g \in \mathcal{G}_i} \left(P_g^{min} u_{g,t} + p_{g,t}\right) - \sum_{j \in \mathcal{N}} B_{ij}\theta_{j,t} = D_i \quad \forall i, t \tag{2.14}$$

$$-F_{ij}^{lim} \le B_{ij}(\theta_{i,t} - \theta_{j,t}) \le F_{ij}^{lim} \quad \forall i, j, t \tag{2.15}$$

$$u_{g,t} \in \{0,1\} \quad \forall t, g \tag{2.16}$$

Indices

$t \in [1, TI]$	Time intervals
$g \in \mathcal{G}$	Generators
$i \in \mathcal{N}, j \in \mathcal{N}$	Buses

Decision variables

$p_{g,t}$	Power output above the minimum for generator *g* and time period *t*.
$u_{g,t}$	Commitment status for generator *g* and time period *t*.
$v_{g,t}$	Startup flag for generator *g* and time period *t*. $v_{g,t} = 1$ indicates that *t* is the first online period after turning on.
$v_{g,t}^H$	Hot startup flag for generator *g* and time period *t*.
$w_{g,t}$	Shut down flag for generator *g* and time period *t*. $w_{g,t} = 1$ indicates that *t* is the last offline period after shutting down.
$\theta_{i,t}$	Voltage phase angle at bus *i*.

Generator cost

C_g^Q	Quadratic cost coefficient for generator *g*
C_g^L	Linear cost coefficient for generator *g*
C_g^{NL}	No-load cost for generator *g* (fixed cost incurred per period when online)
C_g^{SU}	Startup cost for generator *g* (fixed cost incurred on the period when the generator comes online)
C_g^{HS}	Startup cost for generator *g* when it has been offline less than T_g^{cold}
C_g^{SD}	Shut down cost for generator *g* (fixed cost incurred on the last online period before the generator shuts down)

Generator parameters

P_g^{min}	Minimum output (MW)
$P_g^{\max}$	Maximum output (MW)
T_g^U	Minimum up time (intervals)
T_g^D	Minimum down time (intervals)
T_g^{cold}	Cold startup time (intervals)
RU_g	Maximum ramp-up rate (MW/interval)
RD_g	Maximum ramp-down rate (MW/interval)

Transmission system parameters

B	Admittance matrix
F_{ij}^{lim}	Flow limit of the branch connecting buses i and j.
D_i	Demand at bus i.

In this formulation of the unit commitment problem, the total power output of each generator during a particular time interval is:

$$P_{g,t} = P_g^{min} u_{g,t} + p_{g,t} \tag{2.17}$$

The total cost in (2.4) is the sum of the hourly generator commitment and dispatch costs across all generators and time periods. The generation cost is a quadratic function given by

$$\begin{aligned}
&\mathcal{C}_g^{UC}(P_{g,t}, u_{g,t}, v_{g,t}, v_{g,t}^H, w_{g,t}) \\
&= C_g^Q P_{g,t}^2 + C_g^L P_{g,t} + C_g^{NL} u_{g,t} + C_g^{SU} v_{g,t} \\
&\quad + (C_g^{HS} - C_g^{SU}) v_{g,t}^H + C_g^{SD} w_{g,t} \\
&= C_g^Q (p_{g,t} + P_g^{min} u_{g,t})^2 + C_g^L (p_{g,t} + P_g^{min} u_{g,t}) \\
&\quad + C_g^{NL} u_{g,t} + C_g^{SU} v_{g,t} \\
&\quad + (C_g^{HS} - C_g^{SU}) v_{g,t}^H + C_g^{SD} w_{g,t} \\
&= C_g^Q p_{g,t}^2 + (2C_g^Q P_g^{min} + C_g^L) p_{g,t} \\
&\quad + (C_g^Q (P_g^{min})^2 + C_g^L P_g^{min} + C_g^{NL}) u_{g,t} \\
&\quad + C_g^{SU} v_{g,t} \quad + (C_g^{HS} - C_g^{SU}) v_{g,t}^H + C_g^{SD} w_{g,t}
\end{aligned} \tag{2.18}$$

where the cost of the individual generator during a particular time period has three components:

- A quadratic fuel cost function of the form $C_g^Q P_{g,t}^2 + C_g^L P_{g,t} + C_g^{NL}$ that is paid on every period when the unit is online.

- A startup cost, which is a fixed dollar amount assigned to the first period when the unit is online. Two distinct startup costs are used in this case, depending on whether the unit has cooled down at the time of startup. The hot startup cost is lower than the cold startup cost.
- A shut down cost, which is a fixed dollar amount assigned to the las period before the unit shuts down.

The constraints in this formulation enforce the physical limits of generation and transmission facilities:

- (2.5), (2.6) and (2.7) set the startup and shut down flags.
- (2.8) and (2.9) enforce generation minimum running times.
- (2.10) and (2.11) enforce generation minimum down times.
- (2.12) enforces generator output limits, including startup and shut down limits, and sets the output above minimum $p_{g,t}$ to zero when the generator is offline.
- (2.13) enforces generator ramp rates.
- (2.14) represents the power balance equations in a DC power flow model, which is commonly used in US electricity markets [31]. The admittance matrix (B) is an $N \times N$ matrix, where $N = |\mathcal{N}|$. The elements of the admittance matrix are calculated as follows:

$$B_{ij} = -\frac{1}{x_{ij}} \quad \forall i \neq j$$

$$B_{ii} = \sum_{\substack{j \in \mathcal{N} \\ j \neq i}} -\frac{1}{x_{ij}}$$

  where x_{ij} is the reactance of the branch(es) connecting buses *i* and *j*.
- (2.15) enforces branch flow limits in the positive and negative directions. In this model, the assumption is that only branch limits are monitored, therefore the positive and negative limits are the same and all flow constraints are monitored in both directions.

There are some differences between the formulation adopted for the unit commitment in this work and the formulation used by RTOs. In general, RTOs calculate the cost of serving load based on generation offers and not directly using generation cost parameters. Market rules do not allow

generation offers to deviate greatly from their costs, but they are often submitted as convex piecewise linear functions.

Additional constraints not explicitly included in the formulation above are enforced in RTO unit commitment models. Among them:

- RTOs ensure that sufficient generation is committed to meet spinning reserves and regulation requirements. Spinning reserves requirements are met by online generators with unused available capacity. Regulation services are provided by generators that are outfitted with the automatic controls to adjust their output up or down to maintain target voltage levels.
- RTOs ensure that certain fast-start offline generators will be available to provide non-spinning reserves.
- In addition to the branch flow limits, RTOs enforce flow limits on certain groups of branches (flowgates). Flowgates are often defined as a proxy for operational limits, such as voltage stability limits, that cannot be explicitly represented in a DC power flow model.
- RTOs ensure that no transmission limits are violated under a number of contingency conditions. Contingencies represent the failure of a specific element of the transmission system. The unit commitment formulation that ensures that no limit is violated under contingency conditions is referred to as security-constrained unit commitment (SCUC).

The above requirements are included in the unit commitment model as additional linear constraints. Therefore, the unit commitment formulation used throughout this work, while simplified, captures the main features of real-life unit commitment models.

In practice, constraints other than the power balance equations (2.14) are modeled as "soft constraints" in the unit commitment calculations, by adding a penalty term associated with the limit violation to the objective function instead of explicitly enforcing the constraint.

The business practices manuals published by MISO include detailed information of all their market clearing formulations. The complete formulation of the model used in the MISO market clearing software can be found in [36].

2.4 Economic dispatch formulation

The economic dispatch formulation used in the simulated market clearing process is a reduced version of the unit commitment formulation that fixes the value of the commitment variables. The dispatch cost for a generator is calculated as:

$$\mathcal{C}_g^{ED}(P_{g,t}) = C_g^Q P_{g,t}^2 + C_g^L P_{g,t}. \tag{2.19}$$

Constraints (2.12) - (2.15) are enforced by replacing all commitment variables with fixed values. The remaining constraints are not needed for the economic dispatch problem.

2.4.1 Locational marginal prices

In this section, we show the calculation of the LMP and LMP components for a DC economic dispatch problem as presented in [31].

We can write the economic dispatch problem in terms of the output level of online generators $P_{g,t}$ as:

$$\min \sum_{g,t} \mathcal{C}_g^{ED}(P_{g,t}) \tag{2.20}$$

subject to the power balance equations in (2.14), re-written as

$$\sum_{g \in \mathcal{G}_i} P_{g,t} - \left[\xi_{i,t} + D_i\right] = \sum_{j \in \mathcal{N}} B_{ij}\theta_{j,t} \quad \forall i,t \tag{2.21}$$

where $\xi_{i,t}$ are auxiliary parameters associated with each bus and time period. These parameters are set to zero, and used to parametrize the demand increase at each bus in order to derive the locational marginal price (LMP) at the bus.

The cost minimization problem is also subject to flow limits

$$-F_l^{lim} \le B_l(\theta_{i,t} - \theta_{j,t}) \le F_l^{lim} \quad \forall l,t \tag{2.22}$$

where branch $l \in \mathcal{L}$ is a branch from bus i to bus j, $i, j \in \mathcal{N}$.

The minimum and maximum output levels of generators are also enforced for every generator and time period:

$$P_{g,t}^{min} \le P_{g,t} \le P_{g,t}^{max}. \tag{2.23}$$

The Lagrangian of the economic dispatch can be written as:

$$
\begin{aligned}
\mathcal{L} = & \sum_{g,t} \mathcal{C}_g^{ED}(P_{g,t}) \\
& - \sum_{i \in \mathcal{N}} \sum_{t \in [1,TI]} \lambda_{i,t} \left(\sum_{g \in \mathcal{G}_i} P_{g,t} - \sum_{j \in \mathcal{N}} B_{ij} \theta_{j,t} - \left[\xi_{i,t} + D_i \right] \right) \\
& - \sum_{i \in \mathcal{N}} \sum_{t \in [1,TI]} \mu_{l,t}^{+} \left(F_l^{lim} - B_l(\theta_{i,t} - \theta_{j,t}) \right) \\
& - \sum_{i \in \mathcal{N}} \sum_{t \in [1,TI]} \mu_{l,t}^{-} \left(B_l(\theta_{i,t} - \theta_{j,t}) - F_l^{lim} \right) \\
& - \sum_{g \in \mathcal{G}} \sum_{t \in [1,TI]} \omega_{g,t}^{+} \left(P_{g,t}^{max} - P_{g,t} \right) \\
& - \sum_{g \in \mathcal{G}} \sum_{t \in [1,TI]} \omega_{g,t}^{-} \left(P_{g,t} - P_{g,t}^{\min} \right).
\end{aligned}
\tag{2.24}
$$

Assuming the economic dispatch problem has an optimal solution $\mathcal{C}^*(\xi)$, and based on the envelope theorem, the LMP at each bus is calculated as:

$$
LMP_{i,t} = \frac{\partial \mathcal{C}^*(\xi)}{\partial \xi_{i,t}} = \frac{\partial \mathcal{L}}{\partial \xi_{i,t}} = \lambda_{i,t}. \tag{2.25}
$$

The flow constraint can be written in terms of injection sensitivities and net injections as:

$$
-F_l^{lim} \le \sum_{i \in \mathcal{N}} S_{i,t}^{l} \left(\sum_{g \in \mathcal{G}_i} P_{g,t} - \left[\xi_{i,t} + D_i \right] \right) \le F_l^{lim} \tag{2.26}
$$

where $l \in \mathcal{L}$ represents each of the monitored transmission system elements with bidirectional flow limit F_l^{lim} and the flow sensitivity

$$
S_{i,t}^{l} = \frac{df_{l,t}}{dP_{i,t}} \tag{2.27}
$$

is the incremental change in the flow through l ($f_{l,t}$) due to an incremental power injection at bus i and a corresponding withdrawal at the arbitrarily selected reference bus. Details regarding the calculation of flow sensitivities, also referred to as injection shift factors, can be found in [53].

The economic dispatch can be then re-written in a compact form, where the power balance equation is only enforced at a system-wide level and the branch flows are calculated in terms of injection shift factors:

$$
\begin{aligned}
&\min \sum_{g,t} \mathcal{C}_g^{ED}(P_{g,t}) \\
&s.t. \quad \sum_{g\in\mathcal{G}} P_{g,t} - \sum_{i\in\mathcal{N}} \left[\xi_{i,t} + D_i \right] = 0 \quad \forall t \\
&\quad -F_l^{lim} \le \sum_{i\in\mathcal{N}} S_{i,t}^l \left(\sum_{g\in\mathcal{G}_i} P_{g,t} - \left[\xi_{i,t} + D_i \right] \right) \le F_l^{lim} \quad \forall l \in \mathcal{L}, t \\
&\quad P_{g,t}^{min} \le P_{g,t} \le P_{g,t}^{max} \quad \forall g \in \mathcal{G}, t.
\end{aligned}
\tag{2.28}
$$

The Lagrangian for the economic dispatch problem can be re-written based on (2.28):

$$
\begin{aligned}
\mathcal{L} = &\sum_{g,t} \mathcal{C}_g^{ED}(P_{g,t}) \\
&- \sum_{t\in[1,TI]} \lambda_t^0 \left(\sum_{g\in\mathcal{G}} P_{g,t} - \sum_{i\in\mathcal{N}} \left[\xi_{i,t} + D_i \right] \right) \\
&- \sum_{l\in\mathcal{L}} \sum_{t\in[1,TI]} \mu_{l,t}^+ \left(F_l^{lim} - \sum_{i\in\mathcal{N}} S_{i,t}^l \left(\sum_{g\in\mathcal{G}_i} P_{g,t} - \left[\xi_{i,t} + D_i \right] \right) \right) \\
&- \sum_{l\in\mathcal{L}} \sum_{t\in[1,TI]} \mu_{l,t}^- \left(\sum_{i\in\mathcal{N}} S_{i,t}^l \left(\sum_{g\in\mathcal{G}_i} P_{g,t} - \left[\xi_{i,t} + D_i \right] \right) - F_l^{lim} \right) \\
&- \sum_{g\in\mathcal{G}} \sum_{t\in[1,TI]} \omega_{g,t}^+ \left(P_{g,t}^{max} - P_{g,t} \right) \\
&- \sum_{g\in\mathcal{G}} \sum_{t\in[1,TI]} \omega_{g,t}^- \left(P_{g,t} - P_{g,t}^{\min} \right).
\end{aligned}
\tag{2.29}
$$

The LMP at each bus and time period can then be calculated as:

$$
LMP_{i,t} = \frac{\partial \mathcal{C}^*(\xi)}{\partial \xi_{i,t}} = \frac{\partial \mathcal{L}}{\partial \xi_{i,t}} = \lambda_t^0 - \sum_{l\in\mathcal{L}} \mu_{l,t}^+ S_{i,t}^l + \sum_{l\in\mathcal{L}} \mu_{l,t}^- S_{i,t}^l \tag{2.30}
$$

where λ_t^0 is the LMP at the reference bus, also known as the marginal energy component of the LMP, and

$$
\lambda_{i,t}^c = -\sum_{l\in\mathcal{L}} \mu_{l,t}^+ S_{i,t}^l + \sum_{l\in\mathcal{L}} \mu_{l,t}^- S_{i,t}^l \tag{2.31}
$$

is the marginal congestion component of the LMP at bus *i* and time period *t*.

3. A COORDINATED DAY-AHEAD MARKET SOLUTION

This chapter introduces the concept of consensus optimization using the alternating directions method of multipliers (ADMM). It discusses a heuristic extension of ADMM for nonconvex problems and proposes an algorithm that applies such extension to the coordinated solution of the multi-area unit commitment problem. The proposed algorithm is applied to three sets of test cases to demonstrate its effectiveness compared to the ideal, single-area scenario and to a representation of the existing uncoordinated solution.

3.1 Consensus optimization

The alternating directions method of multipliers (ADMM) discussed in [8] is a distributed solution method developed in the 1970s and is well suited for convex optimization problems. The consensus optimization problem can be solved using ADMM in a fully parallelizable manner.

Consider the problem:

$$\begin{aligned} &\min f(x, y_1, ..., y_N) \\ &\text{s.t.} \\ &\quad y_i \in \mathcal{Y}_i \quad i = 1, ..., N \\ &\quad x \in \mathcal{X}. \end{aligned} \tag{3.1}$$

With the introduction of the auxiliary global variable $z \in \mathbb{R}^M$, the objective function in (3.1) can be decomposed into N parts:

$$\begin{aligned} &\min \sum_{i=1}^{N} f_i(x_i, y_i) \\ &\text{s.t.} \\ &\left.\begin{aligned} x_i - z &= 0 \\ y_i &\in \mathcal{Y}_i \\ x &\in \mathcal{X} \end{aligned}\right\} i = 1, ..., N, \end{aligned} \tag{3.2}$$

where $x_i \in \mathbb{R}^M$ are local copies x in (3.1).

An augmented Lagrangian can be constructed for (3.2) in terms of the local variables $x_1, ..., x_N$ and $y_1, ..., y_N$, the global variable z, and the Lagrangian multipliers $\lambda_1, ..., \lambda_N$ as:

$$\mathcal{L}_\rho(x_1,...,x_N,y_1,...,y_N,z,\lambda_1,...,\lambda_N)=\sum_{i=1}^{N}\left(f_i(x_i,y_i)+\lambda_i^T(x_i-z)+(\rho/2)\left\|x_i-z\right\|_2^2\right), \tag{3.3}$$

where $\rho>0$ is the augmented Lagrangian parameter.

The $(k+1)^{\text{th}}$ updates of the ADMM algorithm are:

$$\begin{aligned}
&\left(x_i^{k+1},y_i^{k+1}\right):=\underset{x_i\in\mathcal{X},y_i\in\mathcal{Y}_i}{\operatorname{argmin}}\left(f_i(x_i,y_i)+\lambda_i^{kT}(x_i-z^k)+(\rho/2)\left\|x_i-z^k\right\|_2^2\right)\\
&z^{k+1}:=\frac{1}{N}\sum_{i=1}^{N}\left(x_i^{k+1}+(1/\rho)\lambda_i^k\right)\\
&\lambda_i^{k+1}:=\lambda_i^k+\rho(x_i^{k+1}-z^{k+1}).
\end{aligned} \tag{3.4}$$

With the average over [1, N] for x_i^{k+1} denoted as $\overline{x}^{k+1}$, (3.4) can be re-written as:

$$\begin{aligned}
&x_i^{k+1}:=\underset{x_i\in\mathcal{X},y_i\in\mathcal{Y}_i}{\operatorname{argmin}}\left(f_i(x_i,y_i)+\lambda_i^{kT}(x_i-\overline{x}^k)+(\rho/2)\left\|x_i-\overline{x}^k\right\|_2^2\right)\\
&\lambda_i^{k+1}:=\lambda_i^k+\rho(x_i^{k+1}-\overline{x}^{k+1}).
\end{aligned} \tag{3.5}$$

On the k^{th} iteration, the primal ($r^k\in\mathbb{R}^{MN}$) and dual ($s^k\in\mathbb{R}^M$) residuals are calculated as:

$$\begin{aligned}
&r^k=\begin{bmatrix}r_1^k\\ \vdots\\ r_N^k\end{bmatrix},\ r_i^k=x_i^k-\overline{x}^k\\
&s^k=-\rho\left(\overline{x}^k-\overline{x}^{k-1}\right).
\end{aligned} \tag{3.6}$$

The norm of the residual vectors in (3.6) is used as the stopping criterion for this algorithm.

3.2 Solution approach for the distributed mixed integer quadratic program

In [48], a heuristic method is proposed for the solution of mixed integer quadratic programs. The method used in this work is based on that heuristic approach, with a modified update rule.

To illustrate the proposed method, assume that in the problem stated in (3.2), while the objective function is convex, the feasible regions $\mathcal{X},\mathcal{Y}_i$ are nonconvex.

The optimization problem in (3.7) represents a convex approximation of (3.2):

$$\min \sum_{i=1}^{N} f_i(x_i, y_i)$$

s.t.

$$\left.\begin{array}{l} x_i - z = 0 \\ y_i \in \tilde{\mathcal{Y}}_i \\ x \in \tilde{\mathcal{X}} \end{array}\right\} i = 1,...,N, \tag{3.7}$$

where $\tilde{\mathcal{X}}, \tilde{\mathcal{Y}}_i$ are convex sets.

With each iteration, we solve each subproblem of (3.7):

$$\left(\tilde{x}_i^{k+1}, \tilde{y}_i^{k+1}\right) := \underset{x_i \in \tilde{\mathcal{X}}, y_i \in \tilde{\mathcal{Y}}_i}{\operatorname{argmin}} \left(f_i(x_i, y_i) + \lambda_i^{kT}(x_i - \bar{\tilde{x}}^k) + (\rho/2)\left\| x_i - \bar{\tilde{x}}^k \right\|_2^2 \right). \tag{3.8}$$

On the $k+1^{\text{th}}$ iteration, the solution for each subproblem $i \in [1, N]$ is a projection of $\tilde{x}_i^{k+1}, \tilde{y}_i^{k+1}$ onto the feasible regions $\mathcal{X}, \mathcal{Y}_i$.

$$\begin{aligned} x_i^{k+1} &\in P_{\mathcal{X}}\left(\tilde{x}_i^{k+1}\right), P_{\mathcal{X}}(\cdot): \tilde{\mathcal{X}} \to \mathcal{X} \\ y_i^{k+1} &\in P_{\mathcal{Y}_i}\left(\tilde{y}_i^{k+1}\right), P_{\mathcal{Y}_i}(\cdot): \tilde{\mathcal{Y}}_i \to \mathcal{Y}_i. \end{aligned} \tag{3.9}$$

In general, computing a projection onto a non-convex region is as hard as solving a non-convex optimization problem. Hence, there is no guarantee that the projection of the solution computed from (3.9) will be found at each iteration. For the specific case in which the nonconvexity arises from limiting some variables to integer values, the projections in (3.9), can be as simple as rounding to the nearest integer.

The dual update on the $k+1^{\text{th}}$ iteration is calculated as:

$$\lambda_i^{k+1} := \lambda_i^k + \rho(\tilde{x}_i^{k+1} - \bar{\tilde{x}}^{k+1}). \tag{3.10}$$

Even if projections in (3.9) are found, there is no guarantee that the corresponding objective value will decrease monotonically with each iteration. Two of the features of the solution presented in [48] are incorporated into our unit commitment solution to overcome this problem:

(i) At each iteration, the feasible solution found in (3.9) is compared to the best solution obtained in the previous iterations. If the objective value resulting from the new feasible solution is better than the current best solution, it is saved as the new best solution.

(ii) The algorithm is initialized several times with a set of randomly generated starting points.

3.3 Multi-area unit commitment

3.3.1 Local decision variables

We solve the unit commitment problem from section 2.3 for an interconnected system with several market operators. The set of market operator areas is denoted by $\boldsymbol{a}$.

For the unit commitment problem, the vector of decision variables for each area $a \in \boldsymbol{a}$, x_a is:

$$x_{a,t} = \begin{bmatrix} u_t^a \\ p_t^a \\ v_t^a \\ v_t^{Ha} \\ w_t^a \\ \theta_t^a \end{bmatrix}, t \in [1, TI] \qquad (3.11)$$

$$x_a = \begin{bmatrix} x_{a,1} \\ \vdots \\ x_{a,TI} \end{bmatrix}.$$

In (3.11), u_t^a represents the vector of commitment statuses for time period t, for all generators in area $a \in \boldsymbol{a}$. The same notation is used for all other variables that define the hourly status of generators. Similarly, θ_t^a represents the phase angles for period t of all buses within, or immediately adjacent to, area a. Buses immediately adjacent to a are external to a, but connected directly by a branch to a bus that is internal to a.

The nonconvexity of the unit commitment formulation used in this work arises from the binary nature of all commitment flags (u, v, v^H, and w). Variables v, v^H, and w are fully determined from the value of u; therefore, it is sufficient to enforce $u_{t,g}^a \in \{0,1\} \quad \forall a,t,g$ to make sure all commitment flags take binary values. To solve the convex approximation of the problem in (3.8), we relax this constraint to $u_{t,g}^a \in [0,1] \quad \forall a,t,g$.

3.3.2 Global variables

The consensus variables are the phase angles corresponding to the buses included in more than one area solution and the tie-line flows. A tie-line is a branch (transmission line or transformer)

where the two ends reside in different areas. Those buses connected to either side of any tie-line are shared buses. We denote the set of shared buses:

$$\mathcal{N}^S = \left\{ i : i \in \mathcal{N}^a \cap \mathcal{N}^b \right\} \quad \forall a \neq b, a \in \mathcal{A}, b \in \mathcal{A}. \tag{3.12}$$

The vector of shared variables represented by z in (3.2) is the set of phase angles of all shared buses θ^S and the set of tie line flows F^{TL}.

The vector of shared bus phase angles calculated within the solution of area a is

$$\theta^{S,a} = \left[\theta^a_{i,t} : i \in \mathcal{N}^S \cap \mathcal{N}^a, t \in [1, TI] \right]. \tag{3.13}$$

The consensus value of the shared bus phase angles is calculated, for each area a, as:

$$\begin{aligned} \bar{\theta}^a &= \left[\bar{\theta}^a_{i,t} : i \in \mathcal{N}^S \cap \mathcal{N}^a, t \in [1, TI] \right] \\ \bar{\theta}^a_{i,t} &= \frac{1}{|\mathcal{A}_i|} \sum_{b \in \mathcal{A}_i} \theta^b_{i,t} \quad \forall i \in \mathcal{N}^S \cap \mathcal{N}^a, \end{aligned} \tag{3.14}$$

where $|\mathcal{A}_i|$ is the cardinality of the subset $\mathcal{A}_i \subset \mathcal{A}$. $\mathcal{A}_i$ is the set of all areas that contain bus i.

Note that only those shared buses within or immediately adjacent to an area a are included in the consensus variable vector for a.

Tie lines flows are calculated in the solutions of more than one area. The vector of tie line flows calculated in the subproblem for area a is:

$$F^{TL,a} = \left[B_{ij} \left(\theta^a_{i,t} - \theta^a_{j,t} \right) : i, j \in \mathcal{N}^S \cap \mathcal{N}^a, t \in [1, TI] \right] \tag{3.15}$$

The average value of the tie-line flows is calculated as:

$$\begin{aligned} \bar{F}^a &= \left[\bar{F}_{ij,t} : i, j \in \mathcal{N}^S \cap \mathcal{N}^a, t \in [1, TI] \right] \\ \bar{F}_{ij,t} &= \frac{1}{2} \left(B_{ij} \left(\theta^a_{i,t} - \theta^a_{j,t} \right) + B_{ij} \left(\theta^b_{i,t} - \theta^b_{j,t} \right) \right) \quad i, j \in \mathcal{N}^a \cap \mathcal{N}^b, \forall a, b \in \mathcal{A} \end{aligned} \tag{3.16}$$

3.3.3 Consensus unit commitment

The unit commitment problem described in section 2.3 can be split into subproblems for each area $a \in \mathcal{A}$. For each subproblem, we minimize the total cost of generation within area a:

$$\min \sum_{g \in \mathcal{G}^a} \sum_{t=1}^{TI} \mathcal{C}^{UC}_g (p^a_{g,t}, u^a_{g,t}, v^a_{g,t}, v^{Ha}_{g,t}, w^a_{g,t}) \tag{3.17}$$

subject to constraints (2.5) to (2.16). $\mathcal{C}^{UC}_g(\cdot)$ is a quadratic cost function given in (2.18).

With the vector of decision variables x_a defined in (3.11), (3.17) can be rewritten as:

$$\min_{x_a \in \mathcal{X}_a} \left(\frac{1}{2} x_a^T Q x_a + c_a^T x_a \right). \tag{3.18}$$

The feasible region $\mathcal{X}_a$ for the area subproblem is defined by constraints (2.5) to (2.16), for $t \in [1, TI]$, $i, j \in \mathcal{N}^a$ and $g \in \mathcal{G}^a$. The power balance constraint in (2.14) is only enforced for buses internal to area *a*, not for adjacent buses. Therefore, we rewrite the power balance equation as:

$$\sum_{g \in \mathcal{G}_i} \left(P_g^{min} u_{g,t}^a + p_{g,t}^a \right) - \sum_{j \in \mathcal{N}^a} B_{ij} \theta_{j,t}^a = D_i \quad \forall i \in \mathcal{N}^a, i \notin \mathcal{N}^S, t \in [1, TI]. \tag{3.19}$$

We build a convex approximation of the unit commitment problem by replacing the binary constraint on $u_{g,t}^a$ in (2.16) with:

$$u_{g,t}^a \in [0,1] \quad \forall g \in \mathcal{G}^a, t \in [1, TI]. \tag{3.20}$$

The set of constraints (2.5) to (2.13), (3.19), (2.15) and (3.20) is convex and define the region $\tilde{\mathcal{X}}_a$. The ADMM update of the convex approximation of the unit commitment for area a is:

$$x_a^{k+1} := \underset{x_a \in \tilde{\mathcal{X}}_a}{\operatorname{argmin}} \begin{pmatrix} \frac{1}{2} x_a^T Q_a x_a + c_a^T x_a \\ + \lambda_a^{kT} (\theta^{S,a} - \bar{\theta}^{ak}) + (\rho/2) \left\| \theta^{S,a} - \bar{\theta}^{ak} \right\|_2^2 \\ + \mu_a^{kT} (F^{TL,a} - \bar{F}^{ak}) + (\rho/2) \left\| F^{TL,a} - \bar{F}^{ak} \right\|_2^2 \end{pmatrix}, \tag{3.21}$$

where λ_a^k and μ_a^k are the k^{th} iteration dual variable values associated with the shared bus phase angles and tie-line flows, respectively. The dual update in (3.10) is calculated for the relaxed unit commitment as:

$$\begin{aligned} \lambda_a^{k+1} &:= \lambda_a^k + \rho \left(\theta^{Sa} - \bar{\theta}^{ak} \right) \\ \mu_a^{k+1} &:= \mu_a^k + \rho \left(F^{TLa} - \bar{F}^{ak} \right) \end{aligned} \tag{3.22}$$

At each iteration, the primal residual vector for area *a*, $\varepsilon_{p,a}$, is calculated as:

$$\varepsilon_{p,a}^k := \begin{bmatrix} \theta^{Sa} - \bar{\theta}^{ak} \\ F^{TLa} - \bar{F}^{ak} \end{bmatrix} \tag{3.23}$$

The dual residual vector for area a, $\varepsilon_{d,a}$,is calculated as:

$$\varepsilon_{d,a}^k := \rho \begin{bmatrix} \bar{\theta}^{ak} - \bar{\theta}^{ak-1} \\ \bar{F}^{ak} - \bar{F}^{ak-1} \end{bmatrix} \tag{3.24}$$

The projection of x_a^{k+1} onto the feasible in (3.9) is calculated by selecting a commitment threshold $0 < \xi < 1$ and setting the values of the commitment flag *u* for all generators, periods and areas accordingly. The commitment variables that result from fixing the output of the relaxed unit commitment problem are used as input for an economic dispatch solution. The formulation of the economic dispatch problem corresponds to the one shown in section 2.4.

The generator commitment flag that will be used as an input to the economic dispatch solution, $u_{g,t}^{ED}$, is determined based on the pre-defined commitment threshold:

$$u_{g,t}^{ED} = \begin{cases} 1 & if\ u_{g,t}^{k} \geq \xi \\ 0 & if\ u_{g,t}^{k} < \xi. \end{cases} \tag{3.25}$$

The output of generators with commitment flag $u_{g,t}^{ED} = 0$ will be set to zero in the economic dispatch problem. For the purpose of calculating the total commitment and dispatch costs, the remaining commitment-related variables are calculated from the commitment flag:

$$v_{g,t}^{ED} = \begin{cases} 1 & if\ u_{g,t}^{ED} >^{ED}_{g,t-1} \\ 0 & else \end{cases} \tag{3.26}$$

$$w_{g,t}^{ED} = \begin{cases} 1 & if\ u_{g,t}^{ED} < u_{g,t-1}^{ED} \\ 0 & else \end{cases} \tag{3.27}$$

If for a generator and time interval the startup flag $v_{g,t}^{ED} = 1$ and the number of intervals during which the generator has been offline prior to coming back online is less that the cold start time parameter T_g^{cold} in (2.6), then the hot startup flag $v_{g,t}^{H\,ED} = 1$. Otherwise it is set to zero.

From the resulting fixed set of commitment variables, an economic dispatch calculation is performed to compute the optimal dispatch level for each online generator. The economic dispatch is computed for the multi-area case using a consensus algorithm. Since it is a convex problem, the consensus solution of the economic dispatch should converge towards the optimal solution for the fixed commitment.

The $k+1^{\text{th}}$ ADMM iteration for the consensus economic dispatch problem is:

$$x_a^{ED,k+1} := \underset{x_a^{ED} \in \mathfrak{X}_a^{ED}}{\operatorname{argmin}} \left(\begin{array}{l} \frac{1}{2} x_a^{EDT} Q_a^{ED} x_a^{ED} + c_a^{ED\,T} x_a^{ED} \\ + \lambda_{EDa}^{kT} (\theta_{ED}^{S(a)} - \overline{\theta}_{ED}^{(a)k}) + (\rho_{ED} / 2) \left\| \theta_{ED}^{S(a)} - \overline{\theta}_{ED}^{(a)k} \right\|_2^2 \\ + \mu_{EDa}^{kT} (F_{ED}^{TL(a)} - \overline{F}_{ED}^{(a)k}) + (\rho_{ED} / 2) \left\| F_{ED}^{TL(a)} - \overline{F}_{ED}^{(a)k} \right\|_2^2 \end{array} \right) \tag{3.28}$$

The economic dispatch update in (3.28) is similar to (3.21), but the commitment variables are fixed. The decision variables in the economic dispatch problem for area *a* are:

$$x_a^{ED} = \begin{bmatrix} x_{a,1}^{ED} \\ \vdots \\ x_{a,TI}^{ED} \end{bmatrix} \qquad x_{a,t}^{ED\,T} = \begin{bmatrix} p_{ED\,t}^{(a)} \\ \theta_{ED\,t}^{(a)} \end{bmatrix} \tag{3.29}$$

The global variables in the multi-area economic dispatch problem are the shared buses and tie line flows, defined in the same way they are defined for the unit commitment problem in (3.13) and (3.15). The consensus value of global variables is calculated as shown in (3.14) and (3.16) for the shared bus phase angles and tie-line flows, respectively.

For the area *a* economic dispatch subproblem, the Lagrangian multipliers associated with the constraints that match the local values of shared bus phase angles with the corresponding consensus values are represented by the vector $\lambda_{ED\,a}$. Similarly, the Lagrangian multipliers associated with the constraints that match the local values of tie-line flows with the corresponding consensus values are represented by the vector $\mu_{ED\,a}$. The Lagrangian multiplier updates are calculated as shown in (3.22).

The cost parameters Q_a^{ED} and c_a^{ED} are calculated from the generator quadratic dispatch cost function in (2.19) for all generators in area *a*.

Residual and dual updates for the economic dispatch ADMM solution are calculated as shown in (3.23) and (3.24).

3.3.4 Heuristic multi-area unit commitment algorithm

The multi-area unit commitment solution discussed in the previous sections is presented below as Algorithm 1 and summarized in Figure 3.1. This algorithm achieves a considerable portion of the benefits that could be derived from fully integrating the market operations of neighboring regions, with very limited information sharing. Information shared across regions is limited to shared bus phase angles and tie-line flows. No internal model or bidding information is shared across areas.

The algorithm applies the general approach presented in [48] for the solution of mixed integer programs using ADMM to the distributed solution of the unit commitment problem.

Algorithm 1: Multi-area unit commitment

Step 0: Set simulation parameters: the number of initial conditions generated for the unit commitment (UC) problem (N_{IC}), the maximum number of UC ADMM iterations (N_{UC}), the maximum number of economic dispatch (ED) ADMM iterations (N_{ED}), the commitment threshold $0 < \xi < 1$, the economic dispatch primal and dual tolerances ($\epsilon_{ED}^{p} > 0, \epsilon_{ED}^{d} > 0$)

Step 1: Initialize the best unit commitment solution vector and the best unit commitment cost value by setting $x_{best} = 0$, $C_{best} = \infty$. Set the counter for random initializations of the UC $n=0$.

Step 2: Set $n=n+1$. If n>NIC, STOP and return x_{best}, C_{best}. Otherwise randomly generate initial conditions for x_a^0, λ_a^0 and μ_a^0 for all $a \in \mathcal{A}$. Calculate consensus values for $\bar{\theta}^{a0}$ and $\bar{F}^{a0}$ for all $a \in \mathcal{A}$ using (3.14) and (3.16). Set the UC ADMM iteration counter $k=0$.

Step 3: Set $k=k+1$. If k> N_{UC}, go to Step 2.

Step 4: For each area $a \in \mathcal{A}$, calculate relaxed UC solution from (3.21). Update dual variables from (3.22).

Step 5: Calculate commitment statuses from the relaxed UC solution for all generators $g \in \mathcal{G}$ and all time periods $t \in [0, TI]$ using:

$$u_{g,t}^{ED\,k} := \begin{cases} 0 & if\ u_{g,t}^{k} < \xi \\ 1 & f\ u_{g,t}^{k} \geq \xi. \end{cases}$$

Set all other commitment variables based on $u_{i,t}^{ED\,k}$ using (3.26) and (3.27).

Step 6: Calculate ADMM ED solution with the commitment variables from Step 5 and with $\theta^{0,ED} = \theta^{k}, p^{0,ED} = p^{k}$.

(i) Set $m=0$.

(ii) Set $m=m+1$. If $m>N_{ED}$, stop ED.

(iii) Compute consensus values of shared bus phase angles and tie-line flows from (3.14), (3.16)

(iv) Using (3.28) calculate the ED solution for all areas.

(v) Calculate residuals from (3.23) and (3.24). Stop multi-area ED solution if $\left\| \varepsilon_p^m \right\|_\infty \leq \epsilon_{ED}^{p}$ and $\left\| \varepsilon_d^m \right\|_\infty \leq \epsilon_{ED}^{d}$. Otherwise, go to (ii).

Step 7: Set $x_{best} = x^{ED}$ and $C_{best} = C^{ED}$ if the new solution is feasible and the cost is lower than the current C_{best}.

Step 9: Compute consensus values of shared bus phase angles and tie-line flows for $\bar{\theta}^{a}$ and $\bar{F}^{a}$ for all $a \in \mathcal{A}$ using from (3.14), (3.16). Go to Step 3.

An important difference between the algorithm in [48] and the one presented here is the addition of a distributed convex optimization within each ADMM iteration for the mixed integer program solution. The proposed algorithm contains a nested loop that solves the multi-area economic dispatch problem within every iteration of the multi-area unit commitment problem.

Figure 3.1 highlights the heuristic adjustments implemented to solve the unit commitment problem using ADMM. These adjustments include:

- Solving a convex approximation of the unit commitment by letting the commitment status variables take any value in the [0,1] range. On each iteration, fixing the commitment variables to binary values using a pre-defined commitment threshold.
- With the resulting binary commitment values as input, solving a multi-area economic dispatch using ADMM.
- For each unit commitment solution iteration, saving the current solution as the "best solution" if the economic dispatch solution is feasible and the total commitment and dispatch cost is lower than the cost found in previous iterations.
- Re-initializing the ADMM solution of the convex approximation of the unit commitment problem with randomly generated initial conditions a pre-defined number of times.

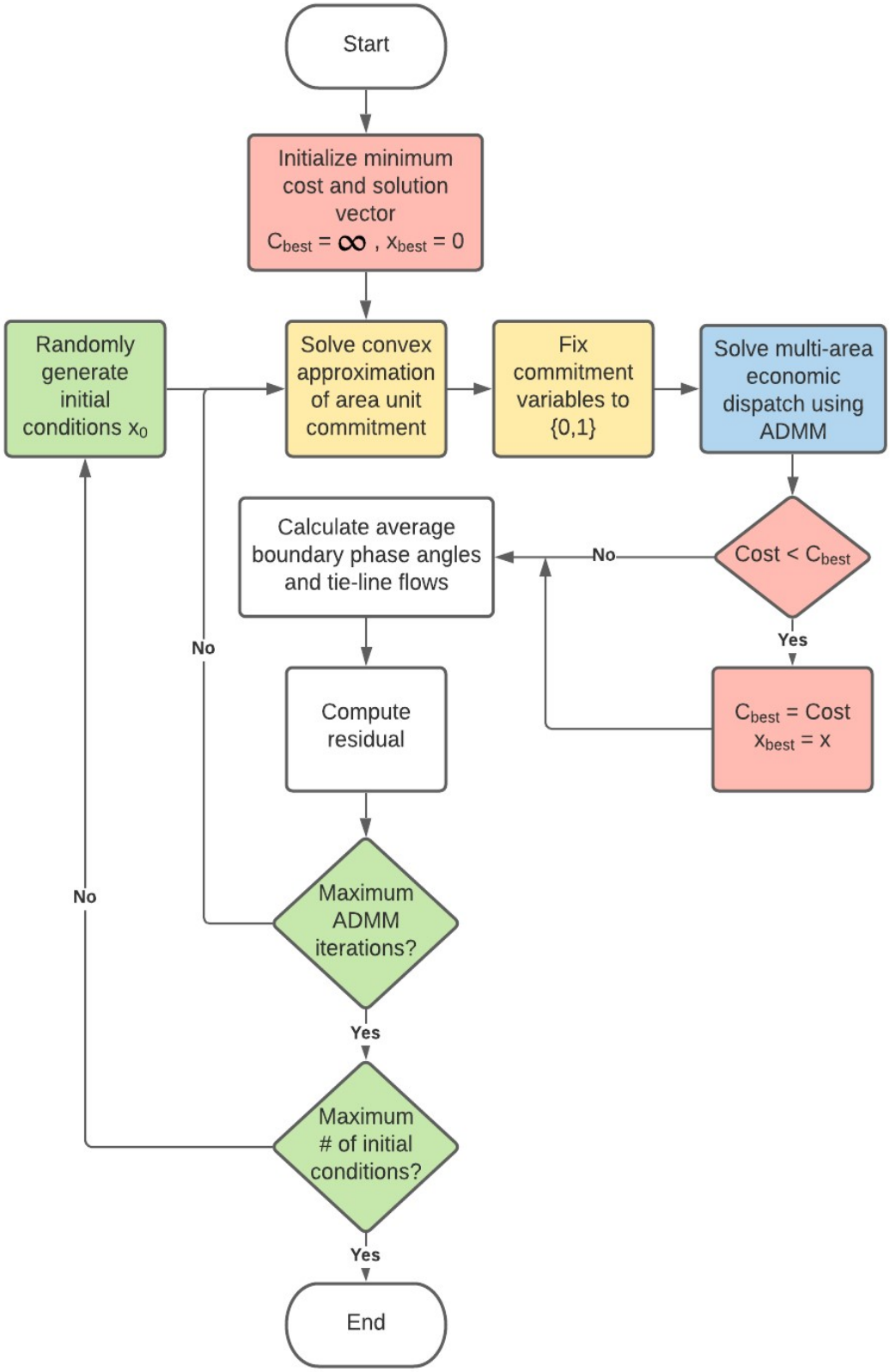

Figure 3.1. Proposed multi-are unit commitment and economic dispatch algorithm

3.4 Simulation cases and results

3.4.1 Test scenarios

To demonstrate the effectiveness of Algorithm 1, we compare its numerical results with two other benchmarking scenarios: joint optimization of all the areas (which we refer to as the single-area model), and uncoordinated optimization.

Single-area model

This represents the unit commitment and economic dispatch results of the entire system modeled as a single area. This model yields the least-cost feasible solution but requires a single market operator to receive bids and offers from all participants and to maintain a model of the entire interconnected transmission system.

Uncoordinated multi-area model

The unit commitment and economic dispatch results are computed separately for each area, with a price-insensitive interchange modeled across pre-defined interfaces. That is, the interchange between areas is modeled by adding fixed energy withdrawal on the buses that represent the interface in the exporting area, and a fixed energy injection at the buses that represent the interface in the importing area. The interfaces are defined as bus aggregates with fixed weights. Additional detail describing the current modeling of inter-regional transactions, which is the basis for the uncoordinated multi-area model, can be found in section 5.3.2.

The interchange amounts in the uncoordinated models are fixed for the 24-hour period.

This model is intended to represent the current coordination methods. While price-sensitive bids and offers may be placed at interchange locations, in practice, the lack of coordination between markets does not guarantee that a transaction to the border in one area will have a corresponding transaction from the border in the other area. Cross border transactions are therefore usually price insensitive. Inter-regional coordination schemes exist in some markets but they are limited to the real-time markets and do not impact day-ahead commitment.

The state of inter-regional coordination and its limitations within the Midcontinent ISO markets is described in the State of the Markets report [44]. The report indicates that external

transactions are overwhelmingly scheduled in a non-price sensitive manner, based on the participant expectation of price differences between markets. Consequently, inter-regional transactions can be uneconomic. Also, it indicates that while some participation in the Coordinated Transaction Scheduling (CTS) process has been observed, it is still a very small fraction of cross-border schedules due mostly to inaccuracy on the interface price forecasts generated by the ISOs that are the basis for the CTS process. As such, the most accurate representation of the current state of day-ahead cross-border schedules is a fixed hourly import or export at each interface, with interfaces defined as fixed aggregates of a number of boundary locations.

Coordinated multi-area model

The unit commitment and economic dispatch results are computed using the distributed algorithm presented in section 3.3.4. Market operators must clear markets in a coordinated fashion but are only required to share a subset of boundary conditions between iterations. Each area can keep bid and offer information private, may have different market rules, and is only required to maintain an accurate model of the internal transmission system and tie-lines.

3.4.2 Test cases

Three transmission network models were used to evaluate the proposed algorithm:

1. A 14-bus, two-area case
2. A 200-bus, three-area case
3. A 500-bus, three-area case

All cases are based on transmission network models obtained from the Texas A&M University electric grid test case repository [49]. All generation cost parameters and inter-temporal constraints were added to the 14-bus case. The 200 and 500 -bus base cases included incremental costs, but no commitment costs and parameters. Commitment costs and constraints were computed for the larger cases from information in [54]. The complete unit commitment model data is included in Appendix A.

3.4.3 System information

Test cases were executed in Matlab R2020b Update 1, calling IBM ILOG CPLEX Optimization Studio version 12.9. They were run on a PC with an Intel Core i7 6560U CPU@2.2GHz, 16 GB RAM and a 64 bit OS.

3.4.4 Simulation parameters

For each case, the ADMM parameters ρ and ρ_{ED} in (3.21) and (3.28), respectively, were selected by evaluating the algorithm performance for a range of parameter values between 0.1 and 100. While reducing simulation times of the ADMM algorithm was not the focus of this work, some approaches for the dynamic selection of ρ_{ED} were explored. While fixed values of ρ_{ED} were used in the final implementation, preliminary results indicate that dynamic parameter setting may improve execution times.

The total number of initializations of the multi-area unit commitment calculation (N_{IC}) was set to $N_{IC} = 4$, so initial conditions are randomly generated four times. All decision variables were initialized using Matlab's built-in random number generator from a uniform distribution, as shown in Table 3.1.

Table 3.1. Random initialization of unit commitment decision variables

Decision variables	Sampled from
Generator status ($u_{g,t}$)	$U(0,1)$
Generator startup ($v_{g,t}$), hot startup ($v_{g,t}^{H}$) and shut down ($w_{g,t}$) flags	$U(0,1)$
Generator output over the minimum ($p_{g,t}$)	$U(0, P_g^{max} - P_g^{min})$
Bus phase angles ($\theta_{i,t}$)	$U(-2\pi, 2\pi)$

For each randomly generated set of initial conditions, *10* ADMM iterations (that is, $N_{UC} = 10$) were completed for the 14 and 200 -bus cases; while for the 500-bus case, $N_{UC} = 12$.

Two approaches for the selection of the commitment threshold ξ in (3.25) were tested: (1) with the parameter set to 0.1 and (2) with the parameter dynamically adjusted. In the dynamic

parameter adjustment, ξ was increased or decreased based on a comparison between the total committed generation and the minimum and maximum system-wide demand, as follows:

1. If the minimum output of committed generation exceeded the minimum demand, ξ was iteratively decreased by 0.01 until the minimum generation output was less or equal to the minimum system-wide demand.
2. If the peak demand exceeded the maximum output of the committed generation, ξ was iteratively increased by 0.01 until the maximum generation output was sufficient to meet the peak demand.

The dynamic selection of the commitment threshold parameter was used for the final simulation.

3.4.5 Simulation results

Table 3.2 shows the 24-hour commitment cost resulting from each scenario and transmission network model.

Table 3.2. Test Case Results

Case	Solution method	Total 24-hour cost (commitment and dispatch)	Execution time (s)
14-bus	Single-area	$ 161,302	0.43
	Uncoordinated	$ 169,269	0.30
	Heuristic multi-area	$ 163,770	120
200-bus	Single-area	$ 454,908	310
	Uncoordinated	$ 699,935	52
	Heuristic multi-area	$ 498,296	3.8×10^3
500-bus	Single-area	$ 1,168,104	3.0×10^3
	Uncoordinated	$ 1,293,572	740
	Heuristic multi-area	$ 1,221,181	15×10^3

Starting from the uncoordinated day-ahead clearing model that represents the current practices, the maximum savings are achieved by clearing the entire system as a single area. For the 14-bus case, the proposed algorithm resulted in a cost reduction of 69% of the savings that

could be achieved by moving to a single-area solution. For the 200 and 500 bus cases, the corresponding cost reductions were 82% and 58%, respectively.

Execution times are noted, highlighting the increased computational burden of the proposed method. The execution times are wall-clock times resulting from running all calculations. For our simulation purposes, area calculations were performed sequentially. While there is room for improvement on the implementation of the proposed algorithm in terms of performance, it is worth noting that increased interregional coordination would certainly require additional computational capabilities.

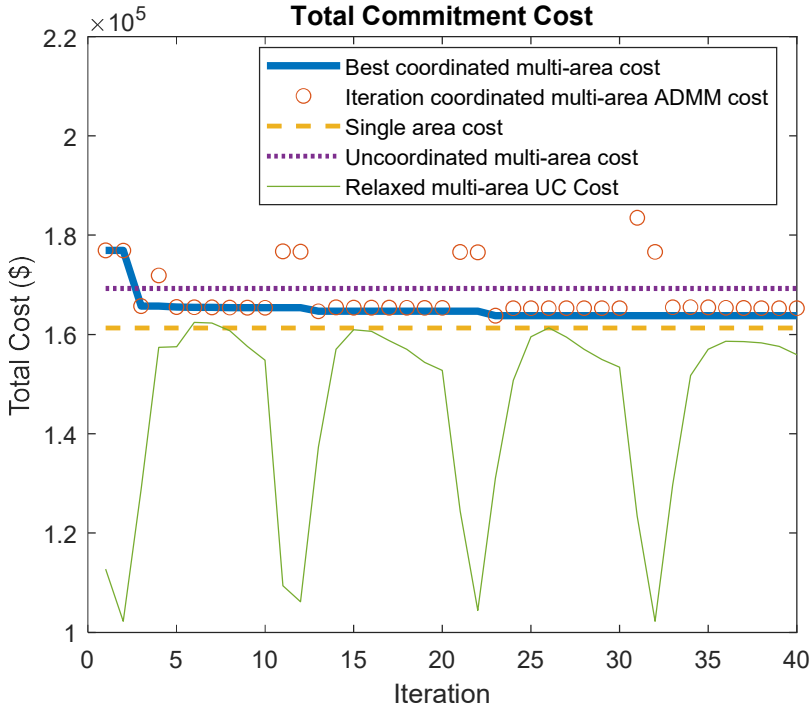

Figure 3.2. Total commitment and dispatch cost comparison for the 14-bus cases

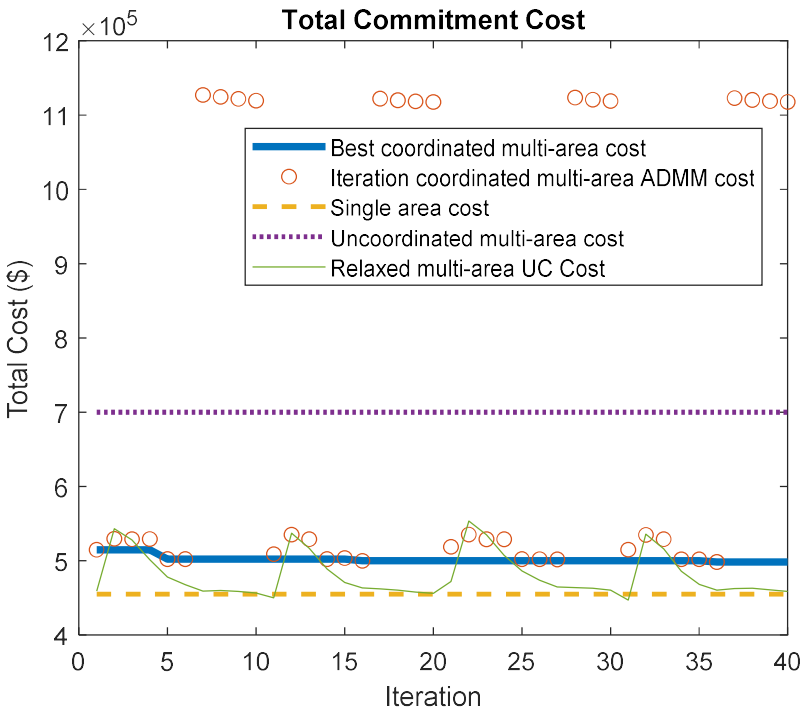

Figure 3.3. Total commitment and dispatch cost comparison for the 200-bus cases

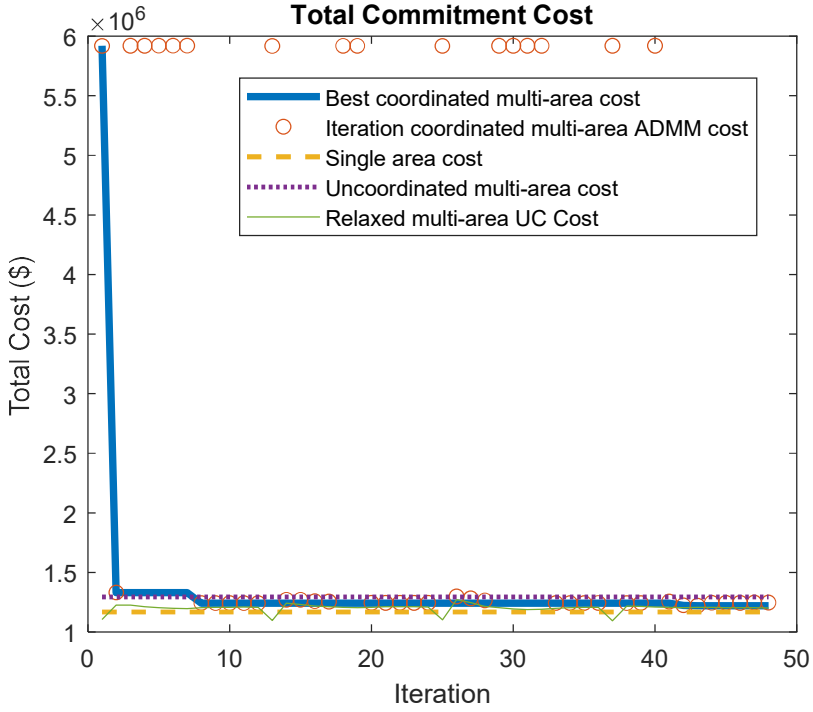

Figure 3.4. Total commitment and dispatch cost comparison for the 500-bus cases

The cost results in each iteration are shown in Figure 3.2, Figure 3.3 and Figure 3.4 for the 14-bus case, the 200-bus case and the 500-bus case, respectively. The total cost corresponding to each ADMM iteration is shown as orange circles. The best cost achieved is retained and shown in the figures as the thick blue line. These values can be compared to the single-area commitment cost in the dashed yellow line and the multi-area uncoordinated cost in the purple dotted line. The uncoordinated multi-area cost represents the current market clearing practices, and the single-area cost should be the lowest; nonetheless, it would require the entire interconnected system to be cleared by a single market operator.

The total cost includes the start-up, shut-down and no-load costs calculated from the projected commitment variable values, plus the dispatch cost in (3.28). In each ADMM iteration of the unit commitment problem, the newly calculated economic dispatch solution replaces the current "best solution" if its associated cost is lower than the best cost, and the corresponding real-time economic dispatch problem is feasible.

In all simulation results, the best multi-area commitment cost was achieved before the last unit commitment ADMM iteration. The experience from test cases indicates that the least-cost relaxed unit commitment solution did not result in the least-cost feasible multi-area economic dispatch solution. This illustrates why one of the algorithms proposed in [17], which completed all ADMM iteration for the convexified unit commitment problem before rounding commitment variable to integer values, did not produce satisfactory results for our test cases.

The very high ADMM costs shown in Figure 3.2, Figure 3.3 and Figure 3.4 are associated with unit commitment solutions for which no feasible multi-area dispatch was found for which boundary conditions across areas match.

Figure 3.5 compares the LMP results from the single-area solution and the multi-area coordinated solution applied to 200-bus case for the 20^{th} hour. While the heuristic multi-area solution did not exactly replicate the single-area results, LMPs do appear to capture the same congestion patterns, creating appropriate price incentives for generators and price-responsive demand to operate in a way that nearly maximizes overall system efficiency. Additionally, the price signals capturing congestion patters across the entire region highlight the location of scarce transmission capacity in a way that may direct optimal investment in transmission capacity.

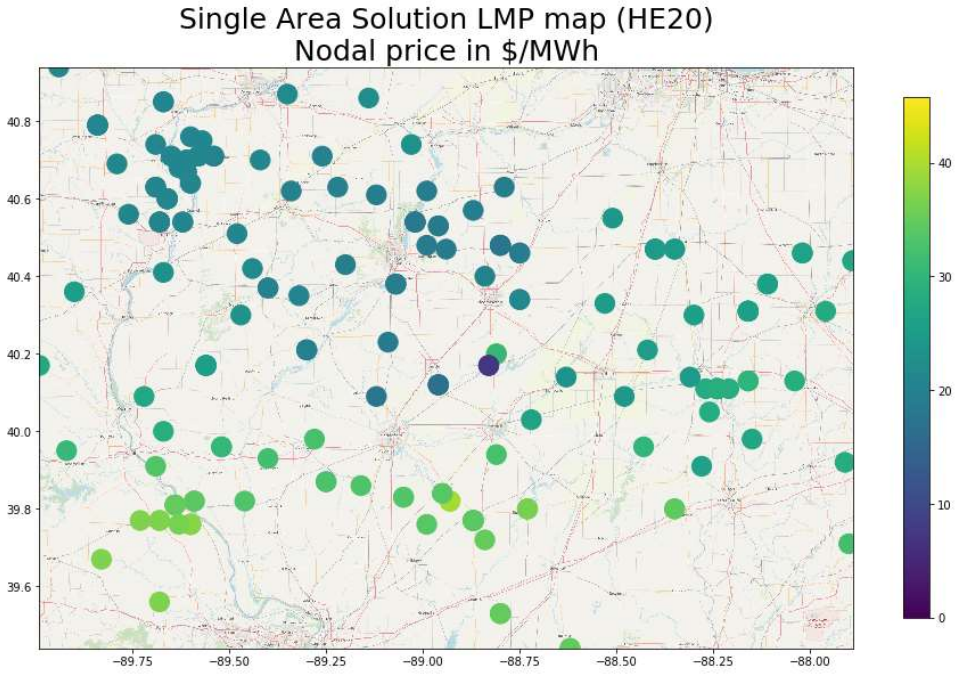

(a)

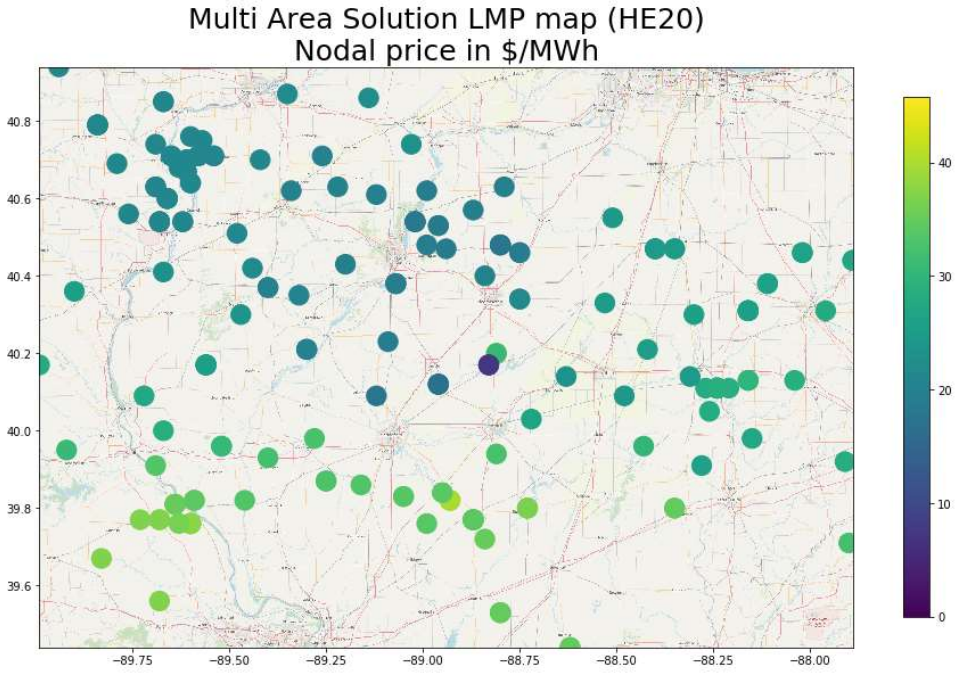

(b)

Figure 3.5. LMP map comparison for the 200-bus case

Figure 3.6 shows LMPs for the same period resulting from the uncoordinated multi-area unit commitment and economic dispatch calculations. The fixed transfer in the uncoordinated case

results in a sub-utilization of the transmission system capacity. Each area has a single, flat LMP. There is a small difference between areas 1 and 2, while prices in area 3 are near zero. This happens because the entirety of area 3 demand in that period is met by renewable resources, which, as shown in appendix A, are modeled as offered into the market with incremental costs of zero dollars per MWh. It is worth noting that because the objective function in the unit commitment problem to minimize includes start-up, shut-down, no-load, and dispatch costs over the 24-hour study period, and the LMPs as computed are driven only by the marginal dispatch cost of generation for the current hour, lower LMPs in one particular hour do not necessarily indicate lower total costs.

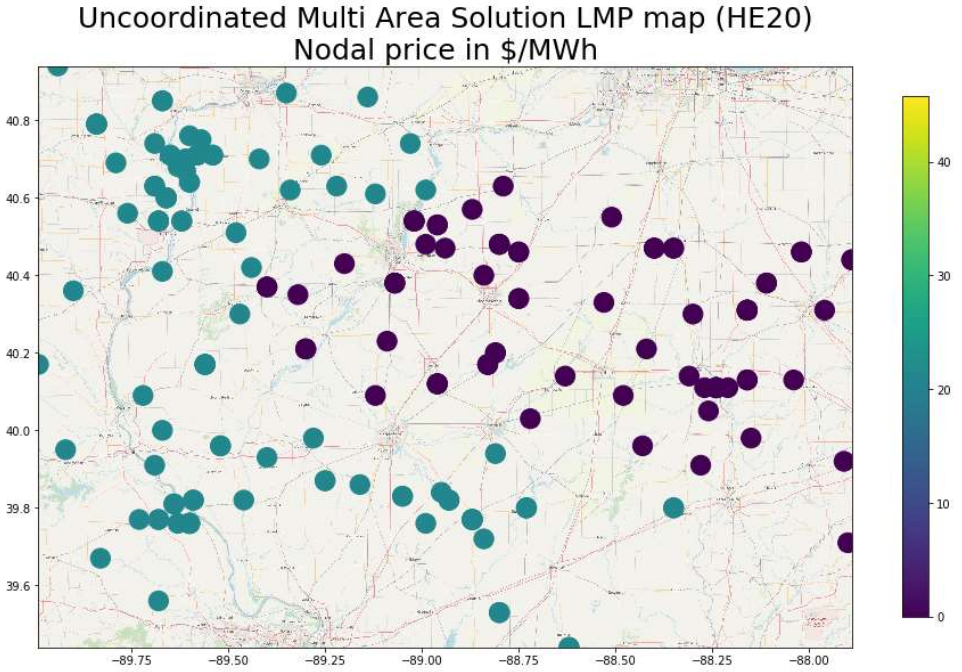

Figure 3.6. LMP map for the uncoordinated multi-area 200-bus case

LMP maps were also generated for the 500-bus case with similar findings. Figure 3.7, Figure 3.8, and Figure 3.9 show the LMPs for a single hour (hour ending 12) for the single area, coordinated and uncoordinated solutions, respectively. In this case it can also be observed that the ideal single area solution and the coordinated solution computed using the proposed algorithm result in similar congestion patterns, while the uncoordinated solution retains considerable price separation between areas due to the under-utilization of transmission capacity.

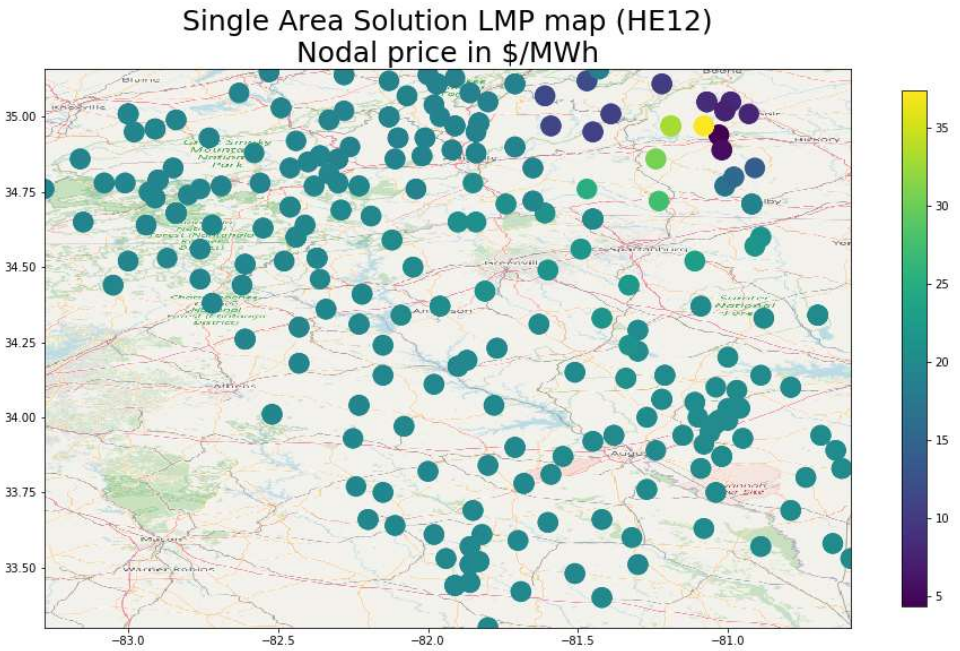

Figure 3.7. LMP map for the 500-bus case (single area solution)

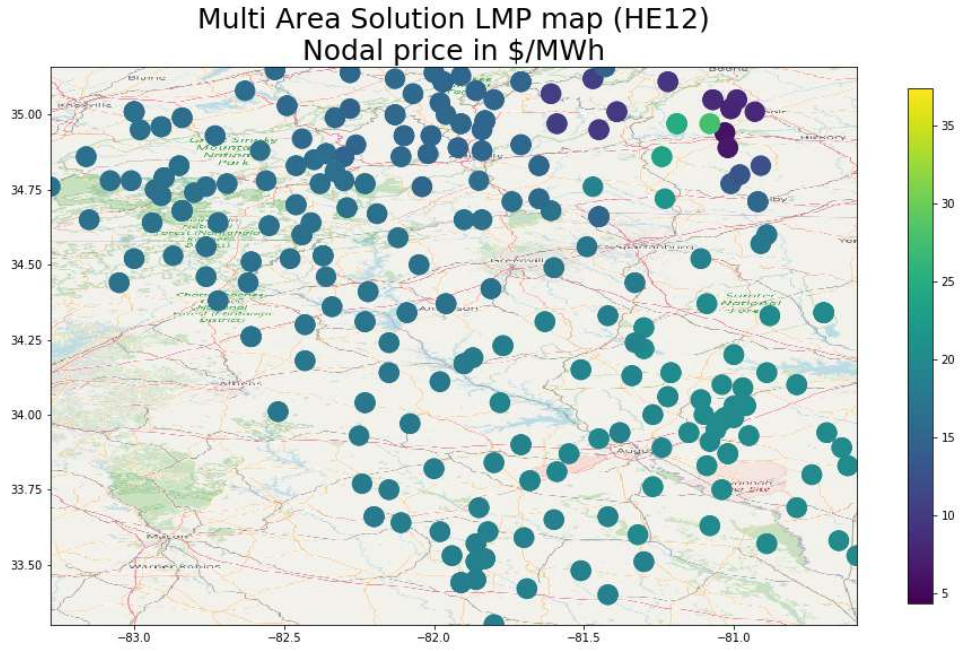

Figure 3.8. LMP map for the 500-bus case (coordinated multi-area solution)

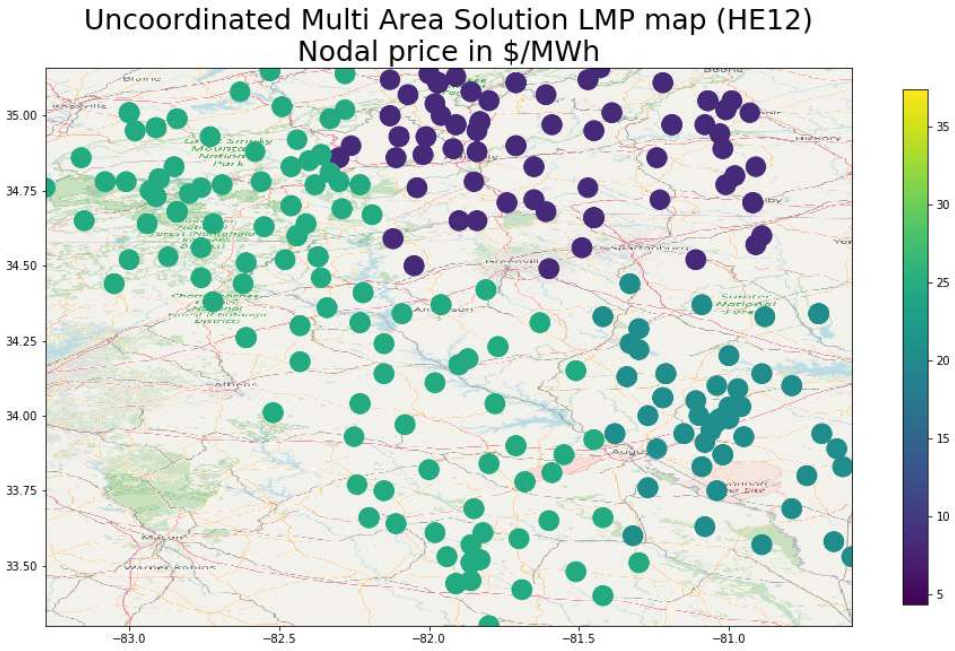

Figure 3.9. LMP map for the 500-bus case (uncoordinated multi-area area solution)

4. COORDINATED FTR AUCTION

LMPs provide entities that participate in wholesale electricity markets with economic incentives to behave in a way that avoids transmission overloads. Within this market-based congestion management structure, load-serving entities (LSEs) must purchase power from the centrally operated market at the LMP of the load location. Because LMPs are highly variable, the transition to LMPs effectively replaced the potential of load and transaction curtailment with considerable price uncertainty.

A simplified illustration of hourly LMP-based generation and load settlement is shown in Figure 4.1 and Table 4.1.

The example presents the hourly settlement of an 80 MW sale from a generator located on node A and an 80 MW purchase from a load on node B. Under this LMP-based market, the load pays the price at its location, $3,600 for 80MW, while the generator gets paid $2,800 for delivering the same amount.

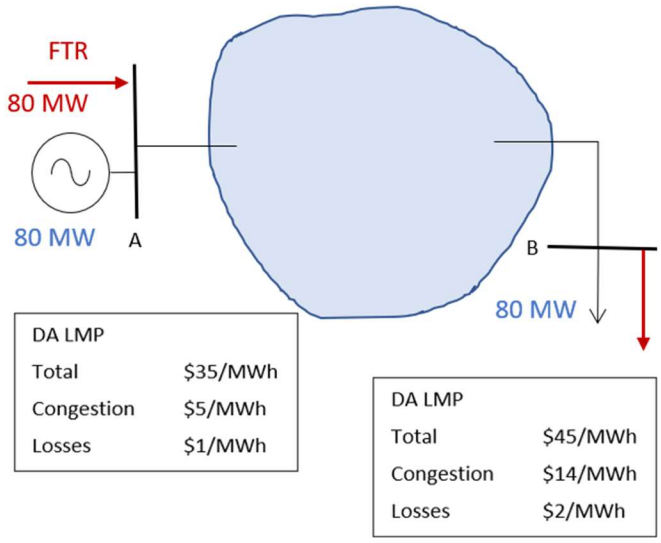

Figure 4.1. FTR hourly settlement illustration.

As illustrated in the example, congestion prices often cause load to pay more into the market than what generators receive. It is usually the case that congestion causes market operators to

charge load more for the energy consumed than what is paid to generators for the energy delivered. This overcollection by the market operator due to congestion is referred to as congestion rents.

Table 4.1. Day-ahead hourly settlement example

Entity	Generator	Load
Location	Node A	Node B
Transaction	80 MWh sale	80 MWh purchase
DA LMP	$35/MWh	$45/MWh
Congestion	$5/MWh	$14/MWh
Losses	$1/MWh	$2/MWh
Hourly settlement	$2,800	-$3,600

Not only do congestion charges increase the cost of electricity at the load locations, but they also introduce considerable price uncertainty, as congestion prices tend to be far more volatile than other LMP components.

Financial Transmission Rights (FTRs) can help manage price uncertainty [26], and provide a mechanism for market operators to redistribute congestion rents [34].

Congestion price risk plays an important role in the evaluation of investment in generation. Added to the difficulty to schedule transactions and meet capacity requirements across market regions, lack of access to adequate hedging instruments can deter investment in generation projects that rely on contracts for delivery across markets, as is often the case for large renewable generation projects.

The importance of the congestion hedging function of FTRs under open access transmission tariffs, and the role of availability of congestion hedging mechanisms in the procurement of power supply arrangements has been affirmed by FERC [32]. Such power supply arrangements are, in turn, often critical to the ability of generation developers to secure financing.

LSEs in PJM, the largest RTO, rely on bilateral power supply arrangements to serve more than 70% of their load [12].

While FTRs offer a mechanism to manage congestion price uncertainty associated with bilateral transactions within an RTO region, the procurement of FTRs to hedge congestion price risk associated with transactions spanning several regions is challenging under existing market structures because (a) acquiring the FTRs requires participation in several auctions that are not

linked, and (b) the FTR settlement does not fully cover the congestion price difference across regions because of the lack of coordination in the day-ahead clearing processes.

Some mechanisms have been proposed to improve pricing of cross-border transactions [35,52]. However, only close day-ahead coordination across RTOs, such as the mechanism proposed in Chapter 3 can result in convergent interface day-ahead prices that may allow to fully hedge the price difference across regions using the adequate set of FTRs.

In this chapter we propose a multi-regional version of the FTR auction that uses a distributed optimization algorithm to allow RTOs to link the clearing of cross-border FTRs, while maintaining all internal bid and offer information private. The proposed auction formulation does not require RTOs to maintain external model information beyond tie-lines, and information exchange within the clearing process is limited to boundary conditions.

The proposed multi-area solution of the FTR auction is based on consensus optimization using ADMM. Because the FTR auction is a convex optimization problem the heuristics applied to the unit commitment calculations in the day-ahead market clearing presented in Chapter 3 are not needed for the ADMM solution to converge to an equivalent single-area auction solution. The next section presents an introduction to FTRs and congestion settlement in RTO markets and illustrates the use of FTRs as congestion hedging mechanisms. Section 4.2 shows the formulation of the FTR auction, which is extended to the multi-area case in section 4.3. Section 4.4 presents test case results comparing the proposed multi-regional FTR auction design to an ideal single-area auction and to the current uncoordinated auction clearing process.

4.1 Financial transmission rights

FTRs are financial instruments that entitle the holder to a stream of payments or charges calculated based on the difference between the congestion component of the locational marginal prices (LMPs) at two locations. FTRs are usually settled on day-ahead prices.

FTRs are acquired by submitting bids into an auction or through an allocation usually associated with transmission service or load serving obligations.

FTRs are specified by:

- A source-sink path. Both source and sink are pricing locations in the transmission system and can be individual nodes or node aggregates.
- A volume in MW.

- A duration, usually between several years and one month.
- A time of use, which defines for which group of hours within the duration of the FTR it will be settled. For example, an FTR can be settled only during peak hours, off-peak hours, or around the clock.
- The type of settlement. An FTR may be acquired as an obligation, which will be settled whether it represents a credit or a charge to its holder, or as an option, settled only when it results in a payment to its holder.

To illustrate the use of FTRs as hedging instruments, we consider the FTR shown in Figure 4.1 which matches the hourly transaction from generation to load shown in the same figure. The settlement of the FTR is shown in Table 4.2. In this example, the FTR settlement, which pays $720 to the FTR holder, offsets the congestion portion of the difference between the load charge and generation payment.

The total difference between the load charge and generation payment is $800, of which $80 corresponds to loss charges and are not offset by FTR payments.

Table 4.2. FTR hourly settlement example

FTR source		A
FTR sink		B
FTR volume		80 MW
DA congestion price	Source	$5/MWh
	Sink	$14/MWh
Hourly FTR payment per MW		$14 - $5 = $9
Hourly FTR settlement		$720

A power supply agreement may allow the LSE to remove uncertainty around the generator payment, but it would leave the LSE exposed to the – usually volatile – price difference between the generator location and the load location. This price difference will be the result of congestion and losses.

If the FTR of the example is held by the load, the total hourly settlement of $2,880 is equivalent to the load paying the congestion price at the FTR source. Within existing RTO markets,

there is no mechanism to hedge exposure to loss prices, but those tend to be far less variable than congestion prices.

In the example, the FTR completely offsets the difference between the load and generation congestion prices. In practice, however, there are several reasons why FTRs do not always constitute a perfect hedge against congestion exposure for load serving entities. Among them, the uncertainty around acquiring the desired FTR volumes through allocations and auctions, the limited granularity of the FTR validity periods, the potentially varying volume associated to some power purchase agreements, and FTR underfunding.

Still, while imperfect, FTRs are widely used as a mechanism to protect transmission customers against the financial risk related to congestion in the day-ahead market.

When power is to be transferred across electricity market regions, congestion hedging becomes considerably more challenging. In addition to the reasons listed above, cross-border congestion hedging through FTRs presents considerable challenges:

a. There is no coordinated way to acquire an FTR for the entire delivery path, across market regions. Participants must submit bids that are internal to each region, sourcing or sinking at the interface, but there is no way to tie the bids to ensure that the same MW amount is awarded on every segment for a given time period.
b. Because of lack of coordination in the day-ahead market clearing processes, the LMPs at the interface connecting two market regions do not usually converge to the same value in the two market clearing processes.

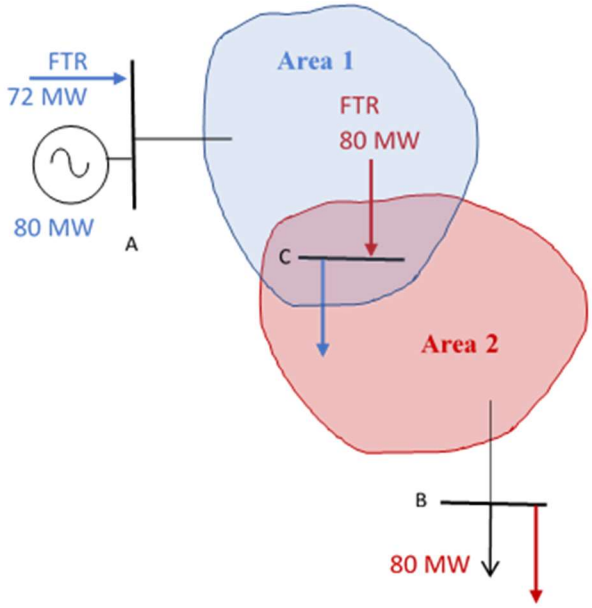

Figure 4.2. Inter-regional transaction and FTR illustration.

To illustrate the effect of the problems described above, Figure 4.2 shows the same transaction as Figure 4.1, but with generation and load residing in separate market areas. For this multi-area example, day-ahead prices and energy settlement are shown in Table 4.3.

Table 4.3. Day-ahead inter-regional transaction settlement settlement example

Entity	Generator	Load
Location	Node A (Area 1)	Node B (Area 2)
Transaction	80 MWh sale	80 MWh purchase
DA LMP	$33/MWh	$46/MWh
Congestion	$4/MWh	$15/MWh
Hourly settlement	$2,640	-$3,680

Because generation and load are not in the same area, it is not possible to acquire through the RTO an FTR from node A to node B. Instead, the LSE can submit separate bids into the FTR auctions of each market, one from the generator to the interface, and one from the interface to the load, with no guarantee that the entire path can be acquired. In this example, the LSE was able to acquire all 80 MW from the interface to the load, but the FTR from the generator to the interface was partially cleared.

In the example from Figure 4.2, the interface between the two regions is represented by node C. Each market calculates interface LMPs based on their internal day-ahead bids and offers, so it is very likely that there will be a difference between the LMP for node C calculated by area 1 and the LMP for node C calculated by area 2. It is not always the case that interface points between markets are defined at the same location, which exacerbates this price mismatch problem.

Table 4.4. FTR hourly settlement example (inter-regional transaction)

FTR area		1	2
FTR source		A	C
FTR sink		C	B
FTR volume		72 MW	80 MW
DA congestion price	Source	\$4/MWh	\$10/MWh
	Sink	\$7/MWh	\$15/MWh
Hourly FTR payment per MW		\$7 - \$4 = \$3	\$15 - \$9 = \$6
Hourly FTR settlement		\$216	\$480

Table 4.4 shows the settlement of each FTR in the example of Figure 4.2. The congestion price difference between nodes A and B is \$11/MWh, which results in a congestion charge for the transaction of \$880. The hourly payment received from the FTR settlement is \$696. Even if the LSE had been able to procure 80 MW of FTRs in area 1, the corresponding settlement for both FTRs would be \$720. The pair of FTR paths is an imperfect hedge against the total congestion cost on paths across areas because the interface price difference between areas is not covered by any FTR.

4.2 FTR auction formulation

Market operators sell FTRs on a regular basis through auctions. The FTR auction process is a social welfare maximization subject to the limits of the transmission system. The market operator receives bids to buy FTRs and offers to sell existing ones and clears the auction by solving (4.1):

$$\max_{p,s,\theta} \sum_{n \in \mathcal{B}} C_n^B(p_n) - \sum_{m \in \mathcal{S}} C_m^S(s_m)$$

$$s.t. \qquad (4.1)$$

$$0 \le p_n \le p_n^{max} \qquad \forall n \in \mathcal{B}$$

$$0 \le s_m \le s_m^{max} \qquad \forall m \in \mathcal{S}$$

$$F_l^{min} \le b_l(\theta_{l,from} - \theta_{l,to}) \le F_l^{\max} \qquad \forall l \in \mathcal{L}$$

$$NI_i = \sum_{j \in \eta_i} B_{ij}(\theta_i - \theta_j)$$

$$with\ NI_i = \sum_{n \in \mathcal{B}^{(i)}} p_n - \sum_{n \in \mathcal{B}^{(-i)}} p_n - \sum_{m \in \mathcal{S}^{(i)}} s_m + \sum_{m \in \mathcal{S}^{(-i)}} s_m \qquad \forall i \in \mathcal{N},$$

where

Sets

$\mathcal{B}$	FTR buy bids submitted into the auction
$\mathcal{S}$	FTR sell offers submitted into the auction
$\mathcal{L}$	Transmission limits enforced in the auction
$\mathcal{N}$	Nodes in the transmission system
η_i	Nodes directly connected to node *i*
$\mathcal{B}^{(i)}$	Buy bids sourcing at node *i*
$\mathcal{B}^{(-i)}$	Buy bids sinking at node *i*
$\mathcal{S}^{(i)}$	Sell offers sourcing at node *i*
$\mathcal{S}^{(-i)}$	Sell offers sinking at node *i*

Decision variables

p_n	Awarded quantity (in MW) for FTR bid *n*
s_m	Awarded quantity (in MW) for FTR offers *m*
θ_i	Phase angle at bus *i*

Other

NI_i	Net FTR injection at node *i*

Cost function

$C_n^B(\cdot)$	Bid curve for bid *n*
$C_m^S(\cdot)$	Offer curve for offer *m*

Parameters

p_n^{max}	Maximum quantity (in MW) associated with buy bid *n*
s_m^{max}	Maximum quantity (in MW) associated with sell offer *m*
$F_l^{min}, F_l^{\max}$	Minimum and maximum limits (in MW) for transmission constraint *l*
b_l	Branch admittance of transmission constraint *l*
B_{ij}	ij^{th} element of the system admittance matrix

4.3 Multi-area FTR auction

If several interconnected regions running their own FTR auctions were to run a coordinated version of (4.1), cross-border bids and offers would be split across regions. The subproblem for area $\alpha \in \boldsymbol{\mathcal{A}}$ can be rewritten as:

$$\max_{p^a, s^a, \theta^a} \sum_{n \in \mathcal{B}^a} C_n^B(p_n^a) - \sum_{m \in \mathcal{S}^a} C_m^S(s_m^a) \tag{4.2}$$

s.t.

$$\begin{aligned} 0 \le p_n^a \le p_n^{max} \quad & \forall n \in \mathcal{B}^a \\ 0 \le s_m^a \le s_m^{max} \quad & \forall m \in \mathcal{S}^a \end{aligned} \tag{4.3}$$

$$F_l^{min} \le b_l(\theta_{l,from}^a - \theta_{l,to}^a) \le F_l^{\max} \quad \forall l \in \mathcal{L}^a \tag{4.4}$$

$$NI_i^a = \sum_{j \in \eta_i} B_{ij}(\theta_i^a - \theta_j^a)$$

$$with\ NI_i^{(a)} = \sum_{n \in \mathcal{B}^{(i),\alpha}} p_n^{(a)} - \sum_{n \in \mathcal{B}^{(-i),\alpha}} p_n^{(a)} - \sum_{m \in \mathcal{S}^{(i),a}} s_m^{(a)} + \sum_{m \in \mathcal{S}^{(-i),a}} s_m^{(a)} \quad \forall i \in \mathcal{N}^a, i \notin \mathcal{N}^b . \tag{4.5}$$

Bids and offers that either source or sink at area *a* are included in the subproblem corresponding to that area. The same applies to transmission facilities where either end resides within the area. The set of buses $i \in \mathcal{N}^a$ include all buses internal to the area, plus immediately adjacent buses. However, the power balance constraint (4.5) is only enforced for buses internal to *a*.

For a set of interconnected areas $\boldsymbol{\mathcal{A}}$, two conditions must be met to ensure the feasibility of the multi-area FTR auction:

1. The volume awarded for cross-border FTRs must be the same across all areas

$$p_n^a = p_n^a \quad \forall n \in \mathcal{B}^a \cap \mathcal{B}^b, \forall a,b \in \boldsymbol{\mathcal{A}} \tag{4.6}$$

$$s_m^a = s_m^b \quad \forall m \in \mathcal{S}^a \cap \mathcal{S}^b, \forall a,b \in \boldsymbol{\mathcal{A}} \tag{4.7}$$

2. The phase angles at the boundary must match:

$$\theta_i^a = \theta_i^b \quad \forall i \in \mathcal{N}^a \cap \mathcal{N}^b, \forall a,b \in \mathcal{A} \tag{4.8}$$

Applying the formulation for consensus optimization via ADMM from [8], we write the augmented Lagrangian in (3.3) as:

$$\mathcal{L}_\rho^k(x^a,\theta^a) = f^a(x^a) + \gamma_k^{aT}(x_S^a - \bar{x}_k) + \frac{\rho}{2}\left\|x_S^a - \bar{x}_k\right\|_2^2 + \sigma_k^{aT}(\theta_S^a - \bar{\theta}_k) + \frac{\rho}{2}\left\|\theta_S^a - \bar{\theta}_k\right\|_2^2 \tag{4.9}$$

Where x^α is the vector of bid and offer decision variables for area *a*:

$$x^a := \begin{bmatrix} p^a \\ s^a \end{bmatrix}. \tag{4.10}$$

The FTR auction is a maximization of the social welfare. For linear bids and offers, the cost $f^a(x^a)$ is re-written as:

$$\begin{aligned} f^a\left(p^a, s^a\right) &= -\left(\sum_{n\in\mathcal{B}^a} C_n^B(p_n) - \sum_{m\in\mathcal{S}^a} C_m^S(s_m)\right) \\ &= -\left(\left(c_B^a\right)^T p^a - \left(c_S^a\right)^T s^a\right) \\ &= -c^{aT}x^a \end{aligned} \tag{4.11}$$

The vectors x_S^a and θ_S^a are the global decision variables represented by *z* in (3.4). Here, the global variables correspond to bids and offers shared with areas outside *a*, and the set of buses on the boundary with other areas, or immediately neighboring *a*. Boundary buses are internal buses that are directly connected to an external bus through a tie-line. Neighboring or adjacent buses are external buses that are directly connected to an internal bus through a tie-line.

We denote the set of shared bids and offers:

$$\mathcal{B}^S = \left\{n : n \in \mathcal{B}^a \cap \mathcal{B}^b\right\} \quad \forall a \neq b, a \in \mathcal{A}, b \in \mathcal{A} \tag{4.12}$$

$$\mathcal{S}^S = \left\{m : m \in \mathcal{S}^a \cap \mathcal{S}^b\right\} \quad \forall a \neq b, a \in \mathcal{A}, b \in \mathcal{A}\ . \tag{4.13}$$

The vector of shared bids and offers calculated within the solution of area *a* is:

$$\begin{aligned} x_S^a &= \begin{bmatrix} p_S^a \\ s_S^a \end{bmatrix} \\ p_S^a &= \left[\, p_n^a : n \in \mathcal{B}^S \,\right] \\ s_S^a &= \left[\, s_m^a : m \in \mathcal{S}^S \,\right]. \end{aligned} \tag{4.14}$$

The consensus value of the shared bids and offers is calculated, for each area *a*, as:

$$\bar{x}^a = \begin{bmatrix} \bar{p}^a \\ \bar{s}^a \end{bmatrix}, \tag{4.15}$$

with the consensus value of shared bid awards:

$$\begin{aligned} \overline{p}^a &= \left[\overline{p}_n^a : n \in \mathcal{B}^S \cap \mathcal{B}^a \right] \\ \overline{p}_n^a &= \frac{1}{|\mathcal{A}_n|} \sum_{b \in \mathcal{A}_n} p_n^b \quad \forall n \in \mathcal{B}^S \cap \mathcal{B}^a, \end{aligned} \tag{4.16}$$

where $\mathcal{A}_n$ is the set of areas that include bid *n*, and the consensus value of shared offer awards:

$$\begin{aligned} \overline{s}^a &= \left[\overline{s}_m^a : m \in \mathcal{S}^S \cap \mathcal{S}^a \right] \\ \overline{s}_m^a &= \frac{1}{|\mathcal{A}_m|} \sum_{b \in \mathcal{A}_m} s_m^b \quad \forall m \in \mathcal{S}^S \cap \mathcal{S}^a, \end{aligned} \tag{4.17}$$

where $\mathcal{A}_m$ is the set of areas that include offer *m*.

Similarly, the vector of shared bus phase angles, θ_S^a, and the consensus value of shared bus phase angles, $\overline{\theta}^a$, are calculated as follows:

$$\begin{aligned} &\theta_S^a = \left[\theta_i^{(a)} : i \in \mathcal{N}^S \right] \\ &\text{where} \\ &\mathcal{N}^S = \left\{ i : i \in \mathcal{N}^a \cap \mathcal{N}^b \right\} \quad \forall a \neq b, a \in \mathcal{A}, b \in \mathcal{A} \end{aligned} \tag{4.18}$$

$$\begin{aligned} \overline{\theta}^a &= \left[\overline{\theta}_i^a : i \in \mathcal{N}^S \cap \mathcal{N}^a \right] \\ \overline{\theta}_i^a &= \frac{1}{|\mathcal{A}_i|} \sum_{b \in \mathcal{A}_i} \theta_i^b \quad \forall i \in \mathcal{N}^S \cap \mathcal{N}^a \end{aligned} \tag{4.19}$$

where $\mathcal{A}_i$ is the set of areas that include bus *i*.

Bids and offers are included in the optimization for area *a* if either the source or the sink reside in that area. However, to avoid duplicate charges or payments, the bid price is included only in one of the areas. This could be achieved by including the bid or offer only in the RTO area where it was submitted and include it with zero price in all other areas that the FTR spans. For this work, the bid or offer price is included in the area where the original FTR sink resides. The ADMM algorithm updates are calculated for the multi-regional FTR auction as:

$$x_{k+1}^a := \underset{x^a, \theta^a}{\arg\min} \left(-c^{aT} x + \gamma_k^{aT} (x_S^a - \overline{x}_k^a) + \frac{\rho}{2} \left\| x_S^a - \overline{x}_k^a \right\|_2^2 + \sigma_k^{aT} (\theta_S^a - \overline{\theta}_k^a) + \frac{\rho}{2} \left\| \theta_S^a - \overline{\theta}_k^a \right\|_2^2 \right). \tag{4.20}$$

The minimization in (4.20) is subject to constraints (4.3) - (4.5). γ^a is the vector of Lagrangian multipliers associated with the constraints matching the local award volumes of the shared bids and offers with the corresponding consensus value. σ^a is the vector of Lagrangian

multipliers associated with the constraints matching locally calculated shared bus phase angles with their corresponding consensus values.

The dual updates are calculated as follows:

$$\gamma_{k+1}^{a} = \gamma_{k}^{a} + \rho\left(x_{k+1}^{a} - \overline{x}_{k+1}^{a}\right), \tag{4.21}$$

$$\sigma_{k+1}^{a} = \sigma_{k}^{a} + \rho\left(\theta_{k+1}^{a} - \overline{\theta}_{k+1}^{a}\right). \tag{4.22}$$

The primal (ε_p) and dual (ε_d) residuals associated with shared bids and offers and with shared bus phase angles are calculated as:

$$\begin{aligned}
\varepsilon_{p,k}^{x(a)} &= x_k^{(a)} - \overline{x}_k^{(a)}, \\
\varepsilon_{p,k}^{\theta(a)} &= \theta_k^{(a)} - \overline{\theta}_k^{(a)}, \\
\varepsilon_{d,k}^{x(a)} &= \rho\left(\overline{x}_k^{(a)} - \overline{x}_{k-1}^{(a)}\right), \\
\varepsilon_{d,k}^{\theta(a)} &= \rho\left(\overline{\theta}_k^{(a)} - \overline{\theta}_{k-1}^{(a)}\right)
\end{aligned} \tag{4.23}$$

Algorithm 2: Multi-area FTR auction algorithm

Step 0: With some $\rho > 0$, set $k = 0$ and specify initial values $x_0^{(a)}, \theta_0^{(a)}, \gamma_0^{(a)}, \sigma_0^{(a)}$ for every area $a \in \boldsymbol{a}$. Set tolerances $\epsilon_p > 0, \epsilon_d > 0$.

Step 1: Use (4.15) - (4.17) to calculate $\overline{x}^{(a)}$ from the current values of awarded cross border FTR quantities and (4.18) - (3.14) to calculate $\overline{\theta}^{(a)}$ from current boundary and neighboring phase angles for every area.

Step 2: Use (4.21) and (4.22) to update the values of $\gamma^{(a)}, \sigma^{(a)}$.

Step 3: Calculate the primal and dual residuals for all areas:

Step 4: With, Stop if $\left\|\varepsilon_{p,k}^{x(a)}\right\|_\infty \le \epsilon_p, \left\|\varepsilon_{p,k}^{\theta(a)}\right\|_\infty \le \epsilon_p$, $\left\|\varepsilon_{d,k}^{x(a)}\right\|_\infty \le \epsilon_d$, and $\left\|\varepsilon_{d,k}^{\theta(a)}\right\|_\infty \le \epsilon_d$. Otherwise go to the next step.

Step 5: Solve (4.20) to update the values of all decision variables in all areas. Set $k \leftarrow k+1$ and go to step 0.

4.4 Test case results

4.4.1 Solution methods

Single-area FTR auction

This represents the FTR auction results of the entire system modeled as a single area. This model yields the least-cost feasible solution but requires a single market operator to receive bids and offers from all participants and to maintain a model of the entire interconnected transmission system. This model is used as a benchmark that represents the ideal case.

Uncoordinated multi-area FTR auction

FTR auction clearing calculations are performed independently for each area. Bids that span more than one area are separated into sections, each one internal to an area. This splitting of bids and offers must be performed by the market participant submitting the bids. The participant submits each bid or offer section with a price that corresponds only to the portion of the path that is internal to the area.

This model represents the current state, where FTR auctions in interconnected RTOs are run independently. In this simplified version of the current state, only internal facilities are included in each area model.

Coordinated multi-area FTR auction

The FTR auction results are computed using the distributed algorithm presented in section 4.3. Market operators must coordinate the auction clearing but share only boundary conditions between iterations. These boundary conditions include shared bid and offer cleared quantities and boundary bus phase angles. Each area keeps internal bid and offer information private, may have different market rules, and is only required to maintain an accurate model of their internal transmission system and tie-lines.

4.4.2 Test cases

Two transmission network models were used to evaluate the proposed algorithm:

1. A 14-bus, two-area case
2. A 200-bus, three-area case

Transmission network models were obtained from the Texas A&M University electric grid test case repository [49]. FTR bid and offer information was generated for this simulation.

4.4.3 System information

Test cases were executed in Matlab R2020b Update 1, calling IBM ILOG CPLEX Optimization Studio version 12.9. They were run on a PC with an Intel Core i7 6560U CPU@2.2GHz, 16 GB RAM and a 64 bit OS.

4.5 Simulation results

Table 4.5 shows the objective function and execution times for the three auction solution methods. The auction maximizes social welfare, which includes the auction revenue and the buyers and sellers surpluses. The social welfare is calculated as:

$$SW = f(p,s) = -\left(c_B^T p - c_S^T s\right) \tag{4.24}$$

Where p, s are the vectors of cleared bid and offer amounts, respectively, and c_B, c_S are the vectors of bid and offer prices.

Table 4.5. FTR auction test case results

Case	Solution method	Social Welfare	Execution time (s)
14-bus	Single-area	$ 606.69	0.027
	Uncoordinated	$ 362.92	0.16
	Coordinated multi-area	$ 606.68	81.8
200-bus	Single-area	$ 1,258.95	0.4396
	Uncoordinated	$ 1,420.59	0.3907
	Coordinated multi-area	$ 1,258.80	403.6

The proposed distributed method results in virtually the same solution as the benchmark single-area case. Figure 4.4 shows the congestion patterns from the coordinated multi-area solution are the same as those from the single-area solution and very different from the uncoordinated solution shown in Figure 4.5.

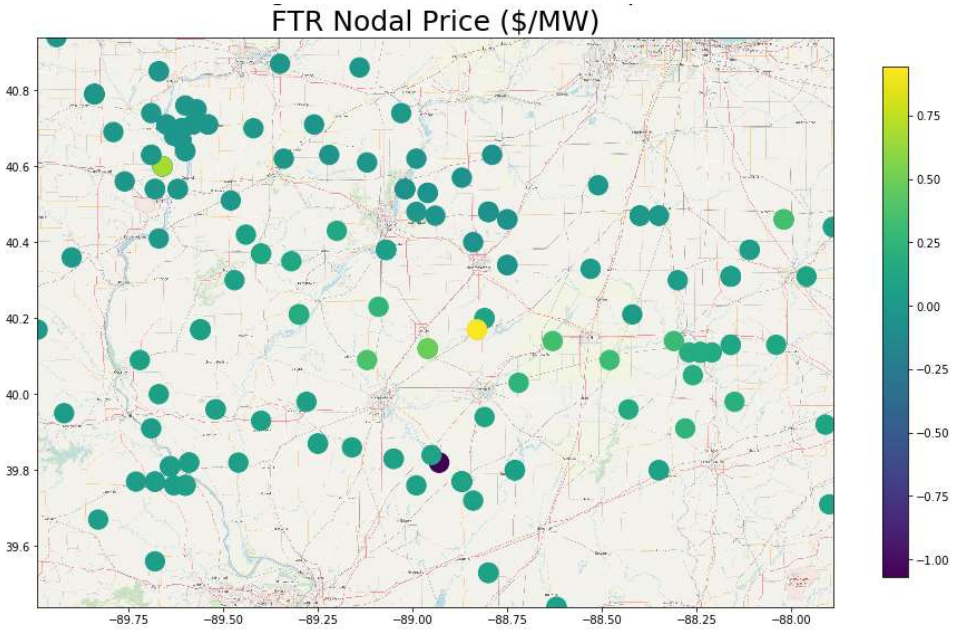

Figure 4.3. Single-area FTR auction nodal price map for the 200-bus case

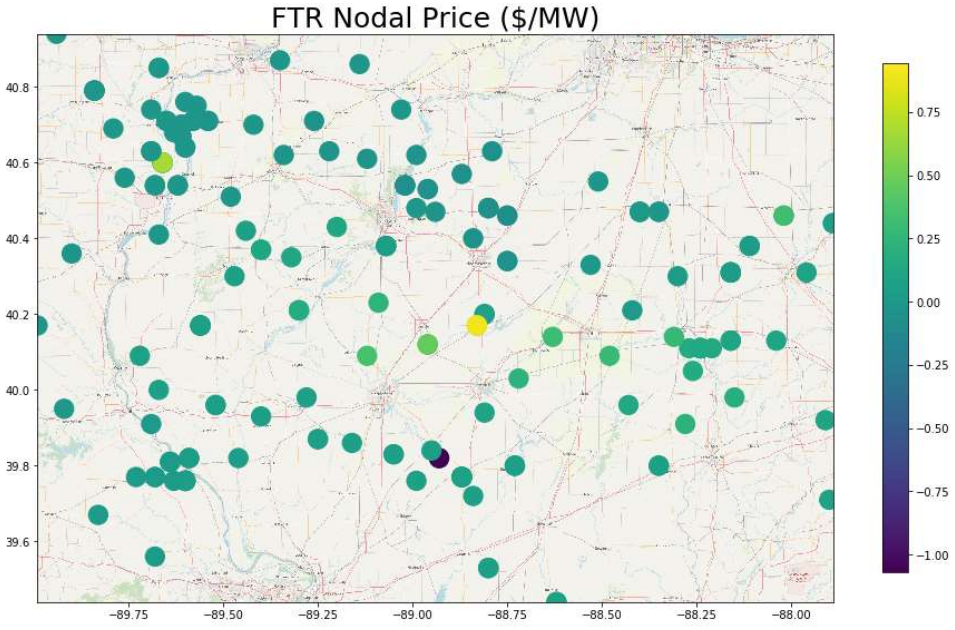

Figure 4.4. Coordinated multi-area auction nodal price map for the 200-bus case

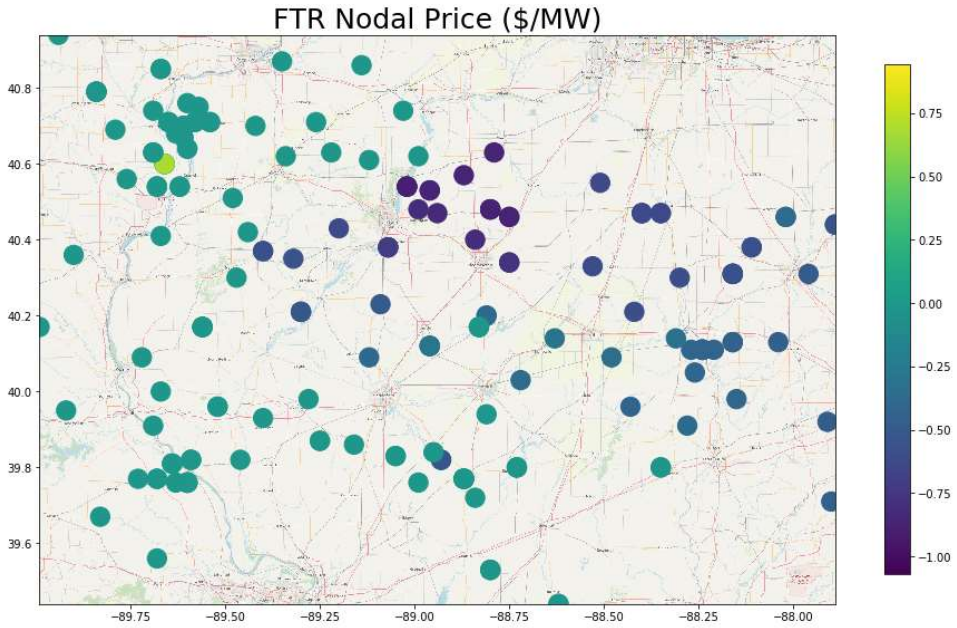

Figure 4.5. Uncoordinated multi-area auction nodal price map for the 200-bus case

The ADMM solution times are considerably larger. Methods to accelerate ADMM have been proposed but are not the focus of this work. Some examples of such methods can be found in [10] and [51].

For the 14-bus case, the uncoordinated solution results in a lower objective function, but that is not the case for the 200-bus case. However, in both cases the final set of outstanding FTRs resulting from the uncoordinated auction are infeasible with respect to the transmission limits of the interconnected system. This occurs because external transmission limits are not enforced in the uncoordinated case.

As will be discussed in the next chapter, the limits of the transmission system are enforced in the FTR auction with the goal of ensuring that congestion revenues from the day-ahead market are sufficient to cover the RTO's obligations to FTR holders. A set of FTRs that is infeasible with respect to the limits of the day-ahead model may result in day-ahead congestion funds being insufficient to cover FTR payments. When transmission facilities that are oversold in the auction bind in the day-ahead market, the congestion rents collected will be insufficient to cover the corresponding FTR obligations. When this occurs, some RTOs prorate FTR payments for all FTR holders, resulting in FTR payments that do not cover the day-ahead congestion charges on the FTR path. Table 4.6 shows the impact of infeasibility in the 14-bus case.

Table 4.6. Revenue adequacy comparison

Item	Amount	
Day-ahead hourly load charges	$ 10,581.86	
Day-ahead hourly generation payments	$ 8,029.90	
Day-ahead hourly congestion rents	$ 2,552.05	
	Uncoordinated FTR Auction	Coordinated FTR Auction
Hourly FTR settlement (net payment)	$ 3,147.86	$ 2,428.28
FTR funding shortfall	$ 595.81	-$ 123.77
Hourly FTR funding	81.1%	100%

In addition to infeasibility, uncoordinated FTR clearing does not enforce FTR bids and offers associated with cross-border transactions to clear at the same level in all areas. Table 4.7 compares the clearing levels of cross-border bids and offers for the 14-bus case. The first column shows the clearing levels for the coordinated and single-area solutions, which are the same. The second and third columns show the cleared levels of the same cross-border bids and offers for the uncoordinated solution. For FTR bids and offers that source in one area and sink in another, there is no guarantee that the same amount will clear in both areas without a coordinated FTR auction. This illustrates part of the difficulty to hedge cross-border transactions in uncoordinated auctions.

Table 4.7. Percent cleared for shared bid and offer (14-bus model)

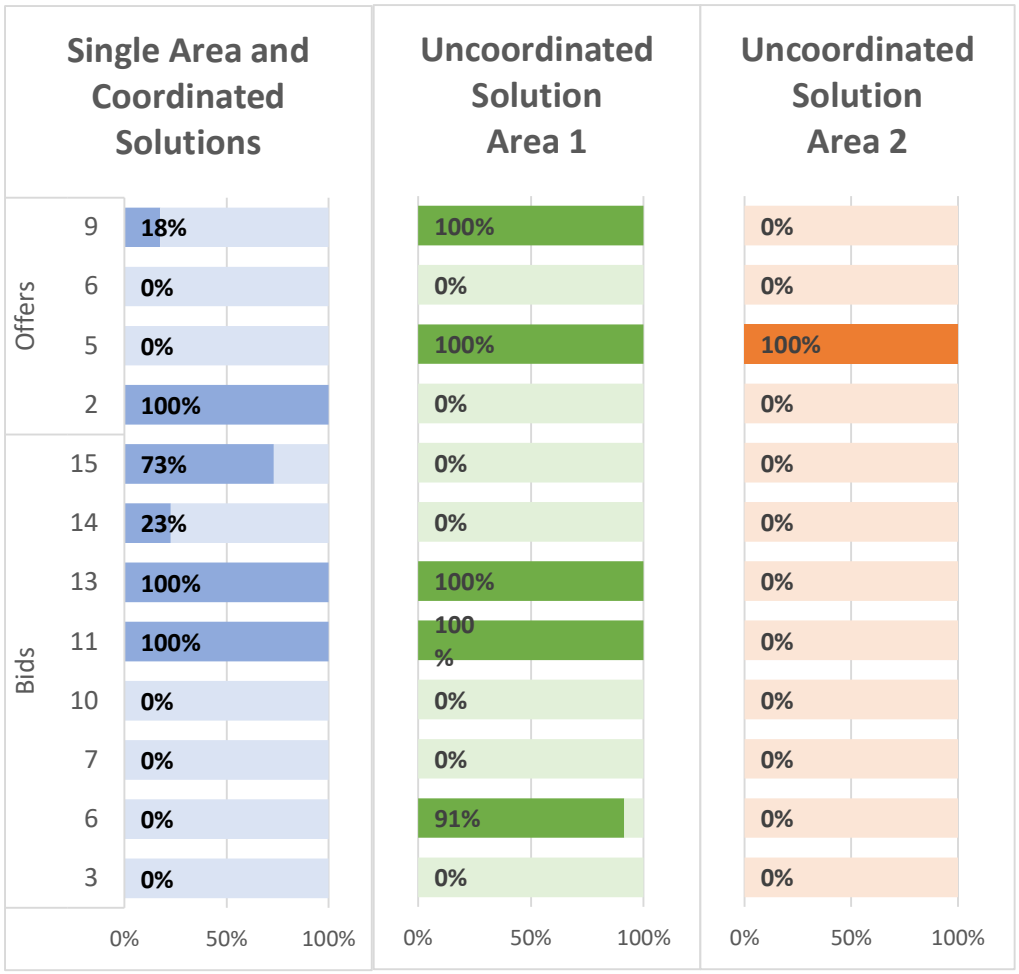

The coordinated solution enforces equal clearing levels for cross-border FTRs. This is a constraint that cannot be enforced without inter-regional coordination of the FTR auction but may result in a lower objective value across the combined interconnected system. It should be noted that in a coordinated FTR auction, market participants can retain the ability to split their bids at the border if they are not concerned about partial clearing of their bid and offer paths.

5. FINANCIAL CONSIDERATIONS

The FTR and day-ahead markets are purely financial markets. The only reason why transactions in both markets are subject to feasibility with respect to the limits of the transmission system is to ensure revenue adequacy: real-time revenues must cover deviations from day-ahead schedules, and day-ahead congestion revenues must cover payments owed to FTR holders.

An important shortcoming of the existing uncoordinated markets is the inability of market operators to accurately model the impact of external generation and load, which can cause considerable revenue inadequacy. In this chapter, revenue adequacy conditions are shown, and the causes of revenue inadequacy associated with poor inter-regional coordination are explained. In this chapter we illustrate how the multi-area market solutions presented in chapters 0 and 4 can improve revenue adequacy.

One of the obstacles in the implementation of improved inter-regional coordination is tied to economic considerations associated to the use of the transmission capacity in one area by transmission customers in another area. In this chapter we show how the revenue transfer across areas that results from the implementation of the coordinated market clearing presented in chapters 0 and 4 constitutes adequate payment for the use of external transmission facilities.

5.1 FTR revenue adequacy

Market operators grant FTRs subject to feasibility with respect to transmission system limits. This is done to ensure that enough funds are collected in the day-ahead market through congestion rents to cover the net obligations to FTR holders. When FTR funding is inadequate, the cost of meeting the funding shortfall is socialized, by charging LSEs or by prorating the payments to FTR holders.

The economic dispatch problem described in section 2.4 is part of the day-ahead market clearing process. As shown in section 2.4.1, locational marginal prices (LMPs) at any location in the system are a byproduct of the economic dispatch solution and, for the linear model used throughout this work, can be decomposed into its energy and congestion components. The congestion component of the LMP at bus i for any time interval t is computed as:

$$\lambda_{i,t}^{c,DA} = \sum_{l \in \mathcal{L}} \mu_{l,t}^{DA} S_{i,t}^{l,DA} \quad , \tag{5.1}$$

where:

$\lambda_{i,t}^{c,DA}$ Congestion component of the LMP at location *i* during interval *t*

$\mu_{l,t}^{DA}$ Shadow price[8] of the constraint associated with transmission limit *l* during interval *t.*

$S_{i,t}^{l,DA}$ Shift factor, as defined in (2.27), of branch *l* to an injection at location *i* for the transmission network topology in interval *t*

$\mathcal{L}$ Set of enforced transmission limits

In this section, we assume that the constraints (2.15) are always defined in the positive direction of the flow. We then re-write (2.15) as

$$B_{ij}(\theta_{i,t} - \theta_{j,t}) \leq F_l^{lim} \quad \forall i, j, t, \tag{5.2}$$

where F_l^{lim} is the flow limit of the branch connecting buses *i* and *j*. The shadow price associated with this constraint in the day-ahead market economic dispatch, $\mu_{l,t}^{DA}$, is non-positive, as the economic dispatch is a cost minimization problem.

It follows that the payment associated to an FTR *n,* with source *i* and sink *j*, for interval *t* will be:

$$\begin{aligned} \pi_n^t &= q_n \left(\lambda_{j,t}^{c,DA} - \lambda_{i,t}^{c,DA} \right) \\ &= q_n \left(\sum_{l \in \mathcal{L}} \mu_{l,t}^{DA} S_{j,t}^{l,DA} - \sum_{l \in \mathcal{L}} \mu_{l,t}^{DA} S_{i,t}^{l,DA} \right) \\ &= -q_n \left(\sum_{l \in \mathcal{L}} \mu_{l,t}^{DA} S_{ij,t}^{l,DA} \right) \end{aligned} \tag{5.3}$$

where:

π_n^t Payment to the owner of FTR *n* (on path *ij*) during interval *t*

q_n Volume (in MW) associated to FTR *n*

$S_{ij,t}^{l,DA}$ Sensitivity of the flow through constraint *l* to a transfer from *i* to *j* for the transmission network topology in interval *t.*

The set of outstanding FTRs for time period *t* ($\mathcal{F}^t$) is defined as the set of FTRs that will be settled based on the day-ahead market results for interval *t.* The total FTR payments for the FTRs in $\mathcal{F}^t$ is:

[8] We assume that all constraints are defined in the direction of the flow, so the shadow price of a binding transmission constraint in the economic dispatch problem is always negative.

$$\begin{aligned}\Pi^t &= -\sum_{n\in\mathcal{F}^t} q_n \left(\sum_{l\in\mathcal{L}} \mu_{l,t}^{DA} S_{ij,t}^{l,DA} \right) \\ &= -\sum_{l\in\mathcal{L}} \mu_{l,t}^{DA} \sum_{n\in\mathcal{F}^t} q_n S_{ij,t}^{l,DA} \\ &= -\sum_{l\in\mathcal{L}} \mu_{l,t}^{DA} \tilde{f}_{l,t}^{FTR}\end{aligned} \tag{5.4}$$

$$\tilde{f}_{l,t}^{FTR} \coloneqq \sum_{n\in\mathcal{F}^t} q_n S_{ij,t}^{l,DA} \tag{5.5}$$

The congestion revenue collected in the day-ahead market for time interval t can be calculated in terms of the net injection $P_{i,t}^{DA}$ and the congestion component of the LMP at each bus in the system.

$$CR_t^{DA} = -\sum_{i\in\mathcal{N}} P_{i,t}^{DA} \lambda_{i,t}^{c,DA} \tag{5.6}$$

If the congestion component of the LMP is disaggregated based on (5.1), we can re-write the congestion revenue in the day-ahead market in terms of the shadow prices of binding transmission constraints (5.2) in the day-ahead economic dispatch solution.

$$\begin{aligned}CR_t^{DA} &= -\sum_{i\in\mathcal{N}} P_{i,t}^{DA} \sum_{l\in\mathcal{L}} \mu_{l,t}^{DA} S_{i,t}^{l,DA} \\ &= -\sum_{l\in\mathcal{L}} \mu_{l,t}^{DA} \sum_{i\in\mathcal{N}} P_{i,t} S_{i,t}^{l,DA}\end{aligned} \tag{5.7}$$

Where the day-ahead market is cleared using a DC power flow approximation, the flows through binding constraints can be calculated as the product of net injections and flow sensitivities:

$$f_{l,t}^{DA} = \sum_{i\in\mathcal{N}} P_{i,t}^{DA} S_{i,t}^{l,DA} \tag{5.8}$$

$$CR_t^{DA} = -\sum_{l\in\mathcal{L}} \mu_{l,t}^{DA} f_{l,t}^{DA} \tag{5.9}$$

To ensure revenue adequacy during any time period t, the congestion revenue collected in the day-ahead market needs to meet or exceed the payments to FTR holders:

$$\begin{aligned}\Pi^t &\le CR_t^{DA} \\ -\sum_{l\in\mathcal{L}} \mu_{l,t}^{DA} \tilde{f}_{l,t}^{FTR} &\le -\sum_{l\in\mathcal{L}} \mu_{l,t}^{DA} f_{l,t}^{DA}\end{aligned} \tag{5.10}$$

The condition in (5.10) ensures hourly FTR revenue adequacy at a system-wide level. A sufficient condition for it to hold is for it to be met on a constraint-by-constraint basis; that is,

$$-\sum_{l\in\mathcal{L}} \mu_{l,t}^{DA} \tilde{f}_{l,t}^{FTR} \le -\sum_{l\in\mathcal{L}} \mu_{l,t}^{DA} f_{l,t}^{DA} \quad \Leftarrow -\mu_{l,t}^{DA} \tilde{f}_{l,t}^{FTR} \le -\mu_{l,t}^{DA} f_{l,t}^{DA} \quad \forall l \in \mathcal{L}. \tag{5.11}$$

Because the shadow price of binding transmission constraints in the day-ahead market clearing process is always non-positive, and the flow through a binding constraints equals the enforced constraint limit, the constraint-level condition in (5.11) can be re-written as:

$$\tilde{f}_{l,t}^{FTR} \le F_{l,t}^{\max,DA} \quad \forall l \in \mathfrak{L} \tag{5.12}$$

Equation (5.12) is a sufficient condition to maintain revenue adequacy in FTR markets during any time interval *t*. It states that for every binding flow constraint of the form (5.2) in the day-ahead market, the flow resulting from applying the outstanding set of FTRs ($\mathfrak{F}^t$) as injections and withdrawals to the transmission system model used in the day-ahead market, must be less than or equal to constraint limit of each branch.

Guaranteeing that (5.12) holds is challenging at the time of clearing the FTR auction, mainly because there is no precise knowledge of each hourly day-ahead transmission topology or limits at the time of clearing the FTR auction.

FTR auctions are cleared for periods with a duration of a month or longer. The resulting cleared FTRs are settled on every hour in the day-ahead market within the validity period of the FTR auction. Day ahead transmission topology and limits can change on an hourly basis. Because a single FTR auction generates FTRs that are valid for a large number of day-ahead models, and because the FTR auction is performed days, and often months before the time when the cleared FTRs become valid, it is impossible to perform the FTR auction using the same transmission system topology and limits that will be used in the day-ahead market.

Consequently, we re-write (5.12) in terms of the representation of the transmission network used for the FTR auction:

$$f_l^{FTR} \le F_l^{\max,FTR} \quad \forall l \in \mathfrak{L}. \tag{5.13}$$

With the FTR flow through the line calculated using the transmission system topology used for the FTR auction:

$$f_l^{FTR} = \sum_{n \in \mathfrak{F}^t} q_n S_{ij,t}^{l,FTR} \ . \tag{5.14}$$

The condition in (5.13) is enforced in the FTR auction in constraint (4.4). Even with this condition maintained, revenue inadequacy may occur when conditions in (5.12) and (5.13) are not equivalent for a particular binding constraint in the day-ahead market. For a constraint $l \in \mathfrak{L}$, this may happen for one of two reasons:

(a) Shift factors in the FTR model are different from those in the day-ahead model due to differences in the representation of the transmission system.

$$S_{ij,t}^{l,DA} \ne S_{ij}^{l,FTR} \ . \tag{5.15}$$

(b) The transmission constraint limit applied in the FTR model is larger than the one used in the day-ahead model.

$$F_{l,t}^{max,DA} < F_{l}^{max,FTR}. \tag{5.16}$$

To reduce the potential of encountering revenue inadequacy, RTOs often reduce the flow limits of transmission facilities in the FTR model. This directly reduces the potential of a revenue shortfall because of (5.16), and leaves some room for sensitivity errors, which will always occur due to transmission outages, differences in the definition of aggregate pricing locations, system reconfigurations, or differences in the shift factor calculation.

5.2 Real-time revenue adequacy

In the previous section we discussed the conditions to ensure that enough funds are collected in the day-ahead market to pay FTR holders. RTOs need to maintain revenue adequacy across all market processes. It is possible that the settlement of transactions in the real-time market can result in the RTO owing money to market participants. In this section, we explore the conditions required to ensure that the real-time market settlement does not result in a net payment from the RTO to market participants.[9]

In PJM, what is described here as real-time congestion revenue is called "balancing congestion". Until a FERC order issued on September 15, 2016, balancing congestion was combined with FTR revenue, and was a major source of FTR revenue inadequacy[1], much of which was a result of the market-to-market coordination process with MISO. In section 5.3.1 we explain how the limitations of inter-regional coordination can result in revenue inadequacy associated with the real-time market.

If we consider the real-time market as a balancing market where only deviations between the day-ahead schedules and real-time injections and withdrawals are settled, the real-time congestion revenue (CR^{RT}) for a time period *t* can be written in terms of the net injection deviation between the day-ahead and real-time markets $\Delta P_{i,t} = P_{i,t}^{RT} - P_{i,t}^{DA}$:

$$CR_{t}^{RT} = -\sum_{i \in \mathcal{N}} \Delta P_{i,t} \lambda_{i,t}^{c,RT} \tag{5.17}$$

[9] Overall, RTOs will remain revenue neutral. If there is a revenue shortfall it will be resmedied using some charge assessed to market participants.

Decomposing the LMP congestion component:

$$\begin{aligned} CR_t^{RT} &= -\sum_{i\in\mathcal{N}} \Delta P_{i,t} \sum_{l\in\mathcal{L}} \mu_{l,t}^{RT} S_{i,t}^{l,RT} \\ &= -\sum_{l\in\mathcal{L}} \mu_{l,t}^{RT} \sum_{i\in\mathcal{N}} \Delta P_{i,t} S_{i,t}^{l,RT} \end{aligned} \tag{5.18}$$

Most RTOs do not utilize a DC power flow approximation in the real-time market calculations; therefore, in the real-time market the line flows do not vary linearly with the magnitude of a power transfer. We can use a linear approximation to calculate the change in the real-time flow due to the deviation between net real-time schedules and net day-ahead schedules:

$$f_{l,t}^{RT} - \tilde{f}_{l,t}^{DA} = \Delta f_{l,t}^{RT} \approx \sum_{i\in\mathcal{N}} \Delta P_{i,t} S_{i,t}^{l,RT} = \Delta f_{l,t}^{RT,DC} \ , \tag{5.19}$$

where $\tilde{f}_{l,t}^{DA}$ is the branch flow on the real-time transmission network due to day-ahead schedules and $f_{l,t}^{RT}$ is the actual branch flow in the real-time market (for any branch l and time period t).

The congestion revenue collected in the real-time market can then be approximately calculated in terms of the change of line flow between the day-ahead and real-time markets:

$$CR_t^{RT} = -\sum_{l\in\mathcal{L}} \mu_{l,t}^{RT} \Delta f_{l,t}^{RT,DC} \ . \tag{5.20}$$

For the hourly real-time congestion revenue to remain positive, it is sufficient, though not necessary, for the congestion revenue to be positive on a constraint-by-constraint basis. This will hold true if for all real-time binding transmission constraints, the portion of the flow resulting from transactions cleared in the real-time market ($\Delta f_{l,t}^{RT}$) is zero or negative.

$$-\sum_{l\in\mathcal{L}} \mu_{l,t}^{RT} \Delta f_{l,t}^{RT,DC} \geq 0 \quad \Leftarrow \quad \Delta f_{l,t}^{RT,DC} \geq 0 \quad \forall l \in \mathcal{L} \tag{5.21}$$

With the real-time market being a cost minimization, it holds that the shadow price $\mu_{l,t}^{RT}$, corresponding to constraint (5.2) in the real-time economic dispatch problem satisfies $\mu_{l,t}^{RT} \leq 0$.

The constraint-level revenue adequacy condition for any time period t can be re-written based on the approximate relationship in (5.19):

$$f_{l,t}^{RT} - \tilde{f}_{l,t}^{DA} \approx \Delta f_{l,t}^{RT,DC} \geq 0 \quad \forall l \in \mathcal{L} \tag{5.22}$$

For real-time binding constraints, the real-time flow is equal to the real-time limit. Hence, we can write the real-time revenue adequacy condition in terms of actual flows:

$$\begin{aligned} &\tilde{f}_{l,t}^{DA} - f_{l,t}^{RT} \leq 0 \\ &\tilde{f}_{l,t}^{DA} \leq F_{l,t}^{\max,RT} \quad \forall l \in \mathcal{L} \end{aligned} \tag{5.23}$$

The result in (5.23) is similar to (5.12): both establish that to ensure revenue adequacy it is necessary to enforce transmission limits. In the same way that (5.12) cannot be enforced in practice because of insufficient knowledge of the day-ahead transmission system at the time of running the FTR auction, (5.23) cannot be enforced in practice because the topology and limits of the real-time transmission system are not fully known when the day-ahead market is cleared.

Therefore, the flow resulting from applying day-ahead transactions to the real-time model $\tilde{f}_{l,t}^{DA}$ cannot be calculated at the time of clearing the day-ahead market; hence it is replaced with the flow resulting from day-ahead transactions in the day-ahead model $f_{l,t}^{DA}$. Similarly, because real-time limits are not known with certainty when performing the day-ahead market calculations, the flow constraint applied in the day-ahead market to maintain revenue adequacy at a constraint level is:

$$f_{l,t}^{DA} \le F_{l,t}^{\max,DA} \quad \forall t, l \in \mathbf{\mathcal{L}}, \tag{5.24}$$

where $f_{l,t}^{DA}$ are the flows caused by day-ahead schedules, calculated using the model available when clearing the day-ahead market, and $F_{l,t}^{\max,DA}$ is the constraint limit modeled in the day-ahead market.

5.3 Revenue adequacy under existing coordination schemes

Maintaining conditions (5.12) and (5.23) is always challenging due to the unavoidable differences between the FTR and day-ahead models and the day-ahead and real-time models. However, two important drivers of revenue inadequacy could be avoided by improving inter-regional coordination:

a. Errors in the estimated share of the capacity of joint transmission facilities
b. Misrepresentation of the impact of imports and exports due to proxy interface modeling

In the following sections we discuss how the limitations of the existing inter-regional coordination schemes can negatively impact revenue adequacy.

In section 5.3.1 we discussed how the transmission capacity of shared facilities is modeled in markets currently, and how the market-to-market procedures discussed in section 1.1 affect

revenue adequacy conditions. In section 5.3.2 we discuss the impact of modeling transactions across markets using a proxy interface can affect revenue adequacy.

5.3.1 Transmission capacity of shared constraints

The models of the transmission system that an RTO uses for its market clearing processes do not only represent the portion of the transmission system that is under the operational control of the RTO. Some representation of external areas is needed to avoid errors in the calculation of power flows. Flows through transmission facilities internal to an RTO region can be impacted by external generation an load.

Transmission system operators identify constraints, usually near regional boundaries, where the flows are affected by transactions from more than one region. For these shared transmission constraints, operators can agree on what portion of the transmission capacity is owned by entities that reside within each transmission operator area. The limit applied to transmission constraints in the unit commitment and economic dispatch calculations performed by the market operator of area $a \in \boldsymbol{a}$ corresponds to the share of the transmission capacity corresponding to *a.*

$$f_l^a \le F_l^a \quad \forall l \in \boldsymbol{\ell}^a, \forall a \in \boldsymbol{a} \ , \tag{5.25}$$

where the total nominal transmission capacity of shared constraints is divided across neighboring regions such that:

$$\sum_{a \in \boldsymbol{a}} F_l^a = F_l^{max} \ . \tag{5.26}$$

One of the benefits of LMP-based markets is the ability to value incremental transmission capacity in terms of constraint shadow prices. In the long term, the shadow price of the transmission constraints in (2.15), enforced in the day-ahead and real-time economic dispatch calculations, can be used to guide the transmission planning process to invest in the most valuable transmission expansion projects.

In the short term, for shared transmission facilities, the shadow prices of transmission constraints (2.15) in the real-time economic dispatch calculations are an indicator of which RTO would derive the largest benefit from additional transmission capacity.

The market-to-market coordination process described in [33] relies on such real-time constraint shadow prices to decide when to shift transmission capacity of shared constraints between RTOs. Transmission capacity moves to the RTO with the largest shadow price (in

absolute value, as constraint (2.15) is bi-directional). For a transmission constraint *l* shared across regions $a, b \in \boldsymbol{a}$, moving ΔF MW of transmission capacity in the real-time market consists of changing the transmission limit imposed in each area from one time interval to the next such that:

$$\begin{aligned} F_{l,t}^{a,RT} &= F_{l,t-1}^{a,RT} - \Delta F \\ F_{l,t}^{b,RT} &= F_{l,t-1}^{b,RT} + \Delta F. \end{aligned} \tag{5.27}$$

The change in (5.27) would be applied within the market-to-market coordination when the magnitude of the shadow price of the constraint associated with transmission limit l is larger in area *b* than in area *a* ($\left|\mu_{l,t-1}^{a,RT}\right| < \left|\mu_{l,t-1}^{b,RT}\right|$).

For the RTO losing transmission capacity (*a*), this may result in the potential of real-time funding shortfall due to the lower transmission limit applied in the real-time market. That is, for the RTO losing transmission capacity in the real-time market:

$$F_{l,t}^{a,RT} < F_{l,t}^{a,DA} \tag{5.28}$$

So the application of the constraint (5.24) in the day-ahead clearing process is no longer a good proxy for the real-time revenue adequacy requirement in (5.23). Moreover, the transfer of real-time transmission capacity may result in subsequent reduction of day-ahead limits. If this happens, the limit applied in the FTR model may be larger than the day-ahead limit for shared constraints:

$$F_{l,t}^{a,DA} < F_{l,t}^{a,FTR} \tag{5.29}$$

If (5.29) holds, (5.13) is no longer an adequate proxy for the FTR revenue adequacy condition in (5.12).

In summary, while market-to-market procedures may improve the utilization of shared transmission facilities in the real-time markets, the resulting transfer of transmission capacity across areas may cause real-time and, indirectly, FTR revenue inadequacy.

5.3.2 Transactions across regions

RTOs model imports and exports as injected or withdrawn from a proxy interface, which is a collection of buses that represents the interface with a neighboring region.

Figure 5.1 shows a transaction, T, of 100 MW between two areas. In this context, a transaction is a combination of a power sale of a certain MW volume at one location (source) and

a purchase of the same MW volume at a different location (sink). In a transaction across areas, the source and the sink of the transaction reside within different RTO regions or areas.

The flows produced across the transmission network due to T depend only on the network topology. Conceptually, splitting transaction T in Figure 5.1 into a pair of transactions, T-I and T-II, each internal to a single region, sourcing or sinking at the proxy interface aggregate, as shown in Figure 5.2 does not have an impact on the power flow, as long as the representation of the interface is the same across regions.

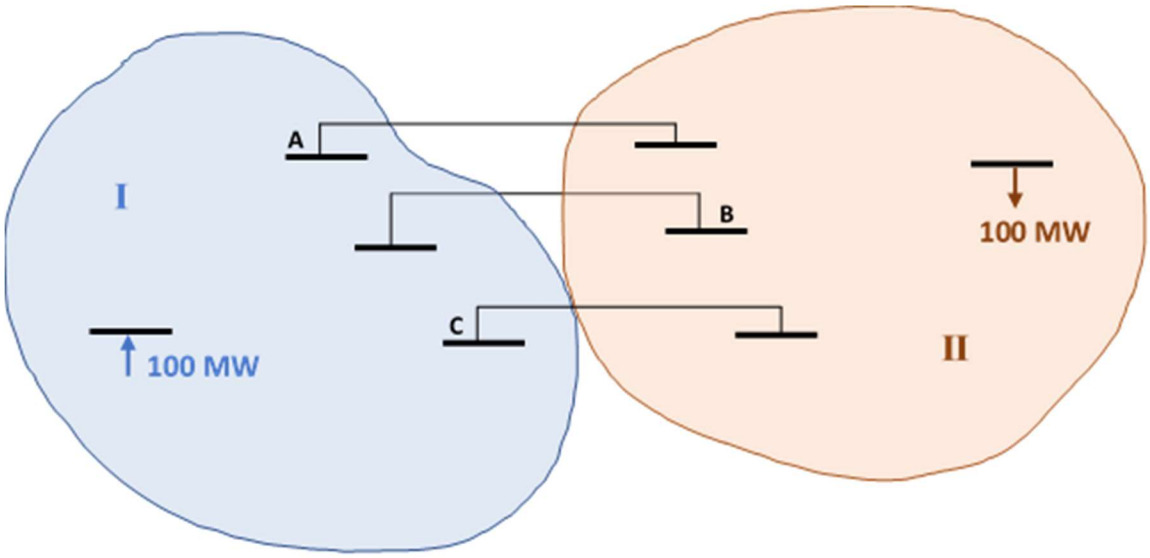

Figure 5.1. Representation of an inter-regional transaction

The net injections and withdrawals in Figure 5.1 and Figure 5.2 are equivalent, as they produce the same flows across the entire system. The proxy interface is arbitrarily defined by the market operator as a bus aggregate with its associated weighting factors. For example, in Figure 5.2, the proxy interface is defined as an aggregate of buses A, B and C, with weights 0.3, 0.4 and 0.3, respectively.

In the model that the exporting region (area I) uses to clear the FTR and day-ahead markets, transaction T is represented only by the internal portion T-I, as shown in Figure 5.3. The flows produced in the exporting system due to T-I depend on the definition of the proxy interface aggregate, which by being fixed and arbitrarily defined, cannot represent the varying way in which the transaction flows into the importing region in real-time. The actual flows across the interconnection between the two regions depend on the transmission system topology and on the

combined dispatch of both systems. Under the existing inter-regional coordination schemes, the representation of the external transmission system is incomplete, and external generation and load are unknown.

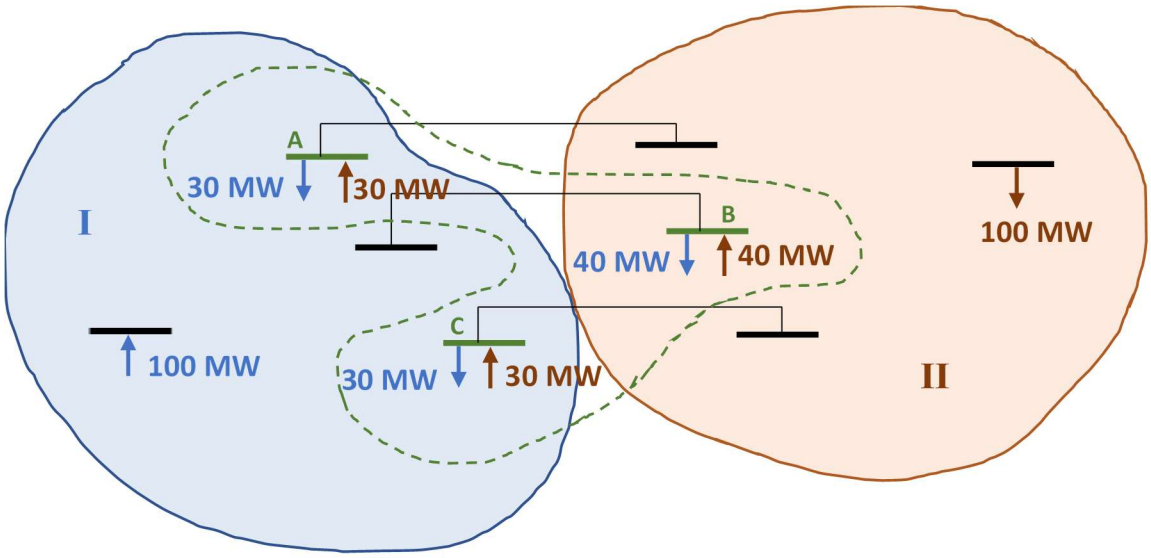

Figure 5.2. Representation of an inter-regional transaction split at the interface

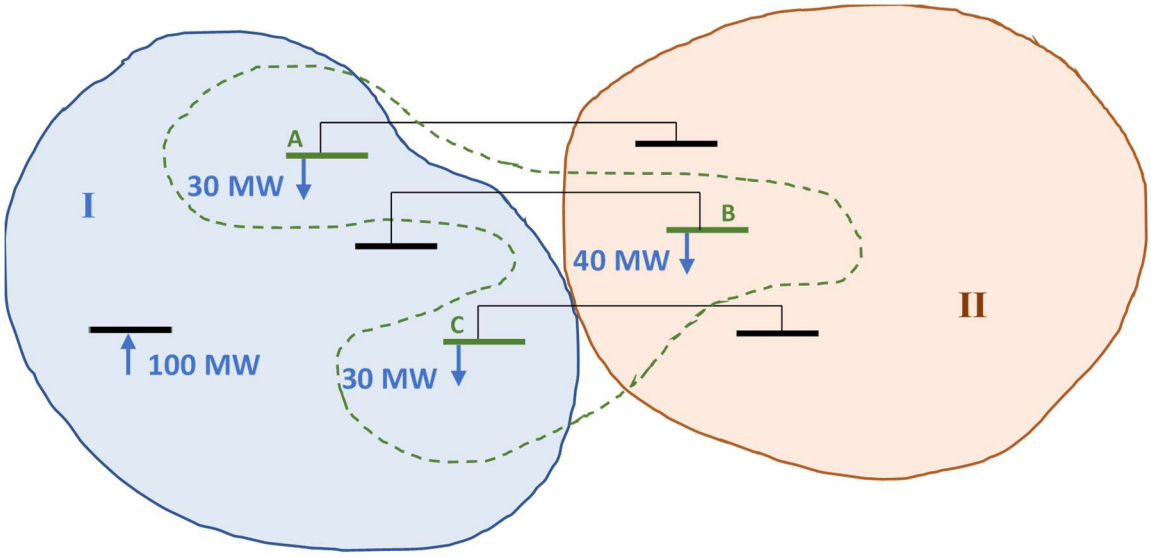

Figure 5.3. Day-ahead representation of an inter-regional transaction (exporting region)

Figure 5.4 represents the transaction T in the real-time market. Flows across the interface depend on the physical state of the transmission system. While settlement of transaction T is still calculated based on the proxy interface aggregate price, in the real-time market an export is measured in terms of the net interchange between areas. The target net interchange is calculated based on scheduled imports and exports, and within each region, generation is dispatched to maintain the interchange at its scheduled values.

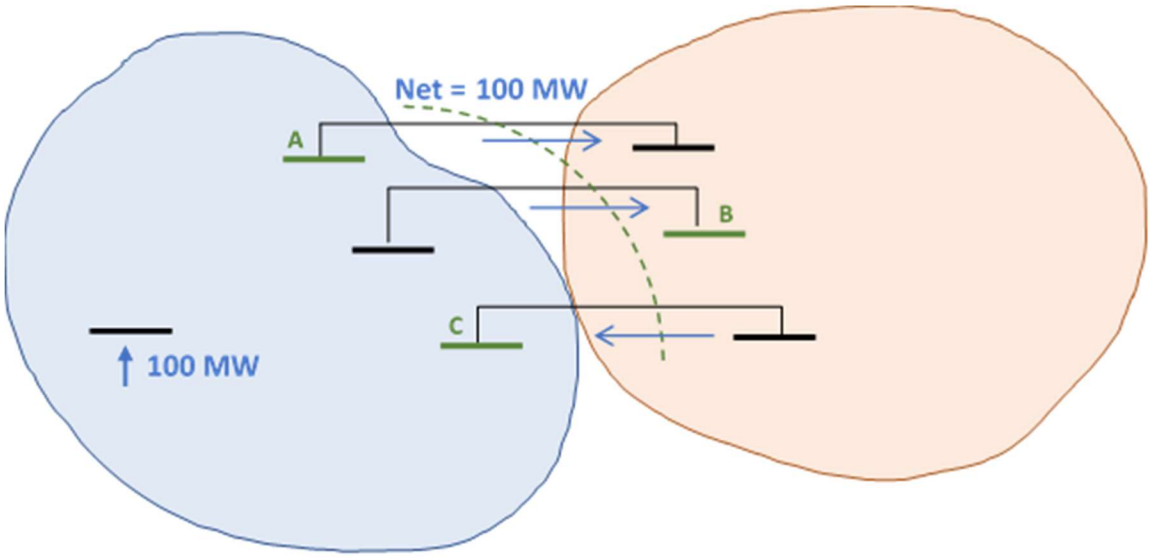

Figure 5.4. Real-time representation of an inter-regional transaction (export region)

The difference between the export as represented in Figure 5.3 and actual physical flow across regions in real-time represented in Figure 5.4 could result in a transaction that is feasible in the day-ahead market to become infeasible in real-time. Because of the representation of cross-border transactions using proxy interface aggregates, the flows in the day-ahead model due to day-ahead schedules deviate from the flows produced by day-ahead schedules applied to the real-time model. That is, $f_{l,t}^{DA} \neq \tilde{f}_{l,t}^{DA}$. As such, feasibility in the day-ahead market (5.24) no longer ensures that the condition for real-time revenue adequacy (5.23) is met.

In the next section, we describe how the coordinated market clearing processes proposed in Chapters 3 and 4 for the day-ahead and FTR markets, eliminate the need to estimate area shares of the capacity of transmission constraints or define proxy interfaces.

5.4 Revenue adequacy under a coordinated day-ahead solution

The coordinated day-ahead clearing algorithm presented in Chapter 3 results in a commitment solution that can reduce considerably the inefficiencies associated with poor inter-regional coordination. While the simulation cases presented showed considerable efficiency gains, the proposed coordinated solution is not guaranteed to be identical to the ideal single-area unit commitment solution.

However, the solution of the coordinated economic dispatch problem will converge towards the single area economic dispatch solution for a given generation commitment state. That is true because, as shown in [8], ADMM is guaranteed to reach the single area solution for a strongly-convex quadratic program. As shown in Appendix B, the power flow equations of the single-area problem are equivalent to the power flow equations of the multi-area coordinated problem when the consensus value of the boundary phase angles are found. That means that the multi-area solution flows are feasible with respect to the single-area solution limits.

In the proposed multi-regional day ahead clearing algorithm, as the primal residual in (3.23) approaches zero, the boundary conditions across regions become equivalent, resulting in a multi-regional power flow solution equivalent to the single area solution. The same holds for the multi-area FTR auction results obtained when the primal residual in (4.23) converges to zero: the multi-area FTR auction solution becomes identical to the single-area auction. This means that both the coordinated day-ahead solution and the coordinated FTR solution produce results that are feasible with respect to the limits of the entire interconnected transmission system.

Neither solution requires the definition of an arbitrary proxy interface aggregate or relies on splitting the transmission capacity of shared constraints to represent the interaction of the interconnected systems. With the proposed coordinated market clearing approach, there is no need to identify which facilities will be impacted by external flows or estimate the extent to which they would have to be derated.

The FTR revenue adequacy condition in (5.10) can be stated for the multi-area system as:

$$\sum_{a\in\boldsymbol{a}} \Pi^{a,t} \le \sum_{a\in\boldsymbol{a}} CR_t^{a,DA} \quad , \tag{5.30}$$

where the total FTR payments can be calculated as a function of the FTR flows in the day-ahead model.

$$\Pi^{a,t} = -\sum_{l\in\boldsymbol{\ell}} \mu_{l,t}^{a,DA} \tilde{f}_{l,t}^{a,FTR} \tag{5.31}$$

The flows in the day-ahead market resulting from the application of outstanding FTRs to the day-ahead model cannot, for the coordinated case, be calculated without knowledge of the external topology. While we can still define, in the same way we do for the single-area problem in (5.5), for the DC power flow approximation, the flow produced by FTRs if applied as injections and withdrawals to the day-ahead model:

$$\tilde{f}_{l,t}^{a,FTR} := \sum_{n \in \mathcal{F}^l} q_n^a S_{ij,t}^{l,DA}. \tag{5.32}$$

The term $S_{ij,t}^{l,DA}$ can only be computed with information of the entire interconnected system.

The hourly revenue adequacy condition for the multi-area case (5.30) is satisfied at a system-wide level if it is satisfied for each binding constraint in every area $a \in \boldsymbol{a}$:

$$-\mu_{l,t}^{a,DA} \tilde{f}_{l,t}^{a,FTR} \leq -\mu_{l,t}^{a,DA} f_{l,t}^{a,DA} \quad \forall l \in \boldsymbol{\mathcal{L}}^a, \forall a \in \boldsymbol{a} \tag{5.33}$$

Because the shadow prices of binding transmission constraints are non-positive, the constraint-level revenue adequacy condition can be written as:

$$\tilde{f}_{l,t}^{a,FTR} \leq F_{l,t}^{\max,DA} \quad \forall l \in \boldsymbol{\mathcal{L}}^a, \forall a \in \boldsymbol{a} \tag{5.34}$$

The day-ahead market model is unknown at the time of clearing the FTR auction. The flow constraints in the FTR auction are calculated based on the topology and limits known at the time of clearing the auction.

$$f_{l,t}^{a,FTR} \leq F_l^{\max,FTR} \quad \forall l \in \boldsymbol{\mathcal{L}}^a, \forall a \in \boldsymbol{a} \tag{5.35}$$

The important difference between the constraint (5.35) enforced in the coordinated FTR auction and (5.25), enforced in the existing coordination schemes, is that there is no need for each area operator to estimate their share of the constraint limit. The right-hand side of (5.35) is the total constraint transmission capacity $F_l^{max,FTR}$ and not a pre-calculated share of the transmission capacity $F_l^{(a),FTR}$.

The same applies to the multi-area real-time revenue adequacy condition enforced in the day-ahead market clearing process:

$$f_{l,t}^{a,DA} \leq F_{l,t}^{\max,DA} \quad \forall l \in \boldsymbol{\mathcal{L}}^a, \forall a \in \boldsymbol{a} \tag{5.36}$$

The right-hand side of (5.36) is the actual total MW limit of the transmission constraint, and not an estimate of the transmission constraint capacity corresponding to area a, as in the representation of the current state in (5.25).

In addition to eliminating the need to split the capacity of shared transmission constraints before clearing the FTR and day-ahead markets, the multi-area day-ahead and FTR market solutions proposed in Chapters 3 and 4 eliminate the need to define a proxy interface. Under the proposed coordinated clearing processes, cross-border transactions are not modeled as sourcing or sinking at the proxy interface aggregate. In the coordinated solution, there is no need to split transactions into components that are internal to a single area, as shown in Figure 5.2. Instead, in the day-ahead market, generation and load bids are entered, and the optimal flow of power across areas will be automatically calculated without the need to explicitly represent cross-border transactions. Cross border flows will be calculated based on the physical representation of the transmission systems and will not depend on any arbitrary interface definition. As such, no revenue inadequacy results from the inaccurate representation of cross-border transactions sourcing or sinking at a proxy interface.

5.4.1 Regional revenue adequacy and use of external transmission

One of the main implementation challenges that a fully coordinated market may face has to do with the shared use of transmission facilities under a coordinated scheme. Under the coordinated day-ahead clearing process presented in Chapter 3, we attempt to allocate transmission capacity in the optimal manner, without regard of where the generation and load that cause the flow through each transmission element reside. However, the construction and maintenance of the transmission system is paid for by the transmission customers of each RTO, with the expectation that such transmission will be used to deliver power to their load. In a coordinated set of neighboring areas, the transmission owned by entities in one region may be used to serve the load of entities in another region.

In this section we propose a redistribution of congestion revenues that would compensate entities in each RTO for the use of their transmission system by external entities. This section shows the calculation of an inter-RTO settlement that can be done after all markets (FTR, day-ahead and real-time) have been settled within every region. Nothing shown in this section affects the market clearing calculations or change in any way how generation and load are dispatched.

In the previous section we showed that the proposed coordinated FTR auction and coordinated day-ahead clearing process can improve system-wide revenue adequacy. However, inter-regional coordination will not guarantee revenue adequacy within each area. Consequently,

in a coordinated group of interconnected market regions, congestion rents should be aggregated and distributed across all interconnected RTOs to cover financial obligations associated with FTRs and day-ahead schedules.

Since only binding constraints may have nonzero shadow prices, we can re-write the day-ahead congestion rents collected in the day-ahead market (5.9) in terms of the limit of transmission constraints:

$$CR_t^{DA} = -\sum_{l \in \mathcal{L}} \mu_{l,t}^{DA} F_{l,t}^{\max,DA} \tag{5.37}$$

Transmission facilities may be jointly owned by transmission companies that are members of separate RTOs. If F_l^a is the portion of the transmission capacity of a line that is owned by members of the RTO that operates area *a*, the congestion revenue that should be allocated to entities in *a* can be written as:

$$CR_t^{a,DA} = -\sum_{l \in \mathcal{L}^a} \mu_{l,t}^{DA} F_{l,t}^{a,DA} \quad . \tag{5.38}$$

Based on (5.38), only the revenues associated with the portion of a transmission constraint that is owned by entities in *a* is kept by the operator of area *a*.

As shown in (5.26), the sum across all areas in $\mathcal{A}$ of the area share of the transmission capacity of a branch must be equal to the flow limit of the branch,. Therefore, the sum of (5.38) for all areas equals the congestion rents collected across the entire interconnected system.

$$CR_t^{DA} = \sum_{a \in \mathcal{A}} CR_t^{a,DA} = -\sum_{a \in \mathcal{A}} \sum_{l \in \mathcal{L}^a} \mu_{l,t}^{DA} F_{l,t}^{a,DA} \quad . \tag{5.39}$$

Let $\hat{f}_{l,t}^{(a),DA}$ be the flows caused by serving the day-ahead load in area *a*. For a DC power flow, the total flow through a line is the sum of the flow caused by all contributing transactions.

$$f_{l,t}^{DA} = \sum_{a \in \mathcal{A}} \hat{f}_{l,t}^{a,DA} \tag{5.40}$$

The congestion charges incurred by entities in area *a* can be written as:

$$CC_t^{a,DA} = -\sum_{l \in \mathcal{L}^a} \mu_{l,t}^{DA} \hat{f}_{l,t}^{a,DA} \tag{5.41}$$

The congestion rents collected by area *a* if the regional congestion rents are distributed across areas based on (5.38) may not be equivalent to the congestion charges paid by entities in *a*, as calculated in (5.41). On a constraint-by-constraint basis, the difference between congestion charges and congestion rents is:

$$\omega_{l,t}^{a,DA} = -\mu_{l,t}^{DA} \hat{f}_{l,t}^{(a),DA} - \left(-\mu_{l,t}^{DA} F_{l,t}^{(a),DA}\right) = -\mu_{l,t}^{DA} \left(\hat{f}_{l,t}^{(a),DA} - F_{l,t}^{(a),DA}\right) \tag{5.42}$$

The charge in (5.42) is negative if the owned transmission capacity is larger than the transmission capacity utilized by entities in *a*, and can be viewed as a credit to entities in *a*. With congestion rents distributed based on (5.38), entities in *a* will pay into the multi-regional market a net charge of:

$$\omega_t^{a,DA} = -\sum_{l \in \mathcal{L}} \mu_{l,t}^{DA} \left(\hat{f}_{l,t}^{(a),DA} - F_{l,t}^{(a),DA} \right) . \tag{5.43}$$

The charge in (5.43) can be interpreted as the payment for utilizing external transmission capacity in the multi-area coordinated market clearing. This charge does not have to be explicitly computed: it is included in the hourly load settlement of all entities.

In this chapter we have shown that the multi-regional market clearing processes proposed have the potential of reducing revenue inadequacy in both the FTR and real-time markets across the entire interconnected system. However, revenue adequacy is not maintained at the individual area level. The improved utilization of the transmission system that results from the proposed day-ahead coordination can result in transmission system capacity being utilized by entities that do not pay for their construction and maintenance. In this last section, we present a redistribution of congestion revenues that provides an inter-RTO settlement mechanism for entities in each area to pay for the use of external transmission facilities or to get paid for allowing external entities to use their transmission facilities.

CONCLUSIONS AND FUTURE WORK

LMP-based RTO markets have brought many benefits to the operation of the wholesale electric power system: generation commitment and dispatch based on a cost minimization algorithm has increased the efficiency of the utilization of transmission capacity and reduced the use of transaction curtailment as a congestion management tool. These benefits, however, have not been extended to the coordination across RTO boundaries.

While existing coordination schemes have introduced economic considerations in the scheduling of electric power transactions across RTOs, those schemes are limited to the real-time markets and are not designed to find a system-wide optimal solution. Rather, they are designed to make incremental dispatch changes due to cross-border considerations. Because the day-ahead market is largely cleared without optimizing inter-regional transactions, generation commitment decisions are made without considering the availability of external generation resources.

In this work we proposed an algorithmic framework for clearing electricity markets that extends the benefits of market-based congestion management across RTO boundaries. Distributed optimization techniques have been applied to the economic dispatch problem, which finds the optimal generation schedules for a pre-determined commitment solution. The application of those techniques to the mixed-integer optimization solved in the day-ahead market to calculate generation commitment decisions is challenging. The heuristic approach proposed in this work is designed to overcome such challenges, in part by taking advantage of some of the unique features of the market clearing process, which normally solves the unit commitment mixed-integer program, followed by the, usually convex, economic dispatch calculation. The proposed solution is a heuristic extension of the alternating directions method of multipliers (ADMM) for the consensus optimization problem.

In comparisons between the proposed coordinated solution method, the ideal scenario where the entire system is treated as a single region, and a representation of the current, uncoordinated solution, the proposed algorithm achieved significant cost savings in all of the numerical simulations, ranging from 58% to 82% in terms of maximum potential savings. In the context of

the annual cost of electric generation in the US, this efficiency improvement represents savings of nearly $7 billion per year.[10]

With a large portion of the load in RTO markets being served through bilateral power purchase agreements or generation owned by load serving entities, the availability of longer-term hedging mechanisms is fundamental to the operation of electricity markets. Recognizing that, we propose a design for a multi-regional auction for financial transmission rights (FTRs) based on consensus optimization using ADMM. The proposed auction design allows market participants to acquire FTRs sourcing and sinking in different regions in the same way that they would acquire FTRs within the same region.

In addition to allowing for scheduling and hedging of cross-border transactions, the proposed design addresses the incomplete pricing that arises from uncoordinated market operations.

Finally, we show that the application of the proposed coordinated market mechanisms meets the revenue adequacy conditions for the entire interconnected system and reduces the potential shortfall arising from the usually inaccurate representation of the impact of external transactions in independently cleared markets. While revenue adequacy is not maintained at an internal level, we show that the transfer of congestion rents from one area to the other within the proposed design can be interpreted as a payment made by members of one RTO for the use of transmission facilities owned by members of external RTOs.

Beyond the efficiencies gained by integrating the market clearing processes of neighboring regions, improved inter-regional coordination is a key tool to achieve larger penetration of renewable electric power sources. The change in the generation matrix that will be required to reduce greenhouse emissions will bring considerable shifts in the way we manage electricity markets.

Renewable resources tend to be geographically congregated, often far from load; hence their full utilization may require moving large amounts of electric power across long distances. The highly variable availability of such renewable generation may require the integration of a larger geographic area and a larger number of generators to reduce the risk of loss of load by diversifying sources of power and connecting renewable resources with other technologies.

Several studies, such as [9,20], performed to evaluate the transition to the levels of clean generation required to meet current CO_2 reduction targets, indicate the need for investment in inter-

[10]2019 data from the US Energy Information Administration (https://www.eia.gov/electricity/data.php)

regional transmission. In this work we showed that lack of coordination across markets would create dispatch schedules that under-utilize available cross-border transmission, but also, that lack of transparent price signals may fail to highlight the need for investment in inter-regional transmission.

In order to take full advantage of the expanded set of shared resources available in a multi-area day-ahead market to support resource adequacy, the coordinated market design could potentially be extended to capacity markets.

The proposed coordinated market clearing processes can bring substantial efficiencies under existing operating conditions, and potentially more as the electric power system transitions to cleaner generation technologies. However, their implementation would require harmonizing RTO bidding and clearing schedules and investing in computational resources.

While the proposed clearing mechanisms will unavoidably be more computationally intensive than current clearing methods, more work is needed to optimize algorithm performance. Performance improvements may include a better selection of parameters and changes in the frequency of updates of consensus variables.

APPENDIX A. UNIT COMMITMENT CASES

14-BUS CASE

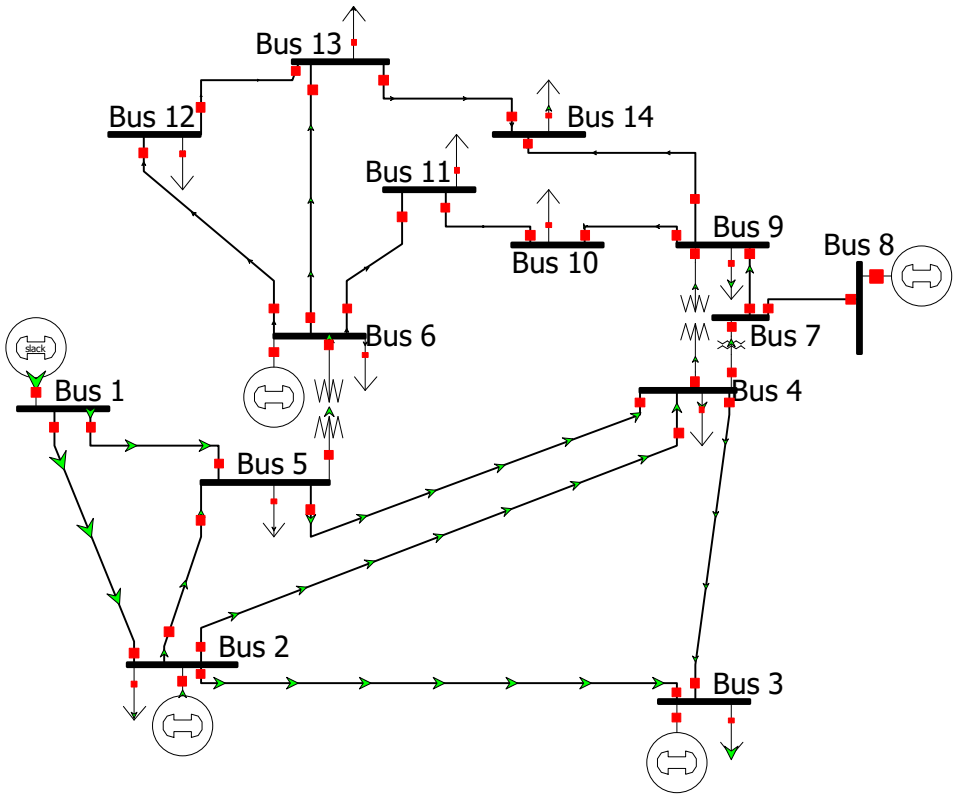

Figure A.1. 14-bus model used for the unit commitment calculations

Table A.1. 14-bus case: Buses

Number	Area Number	Name
1	1	Bus 1
2	1	Bus 2
3	1	Bus 3
4	1	Bus 4
5	1	Bus 5
6	1	Bus 6
7	2	Bus 7
8	2	Bus 8
9	2	Bus 9
10	2	Bus 10
11	2	Bus 11
12	2	Bus 12
13	2	Bus 13
14	2	Bus 14

Table A.2. 14-bus case: Branches

Line ID	Thermal Limit (MW)	x (pu)	From Bus	To Bus
1	200	0.000592	1	2
2	100	0.00223	1	5
3	100	0.00198	2	3
4	100	0.001763	2	4
5	100	0.001739	2	5
6	100	0.00171	3	4
7	100	0.000421	4	5
8	100	0.002091	4	7
9	100	0.005562	4	9
10	100	0.00252	5	6
11	100	0.001989	6	11
12	100	0.002558	6	12
13	100	0.001303	6	13
14	120	0.001762	7	8
15	120	0.0011	7	9
16	100	0.000845	9	10
17	100	0.002704	9	14
18	100	0.001921	10	11
19	100	0.001999	12	13
20	100	0.00348	13	14

Table A.3. 14-bus case: Load

Load ID	Bus ID	Peak MW
1	2	32.55
2	3	141.3
3	4	71.7
4	5	11.4
5	6	16.8
6	9	44.25
7	10	13.5
8	11	5.25
9	12	9.15
10	13	20.25
11	14	22.35

Load was scaled identically across the entire interconnected system model.

Table A.4. 14-bus case: Load profile

HE	Demand factor
1	0.567
2	0.567
3	0.600
4	0.667
5	0.700
6	0.733
7	0.800
8	0.867
9	0.900
10	0.900
11	0.900
12	0.920
13	0.933
14	0.933
15	0.967
16	0.967
17	0.967
18	1.000
19	0.967
20	0.933
21	0.867
22	0.800
23	0.733
24	0.667

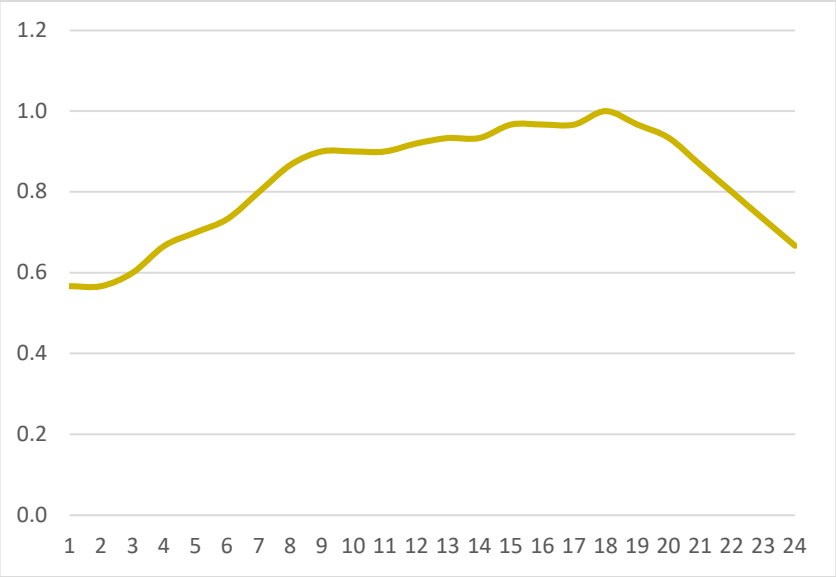

Figure A.2. 14-bus case: Load profile

Table A.5. 14-bus case: Interface definition

Line ID	From Bus	To Bus	From Area	To Area	Weight	Metered side (pricing calculation)
8	4	7	1	2	0.3	1
9	4	9	1	2	0.23	1
11	6	11	1	2	0.07	1
12	6	12	1	2	0.13	2
13	6	13	1	2	0.27	2

Table A.6. 14-bus case: Generators

Gen ID	Bus ID	Output limits (MW)		Maximum ramp rates (MW/h)		Minimum times (h)		T^{init} (h)	T^{cold} (h)	Cost						P^{init} (h)
		Maximum	Minimum	Up	Down	Run	Down			No Load ($)	Linear ($/MW)	Quadratic ($/MW^2)	Shut down($)	Hot Startup($)	Cold Startup($)	
1	1	350	100	225	225	2	2	8	5	1000	16.19	0.00048	0	4500	9000	235
2	2	40	10	60	60	1	1	1	4	450	19.7	0.00398	0	900	1800	31.7
3	8	250	30	60	60	1	1	-1	4	450	18.7	0.00356	0	900	1800	0

200-BUS CASE

Table A.7. 200-bus case: Buses

Number	AreaNumber	Name
1	1	CREVE COEUR 0
2	1	CREVE COEUR 1
3	2	ILLIOPOLIS 0
4	2	ILLIOPOLIS 1
5	3	PAXTON 2 0
6	3	PAXTON 2 1
7	1	PEORIA 9 0
8	1	PEORIA 9 1
9	1	PEORIA 8 0
10	1	PEORIA 8 1
11	2	LOVINGTON 0
12	2	LOVINGTON 1
13	2	LOVINGTON 2
14	2	DECATUR 3 0
15	2	DECATUR 3 1
16	2	DECATUR 3 2
17	2	MASON CITY 0
18	2	MASON CITY 1
19	2	MASON CITY 2
20	2	MASON CITY 3
21	2	MASON CITY 4
22	2	BETHANY 0
23	2	BETHANY 1
24	2	BETHANY 2
25	3	RANKIN 0
26	3	RANKIN 1
27	2	WINDSOR 0
28	2	WINDSOR 1
29	1	PEKIN 2 0
30	1	PEKIN 2 1
31	3	HEYWORTH 0
32	3	HEYWORTH 1
33	3	HEYWORTH 2
34	2	DECATUR 2 0
35	2	DECATUR 2 1
36	3	LINCOLN 0
37	3	LINCOLN 1
38	3	LINCOLN 2
39	2	SHERMAN 0
40	2	SHERMAN 1
41	3	URBANA 2 0
42	2	SPRINGFIELD 8 0
43	1	CARLOCK 0
44	2	PLEASANT PLAINS 0
45	3	LE ROY 0
46	3	LE ROY 1
47	2	DECATUR 1 0
48	3	RANTOUL 2 0
49	3	RANTOUL 2 1
50	3	RANTOUL 2 2
51	3	RANTOUL 2 3
52	3	RANTOUL 2 4
53	3	RANTOUL 2 5
54	2	MACON 0
55	3	ELLSWORTH 2 0
56	3	ELLSWORTH 2 1
57	2	MOUNT PULASKI 0
58	3	WAPELLA 0
59	1	ROANOKE 0
60	1	GREEN VALLEY 0
61	3	BLOOMINGTON 3 0
62	2	SPRINGFIELD 7 0
63	2	BEMENT 0
64	3	PAXTON 1 0
65	3	PAXTON 1 1
66	2	MOUNT ZION 0
67	2	MOUNT ZION 1
68	2	MOUNT ZION 2
69	2	MOUNT ZION 3
70	2	MOUNT ZION 4
71	2	MOUNT ZION 5
72	2	MOUNT ZION 6
73	2	MOUNT ZION 7
74	3	RANTOUL 1 0
75	1	BRIMFIELD 0
76	1	BRIMFIELD 1
77	1	BRIMFIELD 2
78	1	BRIMFIELD 3
79	1	BRIMFIELD 4
80	3	WELDON 0
81	3	GIBSON CITY 2 0
82	3	GIBSON CITY 2 1
83	3	MINIER 0
84	1	HUDSON 0
85	2	ATHENS 0
86	1	PEORIA HEIGHTS 0
87	2	SPRINGFIELD 6 0
88	2	SPRINGFIELD 6 1
89	3	CLINTON 3 0
90	3	CLINTON 3 1

Number	AreaNumber	Name
91	3	CLINTON 3 2
92	3	CLINTON 3 3
93	2	TUSCOLA 2 0
94	2	TUSCOLA 2 1
95	3	KENNEY 0
96	3	MANSFIELD 0
97	1	MANITO 0
98	1	DUNLAP 0
99	1	DUNLAP 1
100	3	CHAMPAIGN 3 0
101	1	PEORIA 7 0
102	3	ELLSWORTH 1 0
103	3	ELLSWORTH 1 1
104	3	ELLSWORTH 1 2
105	3	ELLSWORTH 1 3
106	3	TOWANDA 0
107	3	BLOOMINGTON 2 0
108	1	PRINCEVILLE 0
109	2	DELAVAN 0
110	1	PEORIA 6 0
111	3	SAVOY 0
112	3	NORMAL 2 0
113	3	NORMAL 2 1
114	3	NORMAL 2 2
115	3	NORMAL 2 3
116	1	EAST PEORIA 0
117	1	EAST PEORIA 1
118	1	HANNA CITY 0
119	1	METAMORA 0
120	2	GREENVIEW 0
121	3	CLINTON 2 0
122	3	CLINTON 2 1
123	1	BARTONVILLE 0
124	1	BARTONVILLE 1
125	1	BARTONVILLE 2
126	1	BARTONVILLE 3
127	1	BARTONVILLE 4
128	3	NORMAL 1 0
129	3	NORMAL 1 1
130	3	LEXINGTON 0
131	1	PEORIA 5 0
132	1	MORTON 0
133	1	PEKIN 1 0
134	1	PEKIN 1 1
135	1	PEKIN 1 2
136	1	PEKIN 1 3
137	2	NIANTIC 0
138	3	COLFAX 0
139	1	EL PASO 0

Number	AreaNumber	Name
140	1	TREMONT 0
141	1	PEORIA 4 0
142	1	PEORIA 3 0
143	3	CHAMPAIGN 2 0
144	1	EUREKA 0
145	2	CHATHAM 0
146	3	HOPEDALE 2 0
147	3	HOPEDALE 2 1
148	1	WASHINGTON 0
149	2	SPRINGFIELD 5 0
150	2	SPRINGFIELD 5 1
151	2	SPRINGFIELD 5 2
152	2	SPRINGFIELD 5 3
153	2	SPRINGFIELD 5 4
154	2	SPRINGFIELD 5 5
155	2	SPRINGFIELD 5 6
156	1	PEORIA 2 0
157	1	PEORIA 2 1
158	2	MT ZION 0
159	2	BUFFALO 0
160	2	SPRINGFIELD 4 0
161	2	SPRINGFIELD 4 1
162	1	CONGERVILLE 0
163	3	CHAMPAIGN 1 0
164	3	CHAMPAIGN 1 1
165	3	CHAMPAIGN 1 2
166	3	CHAMPAIGN 1 3
167	3	CHAMPAIGN 1 4
168	3	CHAMPAIGN 1 5
169	3	CHAMPAIGN 1 6
170	3	CHAMPAIGN 1 7
171	3	FISHER 0
172	3	HOMER 0
173	3	TUSCOLA 1 0
174	3	WHITE HEATH 0
175	3	TOLONO 0
176	2	SPRINGFIELD 3 0
177	3	MACKINAW 0
178	3	URBANA 1 0
179	3	URBANA 1 1
180	3	SAINT JOSEPH 0
181	2	SPRINGFIELD 2 0
182	2	SPRINGFIELD 2 1
183	2	SPRINGFIELD 2 2
184	3	MONTICELLO 0
185	2	AUBURN 0
186	1	HOPEDALE 1 0
187	3	CLINTON 1 0
188	3	CLINTON 1 1

Number	AreaNumber	Name
189	3	CLINTON 1 2
190	3	MAHOMET 0
191	3	VILLA GROVE 0
192	3	BLOOMINGTON 1 0
193	1	PEORIA 1 0
194	2	SPRINGFIELD 1 0

Number	AreaNumber	Name
195	3	GIBSON CITY 1 0
196	3	GIBSON CITY 1 1
197	3	GIBSON CITY 1 2
198	1	MAPLETON 0
199	3	GIFFORD 0
200	2	PETERSBURG 0

Table A.8. 200-bus case: Branches

Line ID	Thermal Limit (MW)	x (pu)	From Bus	To Bus
1	100	0.00334	2	1
2	221.1	0.11976	1	119
3	221.1	0.03627	124	1
4	221.1	0.0275	193	1
5	100	0.0033	4	3
6	221.1	0.0581	57	3
7	221.1	0.03804	3	137
8	100	0.00334	6	5
9	221.1	0.04351	48	5
10	221.1	0.05487	5	64
11	100	0.00319	8	7
12	221.1	0.02426	7	86
13	221.1	0.02323	7	101
14	221.1	0.05598	7	148
15	100	0.00397	10	9
16	221.1	0.05512	9	124
17	221.1	0.02673	131	9
18	221.1	0.03097	9	141
19	221.1	0.02524	9	193
20	100	0.00353	12	11
21	100	0.00361	13	11
22	221.1	0.06722	11	15
23	221.1	0.12814	11	93
24	221.1	0.0582	158	11
25	300	0.02753	15	14
26	195	0.0501	14	121
27	195	0.06524	14	149
28	100	0.0032	16	15
29	100	0.00393	18	17
30	100	0.00308	19	17
31	100	0.00334	20	17
32	100	0.00394	21	17
33	221.1	0.0682	109	17
34	221.1	0.07047	17	120
35	100	0.00322	23	22
36	100	0.00307	24	22
37	221.1	0.07349	22	27
38	221.1	0.08677	158	22

Line ID	Thermal Limit (MW)	x (pu)	From Bus	To Bus
39	100	0.00307	26	25
40	221.1	0.05324	25	64
41	221.1	0.064	199	25
42	100	0.00396	28	27
43	221.1	0.17536	27	93
44	221.1	0.13195	27	158
45	100	0.00313	30	29
46	221.1	0.03874	124	29
47	221.1	0.055	29	140
48	100	0.00388	32	31
49	100	0.00364	33	31
50	221.1	0.05856	177	31
51	221.1	0.05525	192	31
52	100	0.00367	35	34
53	221.1	0.04282	34	54
54	221.1	0.04464	34	137
55	100	0.00333	37	36
56	100	0.00351	38	36
57	221.1	0.07439	58	36
58	221.1	0.06699	83	36
59	100	0.0031	40	39
60	221.1	0.06062	39	85
61	221.1	0.05108	159	39
62	221.1	0.02968	41	100
63	221.1	0.02162	41	163
64	221.1	0.06077	41	180
65	221.1	0.08538	44	42
66	221.1	0.05579	181	42
67	221.1	0.0513	43	84
68	221.1	0.0755	43	132
69	221.1	0.10119	44	200
70	160	0.04919	46	45
71	135	0.01853	55	45
72	135	0.02071	102	45
73	135	0.02482	45	187
74	221.1	0.04856	61	46
75	221.1	0.06542	122	46
76	221.1	0.04562	47	54
77	221.1	0.0474	47	66
78	28.9	0.53202	49	48
79	28.7	0.40417	50	48
80	24.3	0.61271	51	48
81	24.3	0.37982	52	48
82	35.3	0.57655	53	48
83	221.1	0.05437	48	74
84	221.1	0.04554	54	66
85	160	0.12465	56	55
86	402.4	0.03905	81	55
87	402.4	0.0089	55	102

Line ID	Thermal Limit (MW)	x (pu)	From Bus	To Bus
88	402.4	0.02976	55	112
89	402.4	0.02439	55	128
90	221.1	0.02983	56	103
91	221.1	0.05137	57	159
92	221.1	0.06353	95	58
93	221.1	0.09597	177	58
94	221.1	0.0724	59	119
95	221.1	0.06243	59	139
96	221.1	0.07928	60	97
97	221.1	0.06275	134	60
98	221.1	0.04556	61	103
99	221.1	0.05898	159	62
100	221.1	0.05314	160	62
101	221.1	0.08324	63	66
102	221.1	0.11602	63	184
103	195.5	0.10157	65	64
104	221	0.158	82	64
105	30	0.14479	67	66
106	73	0.265	68	66
107	70.5	0.09499	69	66
108	70.5	0.19945	70	66
109	68	0.08154	71	66
110	68	0.0746	72	66
111	65	0.14642	73	66
112	221.1	0.03225	66	158
113	221.1	0.06076	74	190
114	24.3	0.78433	76	75
115	7.4	2.19211	77	75
116	65	0.18141	78	75
117	62.1	0.27777	79	75
118	221.1	0.07097	108	75
119	221.1	0.08711	75	157
120	221.1	0.14952	80	100
121	221.1	0.14347	80	143
122	250	0.04237	82	81
123	402.4	0.04714	81	178
124	221.1	0.02627	82	195
125	221.1	0.03677	83	146
126	221.1	0.05517	83	186
127	221.1	0.04544	84	113
128	221.1	0.05029	85	120
129	221.1	0.03307	86	101
130	221.1	0.02314	142	86
131	221.1	0.04266	86	193
132	350	0.03419	88	87
133	402.4	0.01158	149	87
134	221.1	0.03597	88	150
135	221.1	0.02492	176	88
136	221.1	0.02909	88	194

Line ID	Thermal Limit (MW)	x (pu)	From Bus	To Bus
137	8.6	2.27992	90	89
138	32	0.50342	91	89
139	35.3	0.36204	92	89
140	221.1	0.05641	89	95
141	221.1	0.052	188	89
142	62.1	0.2806	94	93
143	221.1	0.14266	93	191
144	221.1	0.07399	122	96
145	221.1	0.10242	96	143
146	221.1	0.07042	96	188
147	221.1	0.08512	97	200
148	250	0.03052	99	98
149	402.4	0.03357	98	123
150	221.1	0.05298	99	142
151	221.1	0.07453	100	174
152	221.1	0.04941	100	179
153	221.1	0.08879	100	184
154	221.1	0.01266	110	101
155	221.1	0.03583	101	117
156	221.1	0.02031	101	141
157	250	0.05458	103	102
158	130	0.08775	104	102
159	260	0.05942	105	102
160	402.4	0.01929	102	128
161	221.1	0.05399	103	106
162	221.1	0.04776	130	106
163	221.1	0.0461	107	113
164	221.1	0.03531	107	129
165	221.1	0.02544	192	107
166	221.1	0.16013	108	198
167	221.1	0.05994	186	109
168	221.1	0.02224	110	193
169	221.1	0.03411	163	111
170	221.1	0.05539	111	175
171	350	0.05862	113	112
172	20	0.43401	114	112
173	200	0.06277	115	112
174	402.4	0.00925	128	112
175	221.1	0.035	113	192
176	300	0.03494	117	116
177	402.4	0.02779	133	116
178	221.1	0.08298	117	132
179	221.1	0.10444	117	162
180	221.1	0.04638	131	118
181	221.1	0.0808	118	134
182	221.1	0.06481	118	198
183	200	0.06302	122	121
184	402.4	0.0636	121	178
185	300	0.00759	187	121

Line ID	Thermal Limit (MW)	x (pu)	From Bus	To Bus
186	420	0.01748	124	123
187	170	0.10456	125	123
188	170	0.06604	126	123
189	170	0.03169	127	123
190	402.4	0.01042	123	133
191	402.4	0.00798	156	123
192	221.1	0.04582	124	193
193	250	0.04445	129	128
194	402.4	0.06826	128	133
195	221.1	0.15799	130	144
196	400	0.01333	134	133
197	225	0.03351	135	133
198	225	0.02748	136	133
199	402.4	0.01399	156	133
200	221.1	0.07136	134	140
201	221.1	0.09341	134	186
202	221.1	0.18445	138	139
203	221.1	0.05637	138	195
204	221.1	0.06582	141	148
205	221.1	0.0187	141	193
206	221.1	0.0485	162	144
207	221.1	0.06011	145	176
208	221.1	0.07551	185	145
209	130.6	0.10181	147	146
210	221.1	0.07708	146	177
211	400	0.02025	150	149
212	20	0.62552	151	149
213	100	0.14169	152	149
214	100	0.1846	153	149
215	100	0.10294	154	149
216	100	0.09984	155	149
217	221.1	0.09193	185	150
218	221.1	0.02144	194	150
219	300	0.04565	157	156
220	180.2	0.08029	161	160
221	221.1	0.02935	160	181
222	58.1	0.11301	164	163
223	65	0.30166	165	163
224	42	0.38207	166	163
225	42	0.1965	167	163
226	40	0.49098	168	163
227	40	0.39642	169	163
228	35.6	0.3749	170	163
229	221.1	0.03956	163	179
230	221.1	0.0674	171	190
231	221.1	0.08112	195	171
232	221.1	0.10656	180	172
233	221.1	0.15504	199	172
234	221.1	0.09929	173	174

Line ID	Thermal Limit (MW)	x (pu)	From Bus	To Bus
235	221.1	0.05536	173	175
236	221.1	0.12264	174	188
237	250	0.03616	179	178
238	221.1	0.18387	180	191
239	221.1	0.0787	180	199
240	60.3	0.29775	182	181
241	65	0.11425	183	181
242	221.1	0.02838	181	194
243	400	0.04476	188	187
244	740	0.00781	189	187
245	87.7	0.06004	196	195
246	87.7	0.19148	197	195

Table A.9. 200-bus case: Load

Load ID	Bus ID	Peak MW
1	2	10.8
2	4	2.68
3	6	10.8
4	8	34.8
5	10	62.5
6	12	0.48
7	13	4
8	16	70.9
9	18	1.13
10	19	1.22
11	20	1.79
12	21	7.29
13	23	2.23
14	24	3.79
15	26	1.84
16	28	3.69
17	30	86.6
18	32	0.7
19	33	8.79
20	35	32.9
21	37	4.87
22	38	40.7
23	39	1.62
24	39	10.1
25	40	3.24
26	41	60.7
27	42	1.69
28	42	15.1
29	43	3.06
30	44	1.5
31	44	5.06
32	46	8.65
33	47	2.44
34	48	2.48
35	54	0.71
36	54	3.51
37	56	1.03
38	56	0.76
39	57	4.46
40	58	1.36
41	58	1.9
42	58	2.51
43	59	1.42
44	59	5.51
45	60	3.43
46	60	2.13
47	61	28.1
48	62	13.5
49	62	20.4
50	63	5.26
51	63	3.48
52	63	3.9
53	74	25.5
54	75	5.27
55	80	0.94
56	80	1.4
57	82	7.48
58	82	2.87
59	83	1.22
60	83	3.06
61	84	5.5
62	85	7.65
63	86	12.1
64	88	74.3
65	89	11.7
66	89	3.12
67	89	3.02
68	89	67.9
69	93	3.33
70	93	1.52
71	95	2.02
72	95	1
73	95	1.08
74	96	4.03
75	97	1.23
76	97	1.06
77	97	8.45
78	99	17.8
79	100	59.2
80	101	0.76
81	106	2.81
82	107	71.7
83	108	0.78
84	108	6.58
85	108	6.44
86	109	2.5
87	109	5.67
88	110	15.9
89	111	14
90	117	49.9
91	118	5.77
92	119	1.28
93	119	24.4
94	120	2.85
95	122	0.84
96	122	0.27
97	122	20
98	129	105
99	130	6
100	131	44.3
101	132	2.22
102	132	2.26

Load ID	Bus ID	Peak MW
103	132	35
104	137	1.84
105	138	2.85
106	139	8.32
107	139	1.7
108	140	12
109	141	2.08
110	142	54.6
111	143	42.4
112	144	13.3
113	145	2.26
114	145	24.2
115	148	46.9
116	157	21.6
117	158	14.2
118	159	2.2
119	162	2.12
120	163	72.5
121	171	5.65
122	171	5.16

Load ID	Bus ID	Peak MW
123	172	1.71
124	172	3.61
125	172	3.19
126	173	1.6
127	173	12.2
128	174	2.44
129	174	1.94
130	175	3.36
131	175	8.2
132	176	28.6
133	177	1.92
134	177	4.18
135	177	9.31
136	179	37.4
137	180	12.3
138	181	2.28
139	181	73.7
140	184	0.85
141	184	1.49
142	184	14.6

Load ID	Bus ID	Peak MW
143	185	2.86
144	185	1.7
145	185	11.7
146	186	3.08
147	190	22.9
148	191	1.16
149	191	4.06
150	191	0.51
151	191	5.7
152	192	72
153	193	32.2
154	194	56.6
155	198	7.87
156	199	3.06
157	199	2.74
158	200	1.12
159	200	1.51
160	200	12.2

Table A.10. 200-bus and 500-bus cases: Load profile

HE	Demand factor
1	0.7592
2	0.7143
3	0.6794
4	0.6602
5	0.6463
6	0.6471
7	0.6597
8	0.6804
9	0.7114
10	0.7515
11	0.7962
12	0.8424
13	0.8854
14	0.9225
15	0.9519
16	0.9751
17	0.9911
18	1.0000
19	0.9940
20	0.9719
21	0.9441
22	0.9150
23	0.8696
24	0.8150

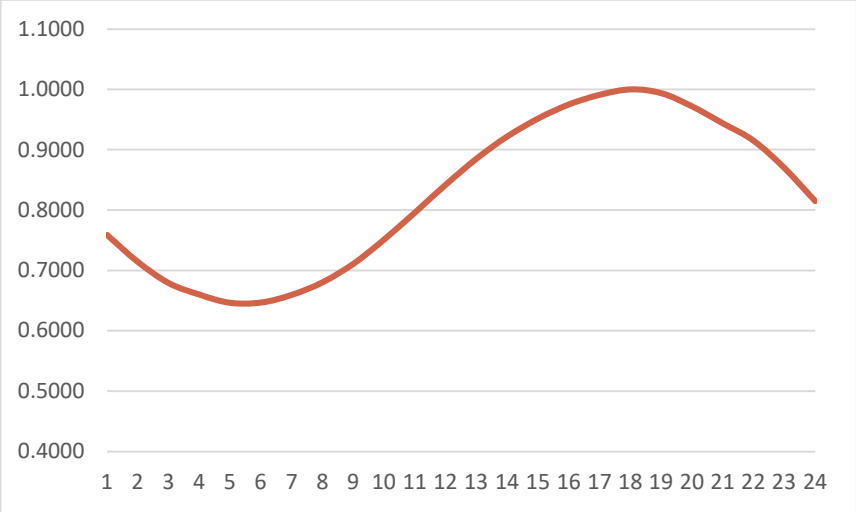

Figure A.3. Load profile curve used for the 200 and 500 bus cases

Table A.11. 200-bus case: Interface definition

Line ID	From Bus	To Bus	From Area	To Area	Weight	Metered side (pricing calculation)
26	14	121	2	3	0.33	2
102	63	184	2	3	0.33	3
126	83	186	3	1	0.2	3
127	84	113	1	3	0.2	1
143	93	191	2	3	0.34	2
147	97	200	1	2	0.5	1
167	186	109	1	2	0.5	2
194	128	133	3	1	0.2	3
195	130	144	3	1	0.2	1
202	138	139	3	1	0.2	3

Table A.12. 200-bus case: Area interchange

From Area	To Area	Interchange amount (MW)	Period
1	2	60	24 hours
1	3	40	24 hours
2	3	30	24 hours

Table A.13. 200-bus case: Generatros

Gen ID	Bus ID	Output limits (MW)		Maximum ramp rates (MW/h)		Minimum times (h)		T^{init} (h)	T^{cold} (h)	Cost						P^{init} (h)	Fuel type
		Maximum	Minimum	Up	Down	Run	Down			No Load ($)	Linear ($/MW)	Quadratic ($/MW^2)	Shut down($)	Hot Startup($)	Cold Startup($)		
1	1	99	29.7	1009.8	1009.8	1	1	5	8	0	0	0	0	0	0	17.9	Wind
2	49	4.53	1.36	10.872	10.872	1	1	8	8	236.12	19.31846	0.001944	81.54	792.75	792.75	4.53	Coal
3	50	4.53	1.36	10.872	10.872	6	6	8	8	236.12	19.88363	0.001944	81.54	792.75	792.75	4.53	Coal
4	51	4.53	1.36	10.872	10.872	6	6	2	8	236.12	20.06757	0.001944	81.54	792.75	792.75	4.53	Coal
5	52	4.53	1.36	10.872	10.872	6	6	4	8	236.12	19.65654	0.001944	81.54	792.75	792.75	4.53	Coal
6	53	9.07	2.72	21.768	21.768	6	6	1	8	236.24	19.10132	0.001944	163.26	1587.25	1587.25	9.07	Coal
7	65	150.4	45.1	1534.08	1534.08	1	1	9	8	0	0	0	0	0	0	4	Wind
8	67	4.7	1.41	11.28	11.28	6	6	8	8	236.13	19.34338	0.001944	84.6	822.5	822.5	4.7	Coal
9	68	27.92	8.38	67.008	67.008	6	6	9	8	236.74	20.50152	0.001944	502.56	4886	4886	27.92	Coal
10	69	27.92	8.38	67.008	67.008	6	6	3	8	236.74	19.65903	0.001944	502.56	4886	4886	27.92	Coal
11	70	27.92	8.38	67.008	67.008	6	6	46	8	236.74	19.74849	0.001944	502.56	4886	4886	27.92	Coal
12	71	27.92	8.38	67.008	67.008	6	6	7	8	236.74	20.05825	0.001944	502.56	4886	4886	27.92	Coal
13	72	27.92	8.38	67.008	67.008	6	6	9	8	236.74	19.56131	0.001944	502.56	4886	4886	27.92	Coal
14	73	27.92	8.38	67.008	67.008	6	6	6	8	236.74	19.40357	0.001944	502.56	4886	4886	27.92	Coal
15	76	4	1.2	36	36	1	1	4	8	606	23.42103	0.002072	32	340	340	1.2	Natural Gas
16	77	2.4	0.72	21.6	21.6	1	1	5	8	603.6	25.44867	0.002072	19.2	204	204	0.72	Natural Gas
17	78	18	5.4	162	162	1	1	-1	8	627	24.88218	0.002072	144	1530	1530	0	Natural Gas
18	79	18	5.4	162	162	1	1	-1	8	627	24.44194	0.002072	144	1530	1530	0	Natural Gas
19	90	3.2	0.96	28.8	28.8	1	1	1	8	604.8	23.27505	0.002072	25.6	272	272	0.96	Natural Gas
20	91	5	1.5	45	45	1	1	1	8	607.5	24.05596	0.002072	40	425	425	1.5	Natural Gas
21	92	6.3	1.89	56.7	56.7	1	1	-5	8	609.45	23.3418	0.002072	50.4	535.5	535.5	0	Natural Gas
22	94	18	5.4	43.2	43.2	6	6	3	8	236.48	19.17243	0.001944	324	3150	3150	18	Coal
23	104	99	29.7	1009.8	1009.8	1	1	5	8	0	0	0	0	0	0	17.9	Wind
24	105	198	59.4	2019.6	2019.6	1	1	9	8	0	0	0	0	0	0	33.6	Wind
25	114	1.7	0.51	17.34	17.34	1	1	8	8	0	0	0	0	0	0	0.4	Wind
26	115	150	45	1530	1530	1	1	8	8	0	0	0	0	0	0	47.7	Wind
27	125	150	39	360	360	6	6	8	8	610.14	20.42032	0.001944	1500	26250	26250	150	Coal

Gen ID	Bus ID	Output limits (MW)		Maximum ramp rates (MW/h)		Minimum times (h)		T^{init} (h)	T^{cold} (h)	Cost						P^{init} (h)	Fuel type
		Maximum	Minimum	Up	Down	Run	Down			No Load ($)	Linear ($/MW)	Quadratic ($/MW^2)	Shut down($)	Hot Startup($)	Cold Startup($)		
28	126	150	39	360	360	6	6	8	8	610.14	19.1717	0.001944	1500	26250	26250	150	Coal
29	127	150	39	360	360	6	6	4	8	610.14	20.36942	0.001944	1500	26250	26250	150	Coal
30	135	446.4	134	1071.36	1071.36	6	6	24	8	1261.33	20.55758	0.001944	8035.2	78120	78120	196.42	Coal
31	136	446.4	134	1071.36	1071.36	6	6	24	8	1261.33	20.55464	0.001944	8035.2	78120	78120	222.55	Coal
32	147	100.5	30.2	1025.1	1025.1	1	1	8	8	0	0	0	0	0	0	13.4	Wind
33	151	5.4	1.62	12.96	12.96	6	6	8	8	236.14	20.7944	0.001944	97.2	945	945	5.4	Coal
34	152	77.22	23.2	185.328	185.328	6	6	8	8	253.01	19.25285	0.001944	1389.96	13513.5	13513.5	77.22	Coal
35	153	77.22	23.2	185.328	185.328	6	6	8	8	253.01	20.86081	0.001944	1389.96	13513.5	13513.5	77.22	Coal
36	154	77.22	23.2	185.328	185.328	6	6	8	8	253.01	20.87739	0.001944	1389.96	13513.5	13513.5	77.22	Coal
37	155	77.22	23.2	185.328	185.328	6	6	8	8	253.01	20.68147	0.001944	1389.96	13513.5	13513.5	77.22	Coal
38	161	138.6	41.6	1247.4	1247.4	1	1	10	8	807.9	24.6386	0.002072	1108.8	11781	11781	41.58	Natural Gas
39	164	12	3.6	108	108	1	1	-8	8	618	25.20297	0.002072	96	1020	1020	0	Natural Gas
40	165	26	7.8	234	234	1	1	-8	8	639	23.84544	0.002072	208	2210	2210	0	Natural Gas
41	166	9.4	2.82	84.6	84.6	1	1	-8	8	614.1	25.32506	0.002072	75.2	799	799	0	Natural Gas
42	167	9.4	2.82	84.6	84.6	1	1	10	8	614.1	24.78685	0.002072	75.2	799	799	2.82	Natural Gas
43	168	9.4	2.82	84.6	84.6	1	1	-2	8	614.1	24.79762	0.002072	75.2	799	799	0	Natural Gas
44	169	9.4	2.82	84.6	84.6	1	1	-2	8	614.1	25.02094	0.002072	75.2	799	799	0	Natural Gas
45	170	9.4	2.82	84.6	84.6	1	1	10	8	614.1	23.599	0.002072	75.2	799	799	2.82	Natural Gas
46	182	17.5	5.25	42	42	6	6	10	8	236.47	19.57337	0.001944	315	3062.5	3062.5	17.5	Coal
47	183	26.6	7.98	63.84	63.84	6	6	10	8	236.71	20.19627	0.001944	478.8	4655	4655	26.6	Coal
48	189	569.2	171	1024.47	1024.47	120	120	300	8	1272.13	7.138956	0.0002	569150	569150	569150	569.14	Nuclear
49	196	67.5	20.3	607.5	607.5	1	1	-2	8	701.25	23.69387	0.002072	540	5737.5	5737.5	0	Natural Gas
50	197	67.5	20.3	607.5	607.5	1	1	8	8	701.25	25.72063	0.002072	540	5737.5	5737.5	20.25	Natural Gas

500-BUS CASE

Table A.14. 500-bus case: Buses

Number	Area Number	Name
1	3	WINNSBORO 0
2	3	WINNSBORO 1
3	3	COLUMBIA 11 0
4	3	COLUMBIA 11 1
5	2	SMYRNA 0
6	2	SMYRNA 1
7	3	EASTOVER 2 0
8	3	EASTOVER 2 1
9	3	EASTOVER 2 2
10	1	CHAPPELLS 2 0
11	1	CHAPPELLS 2 1
12	1	PELZER 0
13	1	PELZER 1
14	1	SENECA 3 0
15	1	SENECA 3 1
16	1	SENECA 3 2
17	1	SENECA 3 3
18	1	SENECA 3 4
19	1	MONETTA 0
20	1	MONETTA 1
21	3	LEXINGTON 2 0
22	3	LEXINGTON 2 1
23	2	WELLFORD 0
24	2	WELLFORD 1
25	2	WELLFORD 2
26	2	WELLFORD 3
27	2	LAURENS 0
28	2	LAURENS 1
29	3	COLUMBIA 10 0
30	3	COLUMBIA 10 1
31	1	WINDSOR 0
32	1	WINDSOR 1
33	1	PROSPERITY 0
34	1	PROSPERITY 1
35	1	NORTH AUGUSTA 2 0
36	1	NORTH AUGUSTA 2 1
37	2	LANDO 0
38	2	LANDO 1
39	2	GAFFNEY 3 0
40	2	GAFFNEY 3 1
41	2	GAFFNEY 3 2
42	1	CLARKS HILL 2 0
43	1	CLARKS HILL 2 1
44	3	JENKINSVILLE 0
45	3	JENKINSVILLE 1
46	2	WOODRUFF 0
47	2	WOODRUFF 1
48	1	IVA 0
49	1	IVA 1
50	1	IVA 2
51	1	IVA 3
52	1	IVA 4
53	3	CAYCE 0
54	3	CAYCE 1
55	1	TROY 0
56	1	TROY 1
57	1	SIMPSONVILLE 2 0
58	1	SIMPSONVILLE 2 1
59	1	SIMPSONVILLE 2 2
60	2	MAYO 0
61	2	MAYO 1
62	3	BELTON 2 0
63	3	BELTON 2 1
64	3	BELTON 2 2
65	1	BRADLEY 0
66	1	BRADLEY 1
67	1	BRADLEY 2
68	2	ENOREE 0
69	2	ENOREE 1
70	1	HONEA PATH 2 0
71	1	HONEA PATH 2 1
72	1	HONEA PATH 2 2
73	1	HONEA PATH 2 3
74	1	SPRINGFIELD 0
75	1	SPRINGFIELD 1
76	2	EDGEMOOR 0
77	2	EDGEMOOR 1
78	1	NEWRY 0
79	1	NEWRY 1
80	1	CLARKS HILL 1 0
81	1	CLARKS HILL 1 1
82	1	CLARKS HILL 1 2
83	1	NEWBERRY 0
84	1	NEWBERRY 1
85	1	AIKEN 3 0
86	1	AIKEN 3 1

Number	Area Number	Name
87	2	ROCK HILL 3 0
88	2	ROCK HILL 3 1
89	3	CAMERON 0
90	3	CAMERON 1
91	1	SENECA 2 0
92	1	SENECA 2 1
93	3	BLAIR 0
94	3	BLAIR 1
95	1	WALHALLA 0
96	1	WALHALLA 1
97	1	ANDERSON 4 0
98	1	ANDERSON 4 1
99	2	PACOLET 0
100	2	PACOLET 1
101	2	PACOLET 2
102	1	ABBEVILLE 0
103	1	ABBEVILLE 1
104	1	AIKEN 2 0
105	1	AIKEN 2 1
106	1	JOHNSTON 0
107	1	JOHNSTON 1
108	2	SPARTANBURG 6 0
109	2	SPARTANBURG 6 1
110	2	GAFFNEY 2 0
111	2	GAFFNEY 2 1
112	1	LEESVILLE 0
113	1	LEESVILLE 1
114	1	LANGLEY 0
115	1	LANGLEY 1
116	1	LANGLEY 2
117	1	DONALDS 0
118	1	DONALDS 1
119	1	GREENVILLE 7 0
120	1	GREENVILLE 7 1
121	3	COLUMBIA 9 0
122	3	COLUMBIA 9 1
123	1	SALEM 3 0
124	1	SALEM 3 1
125	1	SALEM 3 2
126	1	SALEM 3 3
127	1	SALEM 3 4
128	1	SALEM 3 5
129	1	GREENVILLE 6 0
130	1	GREENVILLE 6 1
131	2	COWPENS 0
132	2	COWPENS 1
133	1	WESTMINSTER 2 0
134	1	WESTMINSTER 2 1

Number	Area Number	Name
135	3	SAINT MATTHEWS 0
136	3	SAINT MATTHEWS 1
137	1	GREENWOOD 2 0
138	1	GREENWOOD 2 1
139	2	FINGERVILLE 0
140	2	FINGERVILLE 1
141	2	ROCK HILL 2 0
142	2	ROCK HILL 2 1
143	2	YORK 2 0
144	2	YORK 2 1
145	2	YORK 2 2
146	3	CHAPIN 0
147	3	CHAPIN 1
148	3	CHAPIN 2
149	1	MODOC 0
150	1	MODOC 1
151	2	SPARTANBURG 5 0
152	2	SPARTANBURG 5 1
153	2	SPARTANBURG 5 2
154	2	BOILING SPRINGS 0
155	2	BOILING SPRINGS 1
156	2	GREENVILLE 5 0
157	2	GREENVILLE 5 1
158	3	PELION 0
159	3	PELION 1
160	1	GRANITEVILLE 0
161	1	GRANITEVILLE 1
162	3	IRMO 0
163	3	IRMO 1
164	3	IRMO 2
165	1	SALEM 2 0
166	1	SALEM 2 1
167	1	SALEM 2 2
168	1	SALEM 2 3
169	1	SALEM 2 4
170	1	WEST UNION 0
171	1	WEST UNION 1
172	1	CROSS HILL 0
173	1	CROSS HILL 1
174	1	CROSS HILL 2
175	2	FORT LAWN 0
176	2	FORT LAWN 1
177	2	FORT LAWN 2
178	2	FORT LAWN 3
179	3	NORTH 0
180	3	NORTH 1
181	1	ANDERSON 3 0
182	1	ANDERSON 3 1

Number	Area Number	Name
183	2	BLACKSBURG 2 0
184	2	BLACKSBURG 2 1
185	1	LIBERTY 0
186	1	LIBERTY 1
187	3	ELLOREE 0
188	3	ELLOREE 1
189	1	WAGENER 0
190	1	WAGENER 1
191	1	TRENTON 0
192	1	TRENTON 1
193	1	BATESBURG 0
194	1	BATESBURG 1
195	3	COLUMBIA 8 0
196	3	COLUMBIA 8 1
197	3	COLUMBIA 8 2
198	3	COLUMBIA 8 3
199	3	COLUMBIA 8 4
200	3	LITTLE MOUNTAIN 0
201	3	LITTLE MOUNTAIN 1
202	1	CLINTON 0
203	1	CLINTON 1
204	1	CLINTON 2
205	1	WARRENVILLE 0
206	1	WARRENVILLE 1
207	1	WARRENVILLE 2
208	1	SIMPSONVILLE 1 0
209	1	SIMPSONVILLE 1 1
210	2	DUNCAN 0
211	2	DUNCAN 1
212	1	NORTH AUGUSTA 1 0
213	1	NORTH AUGUSTA 1 1
214	1	GREENWOOD 1 0
215	1	GREENWOOD 1 1
216	1	BELTON 1 0
217	1	BELTON 1 1
218	1	VAUCLUSE 0
219	1	VAUCLUSE 1
220	2	UNION 3 0
221	2	UNION 3 1
222	2	UNION 3 2
223	2	UNION 3 3
224	2	UNION 3 4
225	2	UNION 3 5
226	1	MOUNTAIN REST 0
227	1	MOUNTAIN REST 1
228	1	PICKENS 0
229	1	PICKENS 1

Number	Area Number	Name
230	1	WESTMINSTER 1 0
231	1	WESTMINSTER 1 1
232	3	WEST COLUMBIA 3 0
233	3	WEST COLUMBIA 3 1
234	3	WEST COLUMBIA 3 2
235	1	WARD 0
236	1	WARD 1
237	1	WARD 2
238	2	MOORE 0
239	2	MOORE 1
240	1	WILLISTON 0
241	1	WILLISTON 1
242	3	COLUMBIA 7 0
243	3	COLUMBIA 7 1
244	1	WATERLOO 0
245	1	WATERLOO 1
246	2	BLACKSBURG 1 0
247	2	BLACKSBURG 1 1
248	2	BLACKSBURG 1 2
249	2	BLACKSBURG 1 3
250	2	BLACKSBURG 1 4
251	1	TAYLORS 0
252	1	TAYLORS 1
253	1	GREENVILLE 4 0
254	1	GREENVILLE 4 1
255	1	GREENVILLE 4 2
256	1	GREENVILLE 4 3
257	1	GREENVILLE 4 4
258	1	GREENVILLE 4 5
259	1	GREENVILLE 4 6
260	1	SALEM 1 0
261	1	SALEM 1 1
262	3	COLUMBIA 6 0
263	3	COLUMBIA 6 1
264	3	COLUMBIA 6 2
265	3	COLUMBIA 6 3
266	3	COLUMBIA 6 4
267	1	AIKEN 1 0
268	1	AIKEN 1 1
269	3	POMARIA 0
270	3	POMARIA 1
271	1	RIDGE SPRING 0
272	1	RIDGE SPRING 1
273	1	RIDGE SPRING 2
274	2	GAFFNEY 1 0
275	2	GAFFNEY 1 1
276	3	COLUMBIA 5 0
277	3	COLUMBIA 5 1

Number	Area Number	Name
278	3	COLUMBIA 5 2
279	1	MARIETTA 0
280	1	MARIETTA 1
281	1	ANDERSON 2 0
282	1	ANDERSON 2 1
283	1	SALUDA 0
284	1	SALUDA 1
285	1	FAIR PLAY 0
286	1	FAIR PLAY 1
287	3	HOPKINS 0
288	3	HOPKINS 1
289	1	SUNSET 0
290	1	SUNSET 1
291	3	SALLEY 0
292	3	SALLEY 1
293	1	EDGEFIELD 0
294	1	EDGEFIELD 1
295	2	BUFFALO 0
296	2	BUFFALO 1
297	1	WARE SHOALS 0
298	1	WARE SHOALS 1
299	1	WARE SHOALS 2
300	2	YORK 1 0
301	2	YORK 1 1
302	2	YORK 1 2
303	2	YORK 1 3
304	1	PIEDMONT 0
305	1	PIEDMONT 1
306	1	PIEDMONT 2
307	1	PIEDMONT 3
308	1	CALHOUN FALLS 0
309	1	CALHOUN FALLS 1
310	1	ANDERSON 1 0
311	1	ANDERSON 1 1
312	1	JACKSON 0
313	1	JACKSON 1
314	2	CROSS ANCHOR 0
315	2	CROSS ANCHOR 1
316	2	HICKORY GROVE 0
317	2	HICKORY GROVE 1
318	2	GREAT FALLS 2 0
319	2	GREAT FALLS 2 1
320	3	COLUMBIA 4 0
321	3	COLUMBIA 4 1
322	1	MAULDIN 0
323	1	MAULDIN 1
324	1	GREENVILLE 3 0
325	1	GREENVILLE 3 1

Number	Area Number	Name
326	3	COLUMBIA 3 0
327	3	COLUMBIA 3 1
328	1	PENDLETON 0
329	1	PENDLETON 1
330	2	SPARTANBURG 4 0
331	2	SPARTANBURG 4 1
332	2	CONVERSE 0
333	2	CONVERSE 1
334	2	CONVERSE 2
335	2	CONVERSE 3
336	2	BLACKSTOCK 0
337	2	BLACKSTOCK 1
338	2	FORT MILL 3 0
339	2	FORT MILL 3 1
340	1	LANDRUM 0
341	1	LANDRUM 1
342	1	SILVERSTREET 0
343	1	SILVERSTREET 1
344	1	SILVERSTREET 2
345	3	ORANGEBURG 0
346	3	ORANGEBURG 1
347	1	GREENVILLE 2 0
348	1	GREENVILLE 2 1
349	1	CHAPPELLS 1 0
350	1	CHAPPELLS 1 1
351	1	CHAPPELLS 1 2
352	1	CHAPPELLS 1 3
353	1	CHAPPELLS 1 4
354	3	RIDGEWAY 2 0
355	3	RIDGEWAY 2 1
356	1	FOUNTAIN INN 0
357	1	FOUNTAIN INN 1
358	1	STARR 0
359	1	STARR 1
360	2	SPARTANBURG 3 0
361	2	SPARTANBURG 3 1
362	2	SPARTANBURG 3 2
363	2	SPARTANBURG 3 3
364	2	SPARTANBURG 3 4
365	3	GASTON 2 0
366	3	GASTON 2 1
367	1	SIX MILE 0
368	1	SIX MILE 1
369	1	SENECA 1 0
370	1	SENECA 1 1
371	3	GILBERT 0
372	3	GILBERT 1
373	3	GILBERT 2

Number	Area Number	Name
374	3	SWANSEA 0
375	3	SWANSEA 1
376	2	INMAN 0
377	2	INMAN 1
378	2	GREAT FALLS 1 0
379	2	GREAT FALLS 1 1
380	2	WHITMIRE 0
381	2	WHITMIRE 1
382	2	GRAY COURT 0
383	2	GRAY COURT 1
384	1	WILLIAMSTON 2 0
385	1	WILLIAMSTON 2 1
386	1	CLEMSON 0
387	1	CLEMSON 1
388	1	CLEMSON 2
389	1	CLEMSON 3
390	1	CLEMSON 4
391	1	CLEMSON 5
392	1	CLEMSON 6
393	1	CLEMSON 7
394	1	CLEMSON 8
395	1	CLEMSON 9
396	1	CLEMSON 10
397	1	CLEMSON 11
398	1	CLEMSON 12
399	1	BEECH ISLAND 2 0
400	1	BEECH ISLAND 2 1
401	2	CLOVER 0
402	2	CLOVER 1
403	1	NINETY SIX 0
404	1	NINETY SIX 1
405	2	MC CONNELLS 0
406	2	MC CONNELLS 1
407	1	BEECH ISLAND 1 0
408	1	BEECH ISLAND 1 1
409	1	BEECH ISLAND 1 2
410	1	BEECH ISLAND 1 3
411	1	BEECH ISLAND 1 4
412	1	BEECH ISLAND 1 5
413	1	BEECH ISLAND 1 6
414	1	BEECH ISLAND 1 7
415	3	GADSDEN 0
416	3	GADSDEN 1
417	1	TRAVELERS REST 0
418	1	TRAVELERS REST 1
419	1	DUE WEST 0
420	1	DUE WEST 1
421	3	BLYTHEWOOD 0

Number	Area Number	Name
422	3	BLYTHEWOOD 1
423	2	ROCK HILL 1 0
424	2	ROCK HILL 1 1
425	1	HODGES 0
426	1	HODGES 1
427	1	HODGES 2
428	2	CHESNEE 2 0
429	2	CHESNEE 2 1
430	2	CHESNEE 2 2
431	2	CHESNEE 2 3
432	2	CHESNEE 2 4
433	2	CHESNEE 2 5
434	2	CHESNEE 2 6
435	2	CHESNEE 2 7
436	2	CHESNEE 2 8
437	2	CHESNEE 2 9
438	2	CHESNEE 2 10
439	2	CHESNEE 2 11
440	1	WILLIAMSTON 1 0
441	1	WILLIAMSTON 1 1
442	1	WILLIAMSTON 1 2
443	1	WILLIAMSTON 1 3
444	1	WILLIAMSTON 1 4
445	1	EASLEY 2 0
446	1	EASLEY 2 1
447	2	UNION 2 0
448	2	UNION 2 1
449	2	ARCADIA 0
450	2	ARCADIA 1
451	2	ARCADIA 2
452	2	CATAWBA 0
453	3	GASTON 1 0
454	3	GASTON 1 1
455	3	GASTON 1 2
456	3	GASTON 1 3
457	3	EASTOVER 1 0
458	3	EASTOVER 1 1
459	2	FORT MILL 2 0
460	2	CAMPOBELLO 0
461	1	EASLEY 1 0
462	2	UNION 1 0
463	2	UNION 1 1
464	2	JONESVILLE 0
465	2	JONESVILLE 1
466	2	CHESNEE 1 0
467	1	NORRIS 0
468	1	CLEVELAND 0
469	1	GREER 2 0

Number	Area Number	Name
470	1	CENTRAL 0
471	2	SPARTANBURG 2 0
472	2	SPARTANBURG 2 1
473	1	LONG CREEK 0
474	1	GREENVILLE 1 0
475	3	PEAK 0
476	3	COLUMBIA 2 0
477	2	ROEBUCK 0
478	2	SHARON 0
479	3	RIDGEWAY 1 0
480	3	RIDGEWAY 1 1
481	3	RIDGEWAY 1 2
482	3	RIDGEWAY 1 3
483	3	RIDGEWAY 1 4
484	3	RIDGEWAY 1 5
485	3	WEST COLUMBIA 2 0

Number	Area Number	Name
486	3	WEST COLUMBIA 1 0
487	1	TOWNVILLE 0
488	2	GREER 1 0
489	1	PLUM BRANCH 0
490	1	HONEA PATH 1 0
491	3	COLUMBIA 1 0
492	2	CHESTER 0
493	2	CARLISLE 0
494	2	CARLISLE 1
495	2	SPARTANBURG 1 0
496	2	FORT MILL 1 0
497	2	FORT MILL 1 1
498	2	FORT MILL 1 2
499	3	LEXINGTON 1 0
500	1	MC CORMICK 0

Table A.15. 500-bus case: Branches

Line ID	Thermal Limit (MW)	x (pu)	From Bus	to bus
1	76.5	0.00314	2	1
2	320.3	0.0697	3	479
3	225.1	0.00352	4	3
4	4.5	0.00356	6	5
5	1493.9	0.01375	7	262
6	1493.9	0.01481	7	232
7	320.3	0.01895	8	457
8	320.3	0.03579	8	287
9	567	0.0129	8	7
10	800	0.01362	9	7
11	800	0.01362	9	7
12	320.3	0.01346	10	349
13	4	0.0032	11	10
14	320.3	0.01502	12	441
15	320.3	0.02119	12	304
16	320.3	0.03805	12	216
17	65.5	0.00313	13	12
18	320.3	0.10461	15	230
19	320.3	0.01701	15	369
20	682	0.01122	15	14
21	320.3	0.04609	15	91
22	320.3	0.08462	15	473
23	596	0.01202	16	14
24	930	0.01438	17	14
25	930	0.01438	17	14
26	340	0.05115	18	14
27	320.3	0.04534	19	112
28	320.3	0.02202	19	272

Line ID	Thermal Limit (MW)	x (pu)	From Bus	to bus
29	7.5	0.00389	20	19
30	320.3	0.0489	21	112
31	175	0.02025	21	196
32	254.2	0.00317	22	21
33	1493.9	0.01253	23	464
34	1493.9	0.02385	23	386
35	1493.9	0.00704	23	471
36	626	0.01764	24	23
37	320.3	0.02271	24	360
38	3.6	0.00363	25	24
39	29.5	0.00373	26	24
40	320.3	0.05385	27	68
41	320.3	0.03091	27	382
42	108.6	0.00396	28	27
43	320.3	0.05384	29	491
44	157	0.0033	30	29
45	320.3	0.05093	31	85
46	320.3	0.0548	31	189
47	320.3	0.07945	31	218
48	320.3	0.07487	31	205
49	15.7	0.00343	32	31
50	43.4	0.00328	34	33
51	320.3	0.05412	35	399
52	62.9	0.00303	36	35
53	320.3	0.02918	37	176
54	0.2	0.00382	38	37
55	1493.9	0.0069	39	428
56	1493.9	0.00579	39	332
57	320.3	0.02668	40	131
58	428	0.02531	40	39
59	97.5	0.00392	41	40
60	320.3	0.05842	42	191
61	7.7	0.00312	43	42
62	320.3	0.05026	44	1
63	320.3	0.01931	44	200
64	2.8	0.00388	45	44
65	320.3	0.06348	46	156
66	63	0.00345	47	46
67	57	0.27853	49	48
68	70	0.16356	50	48
69	0.6	0.00367	51	48
70	37.9	0.00334	52	48
71	320.3	0.01442	53	276
72	51.3	0.00306	54	53
73	320.3	0.04157	55	66
74	320.3	0.0411	55	500
75	3.1	0.00331	56	55
76	1493.9	0.02443	57	123
77	675	0.01762	58	57

Line ID	Thermal Limit (MW)	x (pu)	From Bus	to bus
78	320.3	0.04352	58	253
79	675	0.01762	58	57
80	252.9	0.00385	59	58
81	320.3	0.01821	60	131
82	0.3	0.00352	61	60
83	320.3	0.0261	62	3
84	320.3	0.06979	62	457
85	70	0.16353	63	62
86	45.6	0.00327	64	62
87	1493.9	0.01319	65	297
88	320.3	0.06895	66	308
89	405	0.03088	66	65
90	6.7	0.00336	67	66
91	320.3	0.01733	68	314
92	320.3	0.041	68	295
93	27.6	0.004	69	68
94	320.3	0.01951	70	490
95	133	0.04472	71	70
96	60	0.14481	72	70
97	49	0.27303	73	70
98	320.3	0.05408	74	189
99	8.8	0.00334	75	74
100	320.3	0.01416	76	37
101	12.2	0.00331	77	76
102	320.3	0.02261	78	387
103	320.3	0.04983	78	328
104	0.5	0.00328	79	78
105	1493.9	0.01377	80	65
106	320.3	0.02166	81	42
107	529	0.03481	81	80
108	628	0.03113	82	80
109	320.3	0.03952	83	342
110	320.3	0.05076	83	33
111	105.4	0.00366	84	83
112	30	0.0039	86	85
113	325	0.01773	87	141
114	515	0.03504	87	143
115	7.7	0.00357	88	87
116	320.3	0.08267	89	457
117	320.3	0.02032	89	187
118	10.5	0.00386	90	89
119	320.3	0.0484	91	133
120	104.2	0.00362	92	91
121	8.2	0.00328	94	93
122	320.3	0.03932	95	369
123	320.3	0.02027	95	170
124	56.2	0.00325	96	95
125	66.4	0.00399	98	97
126	320.3	0.02582	99	465

Line ID	Thermal Limit (MW)	x (pu)	From Bus	to bus
127	22.7	0.00362	100	99
128	1.4	0.00329	101	99
129	320.3	0.05425	102	308
130	64.6	0.00387	103	102
131	320.3	0.04749	104	191
132	320.3	0.05306	104	31
133	144.2	0.00375	105	104
134	320.3	0.0429	106	191
135	24.5	0.00321	107	106
136	320.3	0.03467	108	495
137	320.3	0.01952	108	472
138	62.9	0.00301	109	108
139	320.3	0.03302	110	316
140	87	0.00371	111	110
141	320.3	0.05115	112	499
142	320.3	0.06078	112	236
143	320.3	0.08276	112	283
144	320.3	0.06781	112	33
145	73	0.00312	113	112
146	320.3	0.05336	114	191
147	320.3	0.06346	114	312
148	6.7	0.00336	115	114
149	5.3	0.00341	116	114
150	320.3	0.0291	117	426
151	12.8	0.00385	118	117
152	320.3	0.02155	119	129
153	46.6	0.00306	120	119
154	320.3	0.06806	121	287
155	320.3	0.02446	121	276
156	70.4	0.00385	122	121
157	320.3	0.07057	124	369
158	320.3	0.01871	124	260
159	488	0.01438	124	123
160	346	0.04064	125	123
161	352	0.02189	126	123
162	378	0.04792	127	123
163	391	0.01585	128	123
164	166	0.00322	130	129
165	320.3	0.02139	131	333
166	41.6	0.00362	132	131
167	320.3	0.05908	133	226
168	320.3	0.05646	133	369
169	66	0.00308	134	133
170	320.3	0.06297	135	457
171	320.3	0.06942	135	287
172	45.6	0.00366	136	135
173	320.3	0.02879	137	426
174	320.3	0.02996	137	214
175	320.3	0.02879	137	426

Line ID	Thermal Limit (MW)	x (pu)	From Bus	to bus
176	122.9	0.00379	138	137
177	320.3	0.0257	139	376
178	0.4	0.00318	140	139
179	209.8	0.00342	142	141
180	400	0.07237	143	247
181	480	0.03896	143	401
182	350	0.07237	143	452
183	320.3	0.01941	143	338
184	650	0.033	144	143
185	650	0.033	144	143
186	650	0.0337	145	143
187	650	0.0337	145	143
188	1493.9	0.00433	146	195
189	1493.9	0.00408	146	162
190	272	0.05565	147	146
191	102.4	0.00394	148	147
192	320.3	0.02641	149	81
193	2.4	0.00369	150	149
194	1493.9	0.00261	151	23
195	570	0.0203	152	151
196	130.1	0.00311	153	152
197	320.3	0.07345	154	488
198	320.3	0.02035	154	429
199	90	0.00301	155	154
200	164.3	0.00358	157	156
201	320.3	0.04929	158	291
202	320.3	0.05593	158	233
203	31.4	0.00387	159	158
204	320.3	0.03683	160	399
205	320.3	0.02465	160	212
206	44.8	0.00357	161	160
207	1493.9	0.00759	162	232
208	1493.9	0.01839	162	220
209	1493.9	0.00328	162	195
210	510	0.01982	163	162
211	510	0.01982	163	162
212	174.5	0.00399	164	163
213	1493.9	0.01042	165	386
214	1493.9	0.00314	165	123
215	606	0.00871	166	165
216	320.3	0.04444	166	228
217	320.3	0.02029	166	289
218	411	0.02157	167	165
219	445	0.03549	168	165
220	543	0.02558	169	165
221	320.3	0.04248	170	226
222	20.9	0.00377	171	170
223	320.3	0.0316	172	244
224	4.7	0.00313	173	172

Line ID	Thermal Limit (MW)	x (pu)	From Bus	to bus
225	12.3	0.00304	174	172
226	1493.9	0.01596	175	220
227	273	0.03857	176	175
228	12.9	0.00365	177	176
229	10.7	0.00316	178	176
230	320.3	0.03624	179	374
231	320.3	0.05727	179	291
232	25.2	0.0033	180	179
233	320.3	0.02873	181	97
234	320.3	0.02642	181	487
235	145.7	0.00372	182	181
236	320.3	0.03527	183	274
237	320.3	0.01887	183	247
238	40.4	0.00301	184	183
239	320.3	0.0185	185	467
240	76.9	0.00307	186	185
241	320.3	0.12704	187	454
242	19.9	0.00314	188	187
243	22.9	0.00301	190	189
244	320.3	0.04959	191	293
245	320.3	0.05114	191	205
246	320.3	0.03704	191	35
247	27.2	0.00376	192	191
248	320.3	0.02753	193	112
249	320.3	0.02132	193	19
250	49.3	0.0038	194	193
251	560	0.01443	196	195
252	597	0.03102	197	195
253	527	0.02185	198	195
254	124	0.00331	199	196
255	320.3	0.02996	200	163
256	14.8	0.00317	201	200
257	320.3	0.03911	202	172
258	6.6	0.00362	203	202
259	72.7	0.00389	204	202
260	320.3	0.06207	205	312
261	4.4	0.00303	206	205
262	30.4	0.0037	207	205
263	141.4	0.0036	209	208
264	320.3	0.02034	210	24
265	54.3	0.00378	211	210
266	320.3	0.03211	212	399
267	155	0.00369	213	212
268	320.3	0.04049	214	403
269	124.1	0.00381	215	214
270	320.3	0.02381	216	70
271	71.7	0.00313	217	216
272	320.3	0.04365	218	399
273	0.6	0.00366	219	218

Line ID	Thermal Limit (MW)	x (pu)	From Bus	to bus
274	1493.9	0.01421	220	471
275	320.3	0.03277	221	493
276	320.3	0.02916	221	478
277	320.3	0.03812	221	447
278	556	0.02901	221	220
279	228	0.02225	222	220
280	248	0.03062	223	220
281	588	0.02404	224	220
282	588	0.02404	224	220
283	628	0.01242	225	220
284	628	0.01242	225	220
285	8.9	0.00335	227	226
286	320.3	0.05975	228	474
287	320.3	0.04697	228	468
288	77.9	0.00359	229	228
289	65	0.18877	231	230
290	1493.9	0.00429	232	453
291	1493.9	0.00653	232	371
292	320.3	0.02167	233	53
293	320.3	0.02176	233	486
294	628	0.0207	233	232
295	95.7	0.00341	234	233
296	1493.9	0.00414	235	271
297	1493.9	0.01637	235	407
298	507	0.02788	236	235
299	320.3	0.02991	236	106
300	4.3	0.00335	237	236
301	320.3	0.02069	238	152
302	320.3	0.03009	238	46
303	64.1	0.00362	239	238
304	320.3	0.10682	240	272
305	320.3	0.04067	240	74
306	27.2	0.00398	241	240
307	320.3	0.06771	242	287
308	320.3	0.02907	242	320
309	130.7	0.0037	243	242
310	320.3	0.03394	244	426
311	15.8	0.00315	245	244
312	1493.9	0.01437	246	471
313	1493.9	0.01337	246	332
314	350	0.0469	247	401
315	370	0.06785	247	246
316	336	0.05441	248	246
317	333	0.05427	249	246
318	628	0.02016	250	246
319	628	0.02016	250	246
320	320.3	0.04155	251	360
321	171.6	0.00386	252	251
322	320.3	0.04892	253	417

Line ID	Thermal Limit (MW)	x (pu)	From Bus	to bus
323	320.3	0.01435	253	119
324	320.3	0.02449	253	347
325	134	0.13453	254	253
326	75	0.10598	255	253
327	65	0.18871	256	253
328	142	0.08097	257	253
329	52	0.25929	258	253
330	11.9	0.00358	259	253
331	320.3	0.01825	260	166
332	31.4	0.00332	261	260
333	1493.9	0.00363	262	232
334	320.3	0.02423	263	326
335	320.3	0.03325	263	491
336	320.3	0.01734	263	476
337	320.3	0.0083	263	276
338	656	0.01827	263	262
339	255	0.05005	264	262
340	241	0.03379	265	262
341	107.2	0.00341	266	263
342	320.3	0.04702	267	31
343	206.9	0.00357	268	267
344	320.3	0.03596	269	93
345	10.9	0.00398	270	269
346	484	0.03765	272	271
347	320.3	0.04047	272	85
348	15.4	0.004	273	272
349	320.3	0.03002	274	110
350	225	0.04081	275	274
351	320.3	0.02412	276	485
352	320.3	0.03082	276	320
353	0.7	0.00366	277	276
354	8.4	0.00385	278	276
355	320.3	0.03077	279	468
356	320.3	0.05728	279	340
357	24.6	0.00308	280	279
358	320.3	0.03678	281	384
359	320.3	0.04556	281	328
360	203.7	0.00362	282	281
361	320.3	0.04143	283	236
362	48.1	0.00399	284	283
363	320.3	0.03109	285	487
364	320.3	0.0264	285	230
365	13.4	0.00327	286	285
366	320.3	0.05236	287	62
367	320.3	0.06826	287	476
368	320.3	0.03927	287	415
369	89.9	0.00382	288	287
370	5.9	0.00381	290	289
371	12.6	0.00322	292	291

Line ID	Thermal Limit (MW)	x (pu)	From Bus	to bus
372	320.3	0.04211	293	149
373	35.7	0.00329	294	293
374	320.3	0.03137	295	447
375	10.8	0.00343	296	295
376	1493.9	0.00935	297	440
377	320.3	0.03112	298	426
378	348	0.03135	298	297
379	20	0.00363	299	298
380	430	0.02449	300	141
381	320.3	0.08031	300	478
382	67	0.08126	301	300
383	75	0.07834	302	300
384	139.2	0.004	303	300
385	320.3	0.02941	304	129
386	28	0.53593	305	304
387	63	0.24992	306	304
388	122.2	0.00347	307	304
389	320.3	0.06668	308	500
390	13.6	0.004	309	308
391	320.3	0.02161	310	281
392	60.5	0.00359	311	310
393	320.3	0.04298	312	267
394	17.9	0.00398	313	312
395	320.3	0.03066	314	295
396	0.7	0.00314	315	314
397	320.3	0.02348	316	5
398	5.5	0.00305	317	316
399	320.3	0.05015	318	336
400	320.3	0.03291	318	176
401	120	0.07586	319	318
402	269.4	0.00362	321	320
403	320.3	0.01939	322	58
404	320.3	0.01939	322	58
405	320.3	0.02746	322	208
406	75.5	0.00311	323	322
407	320.3	0.01442	324	322
408	320.3	0.01723	324	129
409	146.4	0.00371	325	324
410	159.8	0.00319	327	326
411	40.7	0.00303	329	328
412	77.4	0.00388	331	330
413	1493.9	0.00341	332	471
414	508	0.02644	333	332
415	320.3	0.01457	333	330
416	0.9	0.0032	334	333
417	1.3	0.00355	335	333
418	320.3	0.05315	336	93
419	9.7	0.0039	337	336
420	320.3	0.0179	338	459

Line ID	Thermal Limit (MW)	x (pu)	From Bus	to bus
421	50	0.00363	339	338
422	43.3	0.00385	341	340
423	320.3	0.02712	342	10
424	3.7	0.00363	343	342
425	3.3	0.00388	344	342
426	320.3	0.06512	345	415
427	320.3	0.04661	345	179
428	72.4	0.00319	346	345
429	320.3	0.05092	347	417
430	138.5	0.00312	348	347
431	320.3	0.02513	349	403
432	183	0.0716	350	349
433	142	0.07925	351	349
434	150	0.07211	352	349
435	206	0.0722	353	349
436	28.3	0.00376	355	354
437	320.3	0.02735	356	382
438	320.3	0.02452	356	208
439	84.8	0.00342	357	356
440	320.3	0.02689	358	310
441	320.3	0.04128	358	48
442	320.3	0.02455	358	97
443	25	0.00351	359	358
444	320.3	0.07801	360	417
445	52	0.33724	361	360
446	162	0.11798	362	360
447	75	0.11593	363	360
448	40.2	0.00356	364	360
449	320.3	0.02211	365	454
450	320.3	0.02723	365	374
451	101.5	0.00392	366	365
452	320.3	0.07633	367	468
453	320.3	0.05803	367	461
454	320.3	0.01842	367	15
455	17.6	0.00321	368	367
456	62.2	0.00306	370	369
457	1493.9	0.00597	371	195
458	320.3	0.01927	372	112
459	508	0.03602	372	371
460	48.5	0.00318	373	372
461	43.2	0.00301	375	374
462	320.3	0.04503	376	469
463	320.3	0.02156	376	460
464	320.3	0.02636	376	429
465	320.3	0.03194	376	495
466	162.4	0.00335	377	376
467	320.3	0.04877	378	336
468	320.3	0.0125	378	318
469	20.3	0.00382	379	378

Line ID	Thermal Limit (MW)	x (pu)	From Bus	to bus
470	320.3	0.05147	380	202
471	14.4	0.00359	381	380
472	44.5	0.00357	383	382
473	48.1	0.00315	385	384
474	1493.9	0.00455	386	14
475	1493.9	0.00455	386	14
476	320.3	0.01961	387	470
477	320.3	0.0289	387	467
478	658	0.01653	387	386
479	658	0.01653	387	386
480	255	0.04243	388	386
481	374	0.03576	389	386
482	389	0.02728	390	386
483	399	0.02451	391	386
484	297	0.03299	392	386
485	283	0.03349	393	386
486	318	0.022	394	386
487	312	0.05624	395	386
488	313	0.02168	396	386
489	66.7	0.0033	397	387
490	24.4	0.00311	398	387
491	320.3	0.0463	399	312
492	31.7	0.00397	400	399
493	320.3	0.04692	401	5
494	123.7	0.00371	402	401
495	26.2	0.00347	404	403
496	320.3	0.0324	405	300
497	8.2	0.00355	406	405
498	1493.9	0.01082	407	80
499	320.3	0.02765	408	212
500	595	0.01366	408	407
501	320.3	0.01554	408	399
502	326	0.0611	409	407
503	445	0.04197	410	407
504	441	0.02349	411	407
505	431	0.02693	412	407
506	436	0.04036	413	407
507	342	0.04423	414	407
508	8.7	0.00383	416	415
509	320.3	0.03319	417	474
510	320.3	0.04093	417	251
511	320.3	0.04483	417	469
512	320.3	0.03267	417	468
513	109.4	0.00352	418	417
514	320.3	0.04453	419	48
515	320.3	0.03494	419	102
516	8.5	0.00375	420	419
517	320.3	0.04577	421	354
518	320.3	0.05156	421	1

Line ID	Thermal Limit (MW)	x (pu)	From Bus	to bus
519	65.4	0.00311	422	421
520	320.3	0.01763	423	87
521	450	0.03594	423	496
522	273.2	0.00386	424	423
523	1493.9	0.004	425	297
524	554	0.03219	426	425
525	18.8	0.00303	427	426
526	1493.9	0.00601	428	151
527	1493.9	0.01456	428	246
528	320.3	0.01409	429	139
529	320.3	0.01699	429	466
530	646	0.00868	429	428
531	207	0.06355	430	428
532	225	0.03646	431	428
533	204	0.03175	432	428
534	218	0.09098	433	428
535	231	0.02264	434	428
536	458	0.02826	435	428
537	457	0.01431	436	428
538	471	0.01844	437	428
539	492	0.02322	438	428
540	474	0.01452	439	428
541	1493.9	0.00873	440	57
542	1493.9	0.01226	440	386
543	649	0.02873	441	440
544	320.3	0.02819	441	384
545	267	0.04469	442	440
546	385	0.02669	443	440
547	202	0.08953	444	440
548	320.3	0.0282	445	185
549	320.3	0.03179	445	461
550	130.2	0.00358	446	445
551	76.1	0.00384	448	447
552	320.3	0.01991	449	330
553	1.5	0.00333	450	449
554	3.3	0.00319	451	449
555	330	0.01932	452	76
556	320.3	0.02266	454	29
557	634	0.03057	454	453
558	551	0.01616	455	453
559	651	0.01668	456	453
560	207	0.07218	458	457
561	320.3	0.019	459	496
562	320.3	0.03551	460	340
563	320.3	0.04814	462	477
564	320.3	0.03141	462	465
565	80	0.09575	463	462
566	384	0.02723	465	464
567	320.3	0.01931	466	60

Line ID	Thermal Limit (MW)	x (pu)	From Bus	to bus
568	320.3	0.05541	468	289
569	320.3	0.01497	470	467
570	1493.9	0.00613	471	464
571	320.3	0.03186	472	99
572	501	0.01869	472	471
573	320.3	0.04566	473	133
574	320.3	0.03058	475	147
575	320.3	0.03394	475	269
576	320.3	0.02402	476	486
577	320.3	0.03347	477	295
578	320.3	0.04202	479	354
579	221	0.06304	480	479
580	160	0.05504	481	479
581	187	0.03182	482	479
582	187	0.10067	483	479
583	140	0.05489	484	479
584	320.3	0.03462	485	499
585	320.3	0.01969	485	454
586	320.3	0.01707	488	156
587	320.3	0.03564	488	210
588	320.3	0.02347	489	149
589	320.3	0.02751	490	117
590	320.3	0.02294	491	326
591	320.3	0.06069	492	336
592	320.3	0.0415	492	405
593	320.3	0.03274	493	380
594	75	0.0643	494	493
595	320.3	0.01617	495	449
596	350	0.01958	496	143
597	204	0.0647	497	496
598	150	0.11755	498	496
599	320.3	0.04307	500	489

Table A.16. 500-bus case: Load

Load ID	BusID	Peak MW
1	2	30.20
2	4	93.62
3	6	2.18
4	11	1.72
5	13	21.03
6	20	3.15
7	22	104.92
8	25	1.30
9	26	12.36
10	28	35.91
11	30	70.54
12	32	6.78

Load ID	BusID	Peak MW
13	34	17.36
14	36	30.10
15	38	0.09
16	41	33.09
17	43	3.10
18	45	1.43
19	47	24.77
20	51	0.25
21	52	16.24
22	54	24.56
23	56	1.56
24	59	79.77

Load ID	BusID	Peak MW
25	61	0.12
26	64	24.54
27	67	3.17
28	69	9.68
29	75	3.74
30	77	4.72
31	79	0.25
32	84	42.63
33	86	12.21
34	88	3.57
35	90	4.16
36	92	42.97

Load ID	BusID	Peak MW
37	94	3.68
38	96	22.47
39	98	24.51
40	100	7.72
41	101	0.51
42	103	26.94
43	105	55.78
44	107	11.11
45	109	27.15
46	111	35.55
47	113	31.93
48	115	3.51
49	116	2.15
50	118	6.13
51	120	17.91
52	122	37.65
53	130	58.43
54	132	14.38
55	134	28.18
56	136	18.88
57	138	54.64
58	140	0.15
59	142	109.64
60	148	40.51
61	150	1.04
62	153	53.16
63	155	38.14
64	157	59.68
65	159	16.12
66	161	18.02
67	164	69.25
68	171	8.18
69	173	2.18
70	174	5.07
71	177	5.97
72	178	4.63
73	180	9.97
74	182	54.59
75	184	20.51
76	186	29.97
77	188	7.80
78	190	9.77
79	192	11.41
80	194	19.92
81	199	60.96
82	201	6.27
83	203	3.26
84	204	31.71
85	206	2.09
86	207	15.67
87	209	46.33
88	211	19.56
89	213	67.68
90	215	58.65
91	217	31.19
92	219	0.23
93	227	3.58
94	229	35.74
95	234	42.31
96	237	1.88
97	239	22.33
98	241	13.71
99	243	52.54
100	245	8.22
101	252	67.17
102	259	4.62
103	261	12.35
104	266	43.59
105	268	81.33
106	270	4.72
107	273	6.59
108	277	0.29
109	278	4.07
110	280	9.59
111	282	77.51
112	284	22.67
113	286	5.46
114	288	41.00
115	290	2.44
116	292	5.37
117	294	17.78
118	296	4.44
119	299	10.11
120	303	58.95
121	307	43.04
122	309	6.27
123	311	28.96
124	313	8.64
125	315	0.24
126	317	2.55
127	321	106.13
128	323	25.62
129	325	58.56
130	327	85.42
131	329	17.19
132	331	32.63
133	334	0.29
134	335	0.48
135	337	3.85
136	339	51.04
137	341	13.71
138	343	1.74
139	344	1.69
140	346	33.57
141	348	48.90
142	355	14.09
143	357	31.54
144	359	10.13
145	364	17.37
146	366	39.86
147	368	7.57
148	370	23.53
149	373	20.35
150	375	17.47
151	377	51.58
152	379	8.84
153	381	5.78
154	383	17.09
155	385	20.73
156	397	26.40
157	398	11.08
158	400	15.99
159	402	60.03
160	404	13.73
161	406	3.57
162	416	4.28
163	418	36.01
164	420	3.63
165	422	34.70
166	424	106.75
167	427	10.02
168	446	50.19
169	448	32.85
170	450	0.64
171	451	1.26
172	452	7.59
173	459	50.60
174	460	15.03
175	461	51.91
176	465	7.15
177	466	24.73
178	467	0.53
179	468	2.49
180	469	72.75
181	470	28.12
182	472	28.37
183	473	0.66

Load ID	BusID	Peak MW
184	474	43.61
185	474	3.96
186	474	47.07
187	475	0.11
188	476	42.23
189	477	11.83
190	477	6.05
191	478	5.01

Load ID	BusID	Peak MW
192	478	1.21
193	485	19.67
194	486	48.36
195	487	7.71
196	488	55.41
197	489	0.26
198	489	2.30
199	490	19.70

Load ID	BusID	Peak MW
200	491	84.34
201	492	40.46
202	493	2.75
203	495	42.90
204	499	86.31
205	500	2.59
206	500	13.68

Table A.17. 500-bus case: Interface definition

Line ID	From Bus	To Bus	From Area	To Area	Weight	Metered side (pricing calculation)
30	21	112	3	1	0.33	1
34	23	386	2	1	0.15	1
141	112	499	1	3	0.33	1
208	162	220	3	2	0.5	2
320	251	360	1	2	0.15	1
418	336	93	2	3	0.5	2
437	356	382	1	2	0.14	1
444	360	417	2	1	0.14	1
458	372	112	3	1	0.34	1
462	376	469	2	1	0.14	1
470	380	202	2	1	0.14	1
562	460	340	2	1	0.14	1

Table A.18. 500-bus case: Area interchange

From Area	To Area	Interchange amount (MW)	Period
1	2	150	24 hours
1	3	-20	24 hours
2	3	400	24 hours

Table A.19. 500-bus case: Generatros

Gen ID	Bus ID	Output limits (MW)		Maximum ramp rates (MW/h)		Minimum times (h)		T^{init} (h)	T^{cold} (h)	Cost						P^{init} (h)	Fuel type
		Maximum	Minimum	Up	Down	*Run*	*Down*			No Load ($)	Linear ($/MW)	Quadratic ($/MW^2)	Shut down($)	Hot Startup($)	Cold Startup($)		
1	9	771.8	231.54	1852.32	1852.32	6	6	8	8	1424.48	18.99936	0.001944	13892.4	135065	135065	231.54	Coal
2	16	444.45	133.33	800.01	800.01	120	120	400	8	1266.47	5.867	0.0002	444450	444450	444450	133.33	Nuclear
3	17	888.9	266.67	1600.02	1600.02	120	120	400	8	1319.13	8.412	0.0002	888900	888900	888900	266.67	Nuclear
4	18	157.6	47.28	283.68	283.68	120	120	4	8	1076.21	9.275	0.0002	157600	157600	157600	47.28	Nuclear
5	49	1.3	0.39	3.12	3.12	6	6	1	8	236.03	18.99936	0.001944	23.4	227.5	227.5	0.39	Coal
6	50	2.6	0.78	6.24	6.24	6	6	9	8	236.07	18.99936	0.001944	46.8	455	455	0.78	Coal
7	63	3.2	0.96	28.8	28.8	1	1	8	8	604.8	23.15201	0.002072	25.6	272	272	0.96	Natural Gas
8	71	0.58	0	6.264	6.264	1	1	-2	8	0	0	0	0.29	1.74	1.74	0	Hydro
9	72	0.29	0	3.132	3.132	1	1	-2	8	0	0	0	0.145	0.87	0.87	0	Hydro
10	73	0.2	0	2.16	2.16	1	1	-2	8	0	0	0	0.1	0.6	0.6	0	Hydro
11	82	52.04	0	562.032	562.032	1	1	-2	8	0	0	0	26.02	156.12	156.12	0	Hydro
12	125	23.29	0	251.532	251.532	1	1	-2	8	0	0	0	11.645	69.87	69.87	0	Hydro
13	126	23.29	0	251.532	251.532	1	1	-2	8	0	0	0	11.645	69.87	69.87	0	Hydro
14	127	23.29	0	251.532	251.532	1	1	-2	8	0	0	0	11.645	69.87	69.87	0	Hydro
15	128	23.29	0	251.532	251.532	1	1	-2	8	0	0	0	11.645	69.87	69.87	0	Hydro
16	144	602.55	180.76	1084.59	1084.59	120	120	400	8	1363.88	6.87	0.0002	602550	602550	602550	180.76	Nuclear
17	145	602.55	180.76	1084.59	1084.59	120	120	400	8	1060.19	8.143	0.0002	602550	602550	602550	180.76	Nuclear
18	167	27.82	0	300.456	300.456	1	1	-2	8	0	0	0	13.91	83.46	83.46	0	Hydro
19	168	27.82	0	300.456	300.456	1	1	-2	8	0	0	0	13.91	83.46	83.46	0	Hydro
20	169	55.65	0	601.02	601.02	1	1	-2	8	0	0	0	27.825	166.95	166.95	0	Hydro
21	197	293.6	88.08	704.64	704.64	6	6	8	8	1081.02	18.99936	0.001944	5284.8	51380	51380	88.08	Coal
22	198	207.3	62.19	497.52	497.52	6	6	8	8	879.08	18.99936	0.001944	3731.4	36277.5	36277.5	62.19	Coal
23	222	0.75	0	8.1	8.1	1	1	-2	8	0	0	0	0.375	2.25	2.25	0	Hydro
24	223	2.59	0	27.972	27.972	1	1	-2	8	0	0	0	1.295	7.77	7.77	0	Hydro
25	224	73.51	0	793.908	793.908	1	1	-2	8	0	0	0	36.755	220.53	220.53	0	Hydro
26	225	74.03	0	799.524	799.524	1	1	-2	8	0	0	0	37.015	222.09	222.09	0	Hydro
27	231	2.9	0.87	6.96	6.96	6	6	8	8	236.08	18.99936	0.001944	52.2	507.5	507.5	0.87	Coal
28	248	133.2	39.96	1198.8	1198.8	1	1	4	8	799.8	24.03261	0.002072	1065.6	11322	11322	39.96	Natural Gas
29	249	133.2	39.96	1198.8	1198.8	1	1	24	8	799.8	24.03261	0.002072	1065.6	11322	11322	39.96	Natural Gas
30	250	532.8	159.84	4795.2	4795.2	1	1	20	8	2763.98	26.74175	0.002072	4262.4	45288	45288	159.84	Natural Gas
31	254	4.1	1.23	9.84	9.84	6	6	8	8	236.11	18.99936	0.001944	73.8	717.5	717.5	1.23	Coal
32	255	3.3	0.99	7.92	7.92	6	6	8	8	236.09	18.99936	0.001944	59.4	577.5	577.5	0.99	Coal
33	256	2.9	0.87	6.96	6.96	6	6	8	8	236.08	18.99936	0.001944	52.2	507.5	507.5	0.87	Coal
34	257	5.4	1.62	12.96	12.96	6	6	8	8	236.14	18.99936	0.001944	97.2	945	945	1.62	Coal
35	258	1.1	0.33	2.64	2.64	6	6	8	8	236.03	18.99936	0.001944	19.8	192.5	192.5	0.33	Coal

Gen ID	Bus ID	Output limits (MW)		Maximum ramp rates (MW/h)		Minimum times (h)		T^{init} (h)	T^{cold} (h)	Cost						P^{init} (h)	Fuel type
		Maximum	Minimum	Up	Down	*Run*	*Down*			No Load ($)	Linear ($/MW)	Quadratic ($/MW^2)	Shut down($)	Hot Startup($)	Cold Startup($)		
36	264	39.2	11.76	352.8	352.8	1	1	8	8	658.8	23.39547	0.002072	313.6	3332	3332	11.76	Natural Gas
37	265	10.6	3.18	95.4	95.4	1	1	10	8	615.9	23.20122	0.002072	84.8	901	901	3.18	Natural Gas
38	275	101.2	30.36	910.8	910.8	1	1	-8	8	751.8	23.81505	0.002072	809.6	8602	8602	30.36	Natural Gas
39	301	2.9	0.87	6.96	6.96	6	6	-8	8	236.08	18.99936	0.001944	52.2	507.5	507.5	0.87	Coal
40	302	2.9	0.87	6.96	6.96	6	6	-8	8	236.08	18.99936	0.001944	52.2	507.5	507.5	0.87	Coal
41	305	0.14	0	1.512	1.512	1	1	-2	8	0	0	0	0.07	0.42	0.42	0	Hydro
42	306	0.35	0	3.78	3.78	1	1	-2	8	0	0	0	0.175	1.05	1.05	0	Hydro
43	319	6.08	0	65.664	65.664	1	1	-2	8	0	0	0	3.04	18.24	18.24	0	Hydro
44	350	2.16	0	23.328	23.328	1	1	-2	8	0	0	0	1.08	6.48	6.48	0	Hydro
45	351	0.89	0	9.612	9.612	1	1	-2	8	0	0	0	0.445	2.67	2.67	0	Hydro
46	352	2.07	0	22.356	22.356	1	1	-2	8	0	0	0	1.035	6.21	6.21	0	Hydro
47	353	10.64	0	114.912	114.912	1	1	-2	8	0	0	0	5.32	31.92	31.92	0	Hydro
48	361	1.6	0.48	14.4	14.4	1	1	-2	8	602.4	23.14165	0.002072	12.8	136	136	0.48	Natural Gas
49	362	11	3.3	99	99	1	1	8	8	616.5	23.20381	0.002072	88	935	935	3.3	Natural Gas
50	363	3.2	0.96	28.8	28.8	1	1	4	8	604.8	23.15201	0.002072	25.6	272	272	0.96	Natural Gas
51	388	10	3	90	90	1	1	2	8	615	23.19863	0.002072	80	850	850	3	Natural Gas
52	389	173.33	52	1559.97	1559.97	1	1	3	8	859.99	24.30456	0.002072	1386.64	14733.05	14733.05	52	Natural Gas
53	390	173.33	52	1559.97	1559.97	1	1	4	8	859.99	24.30456	0.002072	1386.64	14733.05	14733.05	52	Natural Gas
54	391	173.33	52	1559.97	1559.97	1	1	5	8	859.99	24.30456	0.002072	1386.64	14733.05	14733.05	52	Natural Gas
55	392	116.4	34.92	1047.6	1047.6	1	1	5	8	774.6	23.91865	0.002072	931.2	9894	9894	34.92	Natural Gas
56	393	116.4	34.92	1047.6	1047.6	1	1	8	8	774.6	23.91865	0.002072	931.2	9894	9894	34.92	Natural Gas
57	394	116.4	34.92	1047.6	1047.6	1	1	8	8	774.6	23.91865	0.002072	931.2	9894	9894	34.92	Natural Gas
58	395	116.4	34.92	1047.6	1047.6	1	1	5	8	774.6	23.91865	0.002072	931.2	9894	9894	34.92	Natural Gas
59	396	116.4	34.92	1047.6	1047.6	1	1	2	8	774.6	23.91865	0.002072	931.2	9894	9894	34.92	Natural Gas
60	409	100	30	900	900	1	1	4	8	750	23.80728	0.002072	800	8500	8500	30	Natural Gas
61	410	136.95	41.08	1232.55	1232.55	1	1	3	8	805.42	24.05851	0.002072	1095.6	11640.75	11640.75	41.08	Natural Gas
62	411	136.95	41.08	1232.55	1232.55	1	1	1	8	805.42	24.05851	0.002072	1095.6	11640.75	11640.75	41.08	Natural Gas
63	412	136.95	41.08	1232.55	1232.55	1	1	1	8	805.42	24.05851	0.002072	1095.6	11640.75	11640.75	41.08	Natural Gas
64	413	136.95	41.08	1232.55	1232.55	1	1	8	8	805.42	24.05851	0.002072	1095.6	11640.75	11640.75	41.08	Natural Gas
65	414	111.1	33.33	999.9	999.9	1	1	8	8	766.65	23.88239	0.002072	888.8	9443.5	9443.5	33.33	Natural Gas
66	430	0.14	0	1.512	1.512	1	1	-2	8	0	0	0	0.07	0.42	0.42	0	Hydro
67	431	0.47	0	5.076	5.076	1	1	-2	8	0	0	0	0.235	1.41	1.41	0	Hydro
68	432	0.17	0	1.836	1.836	1	1	-2	8	0	0	0	0.085	0.51	0.51	0	Hydro
69	433	0.96	0	10.368	10.368	1	1	-2	8	0	0	0	0.48	2.88	2.88	0	Hydro
70	434	0.62	0	6.696	6.696	1	1	-2	8	0	0	0	0.31	1.86	1.86	0	Hydro
71	435	28.33	0	305.964	305.964	1	1	-2	8	0	0	0	14.165	84.99	84.99	0	Hydro
72	436	28.33	0	305.964	305.964	1	1	-2	8	0	0	0	14.165	84.99	84.99	0	Hydro
73	437	28.33	0	305.964	305.964	1	1	-2	8	0	0	0	14.165	84.99	84.99	0	Hydro

Gen ID	Bus ID	Output limits (MW)		Maximum ramp rates (MW/h)		Minimum times (h)		T^{init} (h)	T^{cold} (h)	Cost						P^{init} (h)	Fuel type
		Maximum	Minimum	Up	Down	*Run*	*Down*			No Load ($)	Linear ($/MW)	Quadratic ($/MW^2)	Shut down($)	Hot Startup($)	Cold Startup($)		
74	438	28.33	0	305.964	305.964	1	1	-2	8	0	0	0	14.165	84.99	84.99	0	Hydro
75	439	28.33	0	305.964	305.964	1	1	-2	8	0	0	0	14.165	84.99	84.99	0	Hydro
76	442	108	32.4	972	972	1	1	4	8	762	23.86167	0.002072	864	9180	9180	32.4	Natural Gas
77	443	175	52.5	1575	1575	1	1	2	8	862.5	24.31751	0.002072	1400	14875	14875	52.5	Natural Gas
78	444	3.3	0.99	29.7	29.7	1	1	3	8	604.95	23.15201	0.002072	26.4	280.5	280.5	0.99	Natural Gas
79	455	222.83	66.85	2005.47	2005.47	1	1	20	8	934.24	24.64126	0.002072	1782.64	18940.55	18940.55	66.85	Natural Gas
80	456	445.67	133.7	4011.03	4011.03	1	1	20	8	1344.19	26.15123	0.002072	3565.36	37881.95	37881.95	133.7	Natural Gas
81	458	109.6	32.88	1117.92	1117.92	1	1	1	8	0	0	0	0	0	0	32.88	Solar
82	463	7.2	2.16	17.28	17.28	6	6	10	8	236.19	18.99936	0.001944	129.6	1260	1260	2.16	Coal
83	480	8.05	0	86.94	86.94	1	1	-2	8	0	0	0	4.025	24.15	24.15	0	Hydro
84	481	6.47	0	69.876	69.876	1	1	-2	8	0	0	0	3.235	19.41	19.41	0	Hydro
85	482	6.47	0	69.876	69.876	1	1	-2	8	0	0	0	3.235	19.41	19.41	0	Hydro
86	483	3.45	0	37.26	37.26	1	1	-2	8	0	0	0	1.725	10.35	10.35	0	Hydro
87	484	4.03	0	43.524	43.524	1	1	-2	8	0	0	0	2.015	12.09	12.09	0	Hydro
88	494	5.8	1.74	13.92	13.92	6	6	10	8	236.15	18.99936	0.001944	104.4	1015	1015	1.74	Coal
89	497	8.63	0	93.204	93.204	1	1	-2	8	0	0	0	4.315	25.89	25.89	0	Hydro
90	498	2.59	0	27.972	27.972	1	1	-2	8	0	0	0	1.295	7.77	7.77	0	Hydro

APPENDIX B. MULTI-AREA POWER FLOW EQUATIONS

At the solution or the consensus economic dispatch, the distributed problem power flow equations are equivalent to the single-area power flow.

The DC power flow for a single area can be written as:

$$P = B\theta$$

$$B = \left\{ B_{ij} : i, j \in \mathcal{N} \right\}$$

$$B_{ij} = \begin{cases} -\sum_{\substack{k \in \mathcal{N} \\ k \neq j}} \frac{1}{x_{ik}} & i = j \\ \frac{1}{x_{ij}} & i \neq j \end{cases}$$

We re-write the DC power flow equations for the case of two interconnected systems:

$$\begin{bmatrix} P^{(a)} \\ P^{(b)} \end{bmatrix} = \begin{bmatrix} B^{(aa)} & B^{(ab)} \\ B^{(ba)} & B^{(bb)} \end{bmatrix} \begin{bmatrix} \theta^{(a)} \\ \theta^{(b)} \end{bmatrix}$$

$$P^{(a)} = B^{(aa)}\theta^{(a)} + B^{(ab)}\theta^{(b)}$$

The nonzero elements of $Y_{bus}^{(ab)}$ are associated with the tie-lines connecting the two areas. Therefore, the second term of the equation above can be written only in terms of tie-line admittances and boundary bus phase angles:

$$B^{(ab)}\theta^{(b)} = B^{TL}\theta_{BB}^{(b)}$$

As the primal residual in the consensus distributed optimization approaches zero, the phase angles of the buses near the boundary as calculated in each region are nearly equal.

$$\overline{\theta}^* \cong \begin{bmatrix} \theta^{*(a)}_{BB} \\ \theta^{*(a)}_{NB} \end{bmatrix} \cong \begin{bmatrix} \theta^{*(b)}_{NB} \\ \theta^{*(b)}_{BB} \end{bmatrix}$$

Therefore

$$P^{*(a)} = B^{(aa)}\theta^{*(a)} + B^{TL}\theta^{*(a)}_{NB}$$

And the distributed version of the power flow equations used in the consensus is equivalent to the single-area power flow.

$$\begin{bmatrix} P^{*(a)} \\ P^{*(b)} \end{bmatrix} = \begin{bmatrix} B^{(aa)}\theta^{*(a)} + B^{TL}\theta^{*(a)}_{NB} \\ B^{(bb)}\theta^{*(b)} + B^{TL}\theta^{*(b)}_{NB} \end{bmatrix}$$

REFERENCES

[1] *2018 Quarterly State of the Market Report for PJM: January through June*. (2018). http://www.monitoringanalytics.com/reports/PJM_State_of_the_Market/2018/2018q2-som-pjm-sec13.pdf

[2] *2020 State of the Market Report for PJM: January through September*. (2020). https://www.monitoringanalytics.com/reports/PJM_State_of_the_Market/2020/2020q3-som-pjm.pdf

[3] Ahmadi-Khatir, A., Conejo, A. J., & Cherkaoui, R. (2014). Multi-Area Unit Scheduling and Reserve Allocation Under Wind Power Uncertainty. *IEEE Transactions on Power Systems*, *29*(4), 1701-1710. https://doi.org/10.1109/TPWRS.2013.2293542

[4] Ashraphijuo, M., Fattahi, S., Lavaei, J., & Atamtürk, A. (2016, 12-14 Dec. 2016). A strong semidefinite programming relaxation of the unit commitment problem. 2016 IEEE 55th Conference on Decision and Control (CDC),

[5] Baldick, R., & Chatterjee, D. (2014). Coordinated dispatch of regional transmission organizations: Theory and example. *Computers & Operations Research*, *41*, 319-332. https://doi.org/http://dx.doi.org/10.1016/j.cor.2012.12.016

[6] Bertsekas, D. P. (1979). Convexification procedures and decomposition methods for nonconvex optimization problems. *Journal of Optimization Theory and Applications*, *29*(2), 169-197.

[7] Bose, S., Tong, L., Gross, G., Ji, Y., & Ndrio, M. (2020). *Final Report: Coordination Mechanisms for Seamless Operation of Interconnected Power Systems*. PSERC.

[8] Boyd, S., Parikh, N., Chu, E., Peleato, B., & Eckstein, J. (2011). Distributed Optimization and Statistical Learning via the Alternating Direction Method of Multipliers. *Found. Trends Mach. Learn.*, *3*(1), 1-122. https://doi.org/10.1561/2200000016

[9] Brown, P. R., & Botterud, A. (2021). The Value of Inter-Regional Coordination and Transmission in Decarbonizing the US Electricity System. *Joule*, *5*(1), 115-134. https://doi.org/https://doi.org/10.1016/j.joule.2020.11.013

[10] Buccini, A., Dell'Acqua, P., & Donatelli, M. (2020). A general framework for ADMM acceleration. *Numerical Algorithms*, *85*(3), 829-848. https://doi.org/10.1007/s11075-019-00839-y

[11] Chao, H.-P., & Peck, S. (1996). A market mechanism for electric power transmission. *Journal of Regulatory Economics*, *10*(1), 25-59. https://doi.org/10.1007/BF00133357

[12] Chmielewski, B. (2020). *History and Evolution of Financial Transmission Rights in PJM*. Retrieved 12/22/2020 from https://www.pjm.com/-/media/committees-groups/task-forces/afmtf/2020/20200113/20200113-item-04-history-and-evolution-of-ftrs-in-pjm.ashx

[13] Conejo, A. J., & Aguado, J. A. (1998). Multi-area coordinated decentralized DC optimal power flow. *IEEE Transactions on Power Systems*, *13*(4), 1272-1278. https://doi.org/10.1109/59.736264

[14] Correia, P. F. (2006). Decentralised unit commitment in a market structure: problem formulation and solution advancement. *IEE Proceedings - Generation, Transmission and Distribution*, *153*(1), 121-126. https://doi.org/10.1049/ip-gtd:20050161

[15] *Energy primer: A handbook of energy market basics*. (2020). https://www.ferc.gov/sites/default/files/2020-06/energy-primer-2020_0.pdf

[16] Fattahi, S., Ashraphijuo, M., Lavaei, J., & Atamtürk, A. (2017). Conic relaxations of the unit commitment problem. *Energy*, *134*, 1079-1095. https://doi.org/https://doi.org/10.1016/j.energy.2017.06.072

[17] Feizollahi, M. J., Costley, M., Ahmed, S., & Grijalva, S. (2015). Large-scale decentralized unit commitment. *International Journal of Electrical Power & Energy Systems*, *73*, 97-106. https://doi.org/http://doi.org/10.1016/j.ijepes.2015.04.009

[18] FSR. *Electricity markets in the EU*. Florence School of Regulation. Retrieved March 10, 2021 from https://fsr.eui.eu/electricity-markets-in-the-eu/

[19] Gomez, T., Herrero, I., Rodilla, P., Escobar, R., Lanza, S., Fuente, I. d. l., Llorens, M. L., & Junco, P. (2019). European Union Electricity Markets: Current Practice and Future View. *IEEE Power and Energy Magazine*, *17*(1), 20-31. https://doi.org/10.1109/MPE.2018.2871739

[20] Gramlich, R., & Caspary, J. *Planning for the future: FERC's opportunity to spur more cost-effective transmission infrastructure*. A. f. a. C. E. Grid. https://cleanenergygrid.org/wp-content/uploads/2021/01/ACEG_Planning-for-the-Future1.pdf

[21] Granada Echeverri, M., López Lezama, J., & Mantovani, S. (2010). Decentralized AC power flow for multi-area power systems using a decomposition approach based on Lagrangian relaxation. *Revista Facultad de Ingeniería Universidad de Antioquia*, *225-235*. http://www.redalyc.org/exportarcita.oa?id=43019325021

[22] Guo, Y., Bose, S., & Tong, L. (2017). On Robust Tie-line Scheduling in Multi-Area Power Systems.

[23] Guo, Y., Bose, S., & Tong, L. (2018). On Robust Tie-Line Scheduling in Multi-Area Power Systems. *IEEE Transactions on Power Systems*, *33*(4), 4144-4154. https://doi.org/10.1109/TPWRS.2017.2775161

[24] Guo, Y., Ji, Y., & Tong, L. (2018). Generalized Coordinated Transaction Scheduling: A Market Approach to Seamless Interfaces. *IEEE Transactions on Power Systems*, *33*(5), 4683-4693. https://doi.org/10.1109/TPWRS.2018.2803749

[25] Guo, Y., Tong, L., Wu, W., Zhang, B., & Sun, H. (2017). Coordinated Multi-Area Economic Dispatch via Critical Region Projection. *IEEE Transactions on Power Systems*, *32*(5), 3736-3746. https://doi.org/10.1109/TPWRS.2017.2655442

[26] Hogan, W. W. (1992). Contract networks for electric power transmission. *Journal of Regulatory Economics*, *4*(3), 211-242. https://doi.org/10.1007/BF00133621

[27] Ji, Y., & Tong, L. (2018). Multi-Area Interchange Scheduling Under Uncertainty. *IEEE Transactions on Power Systems*, *33*(2), 1659-1669. https://doi.org/10.1109/TPWRS.2017.2727326

[28] Ji, Y., Zheng, T., & Tong, L. (2017). Stochastic Interchange Scheduling in the Real-Time Electricity Market. *IEEE Transactions on Power Systems*, *32*(3), 2017-2027. https://doi.org/10.1109/TPWRS.2016.2600635

[29] Kim, B. H., & Baldick, R. (1997). Coarse-grained distributed optimal power flow. *IEEE Transactions on Power Systems*, *12*(2), 932-939. https://doi.org/10.1109/59.589777

[30] Kim, B. H., & Baldick, R. (2000). A comparison of distributed optimal power flow algorithms. *IEEE Transactions on Power Systems*, *15*(2), 599-604. https://doi.org/10.1109/59.867147

[31] Liu, H., Tesfatsion, L., & Chowdhury, A. A. (2009, 26-30 July 2009). Locational marginal pricing basics for restructured wholesale power markets. 2009 IEEE Power & Energy Society General Meeting,

[32] Long-Term Firm Transmission Rights in Organized Electricity Markets, (2006). https://www.ferc.gov/sites/default/files/2020-05/E-1_78.pdf

[33] Luo, C., Jiang, L., Wen, J., Zhang, X., & Wang, Q. (2015, 26-30 July 2015). Real-time market-to-market coordination in interregional congestion management. 2015 IEEE Power & Energy Society General Meeting,

[34] Lyons, K., Fraser, H., & Parmesano, H. (2000). An Introduction to Financial Transmission Rights. *The Electricity Journal*, *13*(10), 31-37. https://doi.org/https://doi.org/10.1016/S1040-6190(00)00164-0

[35] *MISO-PJM Interface Price Update*. (2017). Retrieved 12/8/2020 from https://www.pjm.com/-/media/committees-groups/stakeholder-meetings/pjm-miso-joint-common/20170228/20170228-item-03a-interface-pricing-update.ashx

[36] Business Practices Manual for Energy and Operating Reserve Markets - Attachment B: Day-ahead Energy and Operating Reserve Market Software Formulations and Business Logic, 2/7/2021 (2019). https://www.misoenergy.org/legal/business-practice-manuals/

[37] Mohammad Javed Feizollahi, M. C., Shabbir Ahmen, Santiago Grijalva. (2015). Large-scale decentralized unit commitment. *Electrical Power and Energy Systems*, *73*, 97-106.

[38] Morales-España, G., Latorre, J. M., & Ramos, A. (2013). Tight and Compact MILP Formulation for the Thermal Unit Commitment Problem. *IEEE Transactions on Power Systems*, *28*(4), 4897-4908. https://doi.org/10.1109/TPWRS.2013.2251373

[39] Muller, N., Irisarri, G., Medina, J., Gonzalez-Perez, C., Yassin, M., Latimer, J., Albuyeh, F., & Mokhtari, S. (2009, 15-18 March 2009). NERC IDC: Managing congestion in the North American Eastern Interconnection. 2009 IEEE/PES Power Systems Conference and Exposition,

[40] Ndrio, M., Bose, S., Guo, Y., & Tong, L. (2019, 4-8 Aug. 2019). Coordinated Transaction Scheduling in Multi-Area Power Systems with Strategic Participants. 2019 IEEE Power & Energy Society General Meeting (PESGM),

[41] Nogales, F. J., Prieto, F. J., & Conejo, A. J. (2003). A Decomposition Methodology Applied to the Multi-Area Optimal Power Flow Problem. *Annals of Operations Research*, *120*(1), 99-116. https://doi.org/10.1023/A:1023374312364

[42] Ouyang, Z., & Shahidehpour, S. M. (1991). Heuristic multi-area unit commitment with economic dispatch. *IEE Proceedings C - Generation, Transmission and Distribution*, *138*(3), 242-252. https://doi.org/10.1049/ip-c.1991.0030

[43] Patton, D. B., LeeVanShcaick, P., & Chen, J. (2011). *2010 Assessment of the Electricity Markets in New England*. https://www.potomaceconomics.com/wp-content/uploads/2017/02/isone_2010_immu_report.pdf

[44] *Potomac Economics - 2019 State of the market report for the MISO electricity markets*. https://www.potomaceconomics.com/wp-content/uploads/2020/06/2019-MISO-SOM_Report_Final_6-16-20r1.pdf

[45] Promoting Wholesale Competition Throuhg Open Access Non-discriminatory Transmission Services by Public Utilities, (1996). https://www.ferc.gov/sites/default/files/2020-05/rm95-8-00v.txt

[46] Regional Transmission Organizations, (1999). https://www.ferc.gov/sites/default/files/2020-06/RM99-2-00K_1.pdf

[47] Schweppe, F. C., Caramanis, M. C., Tabors, R. D., & Bohn, R. E. (1988). *Spot Pricing of Electricity*. Kluwer Academic Publishers.

[48] Takapoui, R., Moehle, N., Boyd, S., & Bemporad, A. (2020). A simple effective heuristic for embedded mixed-integer quadratic programming. *International Journal of Control: Model Predictive Control*, *93*(1), 2-12. https://doi.org/10.1080/00207179.2017.1316016

[49] *Texas A&M University - Electric grid test case repository*. https://electricgrids.engr.tamu.edu/electric-grid-test-cases/

[50] Wang, X., Song, Y. H., & Lu, Q. (2001). Lagrangian decomposition approach to active power congestion management across interconnected regions. *IEE Proceedings - Generation, Transmission and Distribution*, *148*(5), 497-503. https://doi.org/10.1049/ip-gtd:20010490

[51] Wenyi, T. (2019). An Alternating Direction Method of Multipliers with a worst-case O(1/n) convergence rate. *Mathematics of Computation*, *88*(318), 1685-1714. https://doi.org/10.1090/mcom/3388

[52] Xianjun, Z., Chatterjee, D., Tengshun, P., & Sutton, R. (2014, 27-31 July 2014). Interface definition and pricing for economic and efficient interchange transactions. PES General Meeting | Conference & Exposition, 2014 IEEE,

[53] Xu, C., & Overbye, T. J. (2005). PTDF-based power system equivalents. *IEEE Transactions on Power Systems*, *20*(4), 1868-1876. https://doi.org/10.1109/TPWRS.2005.857013

[54] Xu, T., Birchfield, A., Gegner, K., Shetye, K., & Overbye, T. (2017). Application of Large-Scale Synthetic Power System Models for Energy Economic Studies. Proceedings of the 50th Hawaii International Conference on System Sciences, Waikoloa Village, Hawaii, USA.

[55] Zhao, F., Litvinov, E., & Zheng, T. (2014). A Marginal Equivalent Decomposition Method and Its Application to Multi-Area Optimal Power Flow Problems. *IEEE Transactions on Power Systems*, *29*(1), 53-61. https://doi.org/10.1109/TPWRS.2013.2281775